Flow Behaviour of Pellets

Design of a Mass Flow Hopper for Biomass and Waste Pellets in an HTW Gasification Plant

Lars Markman

Delft University of Technology

TU Delft

Flow Behaviour of Pellets

Design of a Mass Flow Hopper for Biomass and Waste Pellets in an HTW Gasification Plant

by

Lars Markman

to obtain the degree of Master of Science
at the Delft University of Technology,
to be defended publicly on Monday August 28, 2023 at 13:00.

Student number:	4586530
Report Number:	2023.MME.8854
Project duration:	September 1, 2022 – August 28, 2023
Supervised by:	Prof.dr.ir. D. Schott, TU Delft
	E. M. Moghaddam, PhD
	Dr.ir. J.T. Padding, TU Delft

An electronic version of this thesis is available at http://repository.tudelft.nl/.

TU Delft Delft University of Technology

Summary

The global energy demand is rising and is primarily met by unsustainable and polluting fossil fuels (Sorrell, 2015). At the same time, the amount of municipal solid waste is rapidly growing due to economic and population growth (Kaza et al., 2018). Landfill space is limited and emits significant greenhouse gases (Kákonyi et al., 2021). Energy and waste management have long been challenging issues, but with the increasing awareness of environmental concerns, there is a growing demand for a solution (Klinghoffer et al., 2013). Waste gasification holds the potential to address energy and waste problems simultaneously. The solid fuel in the gasifier must first undergo a densification process, such as pelletization. Pelletization involves compressing the feedstock at high temperatures (up to 100+°C) and pressures (20 bar) to force small particles to adhere to each other, resulting in larger, denser pellets (Gilvari, 2021).

Plant shutdowns often occur due to failures in the handling systems for feedstock (Basu, 2013; Craven et al., 2015; Dooley et al., 2020). Problems such as flow obstructions, incomplete emptying, and segregation can arise during the discharge of solids from silos (Schulze, 2007). Another prevalent industrial problem in hoppers is arching, where particle cohesion or interlocking blocks the outlet, preventing material flow (Rezaei et al., 2016). Designing handling equipment for waste- and biomass-based pellets is particularly challenging because the materials do not have consistent specifications due to seasonal effects, long-term price fluctuations, and availability (Bradley, 2016). Additionally, pellets mechanically degrade during handling, which may increase the fines content beyond expected levels.

This paper aims to analyze the flow properties of three different biomass and waste pellets with four different testing methods (Schulze ring shear test, angle of repose, angle of tilt and Hausner ratio). The effect of mechanical degradation on the flowability was investigated by varying the fines content. The results from the four different testing methods were correlated to determine their predictive powers. Finally, a hopper was designed based on the flowability measurements and sensitivity analysis of Jenike's hopper design method.

Chapter 2 presents a literature review conducted to discover literature on the flowability of pellets and the factors influencing the flowability of pellets. The overview of the state-of-the-art pellet flowability research reveals that there is no literature relating the pellet properties to flowability. For many powders and other BSMs, the factors influencing the flowability have been researched, and this information is used to determine our experimental plan.

The experimental setups are determined based on measurement standards and literature in **Chapter 3**. These setups are used to determine the pellet properties that may influence the flowability of the pellets, such as the length, shape, density, roughness and mechanical durability. Furthermore, we describe the flowability tests, which were conducted by the Schulze Ring Shear Tester. Finally, three additional flow estimators are described: the angle of repose, angle of tilt and Hausner ratio.

An extensive experimental plan is set up that tests the pellet, BSM and flow properties of three different pellets (RDF, waste wood and fresh wood), mixtures of the pellets, and at four different fines contents (0, 10, 20, 30%)

In **Chapter 4** presents the results of these measurements and compares them with our expectations based on the literature. The fines content negatively influences the flowability of all pellets. The flowability of a BSM with 30% fines content approaches the flowability of the fines fraction. In contrast, an increasing fines content can increase or decrease the wall friction, depending on the pellets. The fines fraction dominates the wall friction at just 10% fines content.

In **Chapter 5** investigates the relationship between the three flow indicators, the angle of repose, the angle of tilt and the Hausner ratio. The findings agree with the literature: an increased angle of repose, angle of tilt and Hausner ratio correspond to a worse flowing BSM. However, one of the relationships are accurate enough to predict the material's flowability and thus cannot be used in silo design.

Finally, in **Chapter 6**, a hopper is designed for the pellets based on the test results and sensitivity analysis. We found that wall friction, flowability, bulk density, and particle size and shape are the most critical material properties in designing a mass flow hopper. Bulk density, particle size and shape are easy to determine. However, the flowability and wall friction require expensive tests. As shown in Chapter 5, there are no cheaper, reliable alternatives to shear testing. Therefore, the design of the hopper is relatively conservative, so it will work even with BSMs that flow worse than we have tested.

Contents

List of Symbols and Abbeviations

Abbreviations

Abbreviation	Definition
BSM	Bulk Solid Material
crit	Critical (conditions at the minimum outlet diameter)
FW	Fresh Wood
L/D	Length over Diameter
PLD	Pellet Length Distribution
PSD	Particle Size Distribution
RDF	Refuse-Derived Fuel
RST	Ring Shear Tester
WW	Waste Wood

Symbols

Symbol	Definition	Unit
A	Area	m^2
AoR	Angle of Repose	$^\circ$
AoT	Angle of Tilt	$^\circ$
d	Outlet Diameter	m
D	Diameter Pellet	m
DU	Mechanical Durability	%
ff	Hopper Flow Factor	-
FFc	Flow Function, flowability	-
g	Gravitational Constant	$m\,s^{-2}$
HR	Hausner Ratio	-
K	Lateral Stress Ratio	-
l	Length	m
m	Mass	kg
m_a	Mass After Mechanical Durability Test	kg
m_b	Mass Before Mechanical Durability Test	kg
r	Polar Coordinate	m
U	Perimeter	m
v	Velocity	$m\,s^{-1}$
V	Volume	m^3
ϕ_e	Effect Angle of Internal Friction	$^\circ$
ϕ_x	Wall Friction Angle	$^\circ$
ρ	Density	$kg\,m^{-3}$
ρ_b	(Loose) Bulk Density	$kg\,m^{-3}$
ρ_t	Tapped Bulk Density	$kg\,m^{-3}$
σ_1	Major Principal Stress, Consolidation stress	Pa
σ_1'	Major Stress in an Arch	Pa
σ_c	Unconfined Yield Strength	Pa
σ_h	Horizontal Stress	Pa
σ_v	Vertical Stress	Pa

Symbol	Definition	Unit
σ_w	Normal Stress Wall Friction	Pa
τ_w	Shear Stress Wall Friction	Pa
θ_c	Hopper Cone Angle (to the vertical)	°

List of Figures

List of Tables

1 Introduction

1.1. Waste and Energy Problem

Today, the increasing global wealth causes an ever-increasing energy demand (Sorrell, 2015). Unsustainable and polluting fossil fuels are responsible for much of the energy produced. Exploiting these fossil fuels is faster than their regeneration, so they will run out. Furthermore, they contribute significantly to CO_2 emission and thus to the planet's warming.

Concurrently, the amount of municipal solid waste produced is growing quickly. Back in 2016, the world produced 2.01 billion tonnes of waste. Projections indicate that this figure will increase to 2.59 billion tonnes by 2030 and to 3.40 billion tonnes by 2050 (Kaza et al., 2018). The landfill space is increasingly limited (Ilic et al., 2018a). Non-managed waste causes various problems: blockage of sewers, diseases, increased respiratory problems, and the low biodegradability of (especially plastic) causes problems mainly in the maritime environment (Sharma & Jain, 2020). Also, valuable resources are lost when waste is sent to landfill (Lopez et al., 2018). Furthermore, waste landfills emit significant greenhouse gases (Kákonyi et al., 2021).

Energy and waste management are two challenges that humans have been facing for a long time (Klinghoffer et al., 2013). During the last decades, growing awareness and concern regarding the state of our planet have increased the demand for a solution to these challenges (Nobre et al., 2020). One promising approach that addresses both energy and waste problems is the gasification of waste materials.

1.2. High-Temperature Winkler Gasification Process

The circular economy uses waste streams as a source of secondary resources and recovers waste for reuse and recycling (Kaza et al., 2018). The concept of circular economy is gaining momentum in high-income countries, specifically in Europe. Products are designed to minimise their impact by not only extending their lifetime but also by minimising the impact of disposal. Some waste cannot be recycled or reused. Non-landfill solutions for this waste include advanced thermal technologies such as pyrolysis, gasification and plasma arc technologies.

Gasification is the thermochemical conversion process through partial oxidation in which carbonaceous solid fuels are converted into gas. It differs from oxidation, as oxidation requires O_2 to be available above the stoichiometric requirements. During gasification, a controlled amount of O_2 below the stoichiometric requirements for combustion is present, inducing thermochemical conversion to syngas. Downstream reactors convert the syngas into different advanced (bio)fuels and chemicals. One of the potential end products is the production of (bio)methanol.

The obtained syngas mainly comprise CO, CO_2, H_2 and CH_4. Unwanted solid byproducts, bottom ash and dust are removed from the reactor and syngas. Gas is of higher energy density and is generally more efficient, versatile and controllable than solid fuels (Zhang et al., 2019). With its ability to convert diverse feedstock, including waste and biomass, through thermochemical processes, gasification technology has recently gained significant attention (Bhaskar & Pandey, 2015).

Gasifiers divide into three types based on their fluidisation regime. The three types are fixed or moving bed gasifiers, fluidised and entrained bed gasifiers (Bell et al., 2011). The (bubbling) fluidised bed gasifier is a common choice for gasifying waste because it can handle an extensive array of solid fuels (Nobre et al., 2020).

Fritz Winkler developed a bubbling fluidised bed gasifier in 1921, which has been used commercially to gasify coal for many years (Basu, 2013). The high-temperature Winkler (HTW) gasifier, was created in the 1970s by RWE and Udeh. It operates under high temperatures and elevated pressure, which directly affects the partial oxidation and gasification reactions. These reactions occur at different timescales, resulting in an increased production of syngas with higher thermal output at the gasifier's outlet (Energy, 2022). The main advantages of fluidised bed reactors are their high heat and mass transfer rates, gas-solid contact, temperature control, solid mixing and flexibility. The gasifier best suits reactive feedstock, such as reactive coal, low-rank coal, biomass, refuse-derived fuel (RDF) and municipal solid waste (Energy, 2022). However, they require high initial investment costs (Lopez et al., 2018).

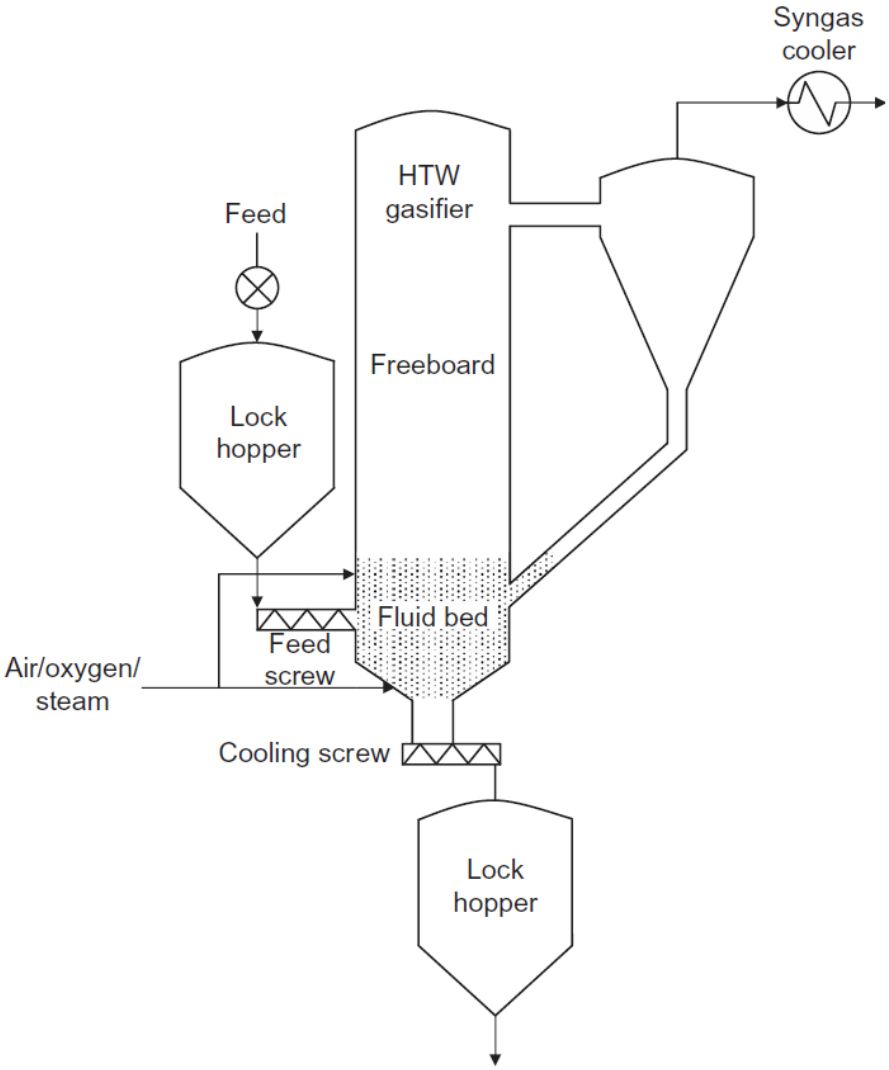

Figure 1.1: Simplified schematic of the HTW gasifier (Basu, 2013)

Figure 1.1 shows a simplified schematic of an HTW gasifier. The HTW gasifier incorporates two thermal zones: the gasification and the post-gasification zone. These zones are designed to accommodate the specific physio-chemical properties of the feedstock by adjusting the temperature accordingly. The gasifying medium, consisting of oxygen and steam, is introduced at different levels. The major part of the conversion occurs in the gasification zone. In the upper part of the gasifier, the post-gasification

zone, additional O_2 is added to complete the gasification. The cyclone removes a large part of the ash and dust from the syngas and returns it to the gasifier for a higher conversion rate. The lock hopper underneath the gasifier captures the bottom ash. Because of the elevated pressure, the feeding, bottom ash and dust removal systems have to be performed by lock hoppers.

1.2.1. Feedstock Preparation for HTW Gasification Process

HTW gasifiers can convert a large range of feedstock, such as Solid Recovered Fuels (SRF) and wood. SRF is a fuel produced from solid waste. It typically consists of municipal solid waste such as biodegradable, recyclable, inert and composite waste. Before the waste enters production, valuable materials such as paper, metal, glass and wood are removed for recycling. The waste is segregated, crushed, mixed and finally pelletised, and *Refuse-Derived Fuel* (RDF) pellets are formed. Another option is pelletizing various types of discarded or unused wood, such as wood chips, sawdust, and wood shavings, resulting in *waste wood* (WW) pellets. Finally, fresh tree wood can also be ground and pelletized, resulting in fresh wood (FW) pellets. Figure 1.2 shows RDF, WW and FW pellets at the top, and the dust and lumps they consist of.

Figure 1.2: From Left to Right: Waste Wood, RDF, Fresh Wood
From Top to Bottom: Pellets, Lumps, Fines

The feedstock used by the HTW process must be able to resist the high pressure of the gasifier, and the moisture content must be less than 15%. Therefore, the solid fuel undergoes a treatment process to reduce its high moisture content and decrease the level of impurities, which is especially necessary for waste solid fuels. Additionally, the fuel is densified or pelletized to improve the bulk density, energy density and flowability behaviour within the lock-hopper system. Pelletisation is a form of densification that uses temperature (up to 100+°C) and pressure (above 20 MPa) to compress the small particles and force them to adhere to one another to create a final larger particle (Gilvari, 2021).

Densification by forming pellets is advantageous for multiple reasons (Berghel et al., 2022; Gilvari, 2021; Rezaei et al., 2016). It increases the mass and energy density, lowers the moisture and ash content, uniforms the size and shape, and increases the strength and durability, furthermore, it enhances the homogeneity of heterogeneous type of solid fuels such as wastes. This results in improved transportation volume and cost, increased storage ease and gasification characteristics. Furthermore, due to the uniformity in size and shape, the flow behaviour of pellets is more predictable and generally

better than the base material (Dai et al., 2012; Wu et al., 2011).

The solid fuel supply to the reactor is an essential part of any gasification plant. A series of solid handling equipment handle the bulk solid material before arriving in the gasifier, such as trucks, conveyor belts, silos and hoppers.

1.3. Bulk Solid Handling Challenges

Many plant shutdowns are related to failures in the feedstock handling systems (Basu, 2013; Craven et al., 2015; Dooley et al., 2020). The discharge of solids from silos and hoppers may cause severe problems, such as flow obstructions, incomplete emptying and segregation (Figure 1.3) (Schulze, 2007). This makes the design of equipment for handling of waste and biomass streams very challenging. The fuel lacks precise specifications due to its origin from byproducts and leftovers of other industries. Therefore, the properties, such as particle size, moisture content, and dust content, can vary daily. Furthermore, seasonal effects can play a role along with long-term price and availability (Bradley, 2016). Furthermore, the degradation of biomass pellets during handling changes their properties. According to Ilic et al. (2018b), there are often up to 25% fines in the plants when only 5-8% is expected.

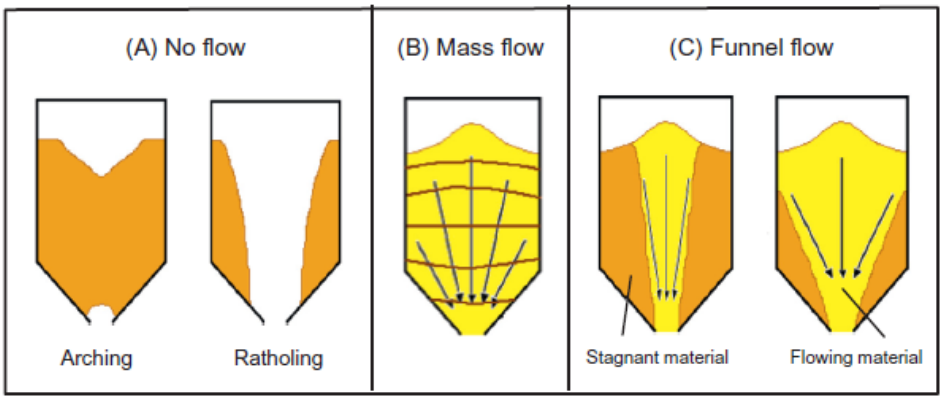

Figure 1.3: Illustration of flow regimes in hopper

The flow regime in a silo or hopper can be defined as mass flow or funnel flow. In the case of mass flow, every particle in the silo moves during discharge. In the case of funnel flow, particles are at rest along the sides of the silo. Achieving mass flow in the silo is desirable to ensure complete emptying and prevent segregation in the outflow. Mass flow occurs when the wall friction is sufficiently low, and the cone's angle is sufficiently steep. Another common problem in hoppers is arching, where the BSM blocks the outlet due to particle cohesion or interlocking, and no material can flow out. Arching can be prevented by having a sufficiently large outlet diameter (Schulze, 2007). Arching biomass particles in a gasifier's feeding system is a common industrial issue (Rezaei et al., 2016).

In an HTW gasification plant pellets must be transported into the reactor. They are handled by a series of equipment, finally ending up in the pressurised lock-hopper handling systems and then the reactor. The gravity lock-hoppers are located above each other. First, the pellets enter the feed hopper. The feed hopper feeds the pellets to the lock hoppers through a chute. The lock hopper is pressurised to the desired pressure. Then, the pellets are fed to the charge bin, where they are finally transported to the gasifier using a star feeder and screw conveyors.

1.4. Problem Statement

Waste streams are unreliable: the quality varies daily, and long-term pricing and availability may force a plant to switch to a different supplier or waste material in the future (Bradley, 2016). Potential issues in the biomass feeding systems for thermochemical reactors have been identified, and it is clear that the physical biomass properties play a substantial role (Dai et al., 2012; Ilic et al., 2018a). Therefore, to prevent problems, one must assess the feedstock regularly, especially when switching suppliers or

waste material. Currently, the pellets are analysed by external laboratories because only they have the necessary knowledge and equipment. The industry is looking for a more straightforward and less time-consuming test procedure to confirm the compatibility between equipment and bulk solids to increase their adaptability in the capricious biomass market.

However, there is a limited amount of research on the effect of the physical properties of pellets on their flow behaviour. A change in the physical and chemical properties of the pellets, such as size and size distribution, chemical composition, and moisture content, might affect the flowability. It is unknown to what extent these parameters influence the flowability of the pellets and, thus, the flow behaviour in the hopper and the correct operation of the plant. Recent literature reviews on biomass flowability, such as Cheng et al. (2021) and Minglani et al. (2020), only identified a few papers focussing on the flowability of pellets. Most of the research on pellets is on the effect of feedstock on chemical pellet properties, the effect of different densification methods and the economic aspects. However, the influence of mechanical pellet properties on the flow behaviour (in the feeding line of gasification plants) is yet unknown.

1.5. Research Questions

"How can we use experiments to establish the pellet, BSM and flow properties of fresh wood, waste wood and refuse-derived fuel pellets to design a lock-hopper for material handling in gasification plants and to develop a quicker approach to establish the flow properties of pellets?"

The following sub-questions help to answer the main research question:

1. Which factors affect the flowability of pellets?
2. How can the pellet properties that influence the flowability and the flow properties of the bulk solid material be measured?
3. What are the experimental results of the relevant pellet and flow properties of the BSM, and how does the fines content influence the flowability?
4. What are the relationships between the various flow indicators that may be used to quickly establish flowability?
5. How must the lock hopper be designed to ensure mass flow of the bulk solid material?

1.6. Outline

Figure 1.4 presents the outline of this thesis. Chapter 2 presents a literature review on the properties of pellets and the factors influencing the flowability of powders and biomass. The factors influencing the flowability of pellets may be used to make predictions about the flowability of pellets without requiring shear testing. In Chapter 3, the experimental setups to measure the pellet and BSM properties and described and the experimental plan is explained. Chapter 4 presents the test results and discusses the findings. Then in Chapter 5, the relationships between the flow indicators and flowability are investigated. In Chapter 6, a lock-hopper is designed based on the experimental results. Finally, the main research question is answered in Chapter 7.

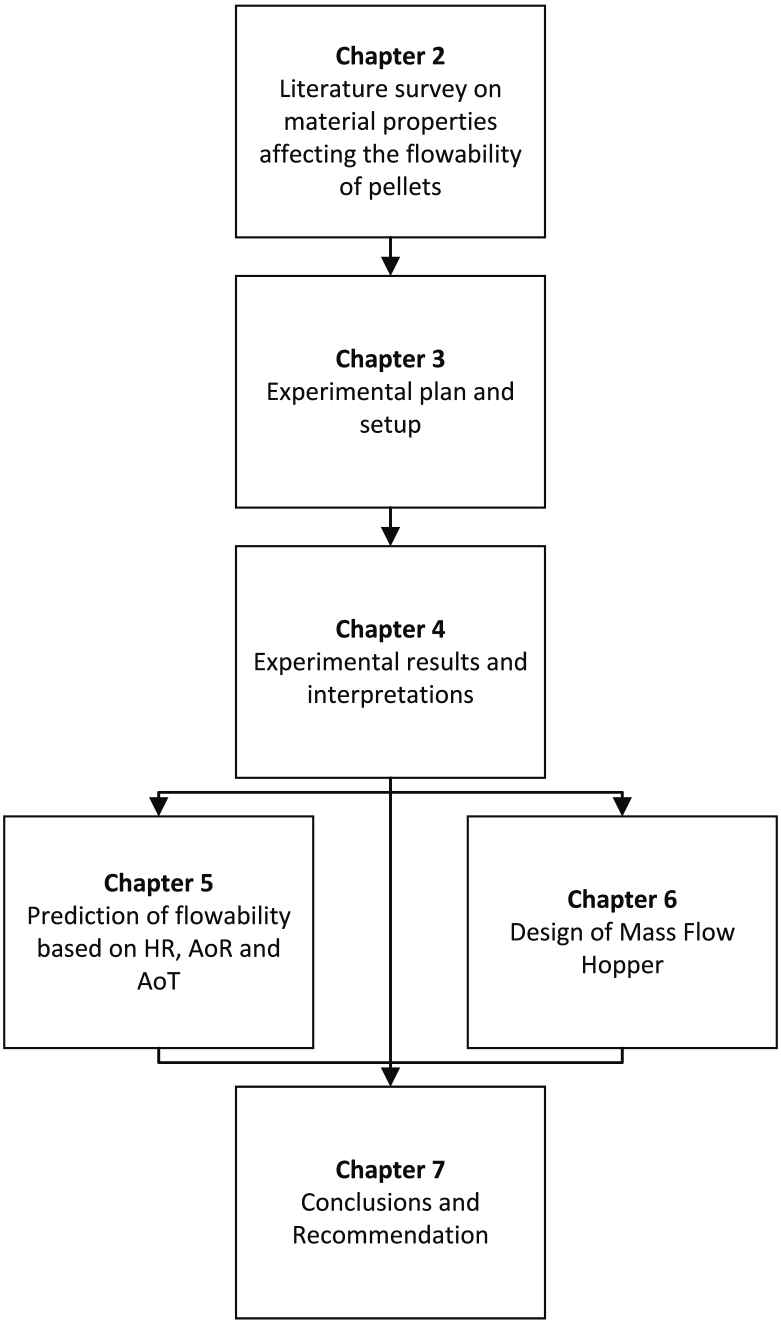

Figure 1.4: Thesis Outline

2

Factors influencing the Flow Behaviour of Pellets

This chapter presents a literature review to discover the factors that influence the flow behaviour of pellets. Quantitative information about how the factors influence flow behaviour may be used to make predictions about flowability when pellet properties change. This first requires knowledge of which factors influence the flow behaviour before measurements can be conducted to quantify the exact behaviour.

This chapter first presents background knowledge of bulk solid material research. Then, it presents an overview of current literature focusing on pellets flowability and research on the factors influencing flowability in biomass and powders.

2.1. Basic principles of BSM behaviour

A bulk solid material consists of individual particles, usually surrounded by air. The particles in the bulk solids are in substantial contact with predominantly contact points instead of planes.

In principle, it is possible to describe the behaviour of the bulk solid by considering the particle-particle interactions. Discrete element modelling uses this approach to simulate bulk solid behaviour. However, it is computationally very intensive due to the many particles involved. Furthermore, the complexity of the interactions and interfacial phenomena (such as liquid arching) that govern the adhesive forces are difficult to calculate.

Another approach is to consider the bulk solid as a continuum. This method uses volume elements that are large compared to individual particles and considers the stresses and deformations on these elements, comparable to the procedures in fluid mechanics.

Due to the complexities inherent in the particle interactions, the flow behaviour is difficult to predict. The flow behaviour depends not only on the properties of the bulk solid itself but also on the environmental conditions and the handling equipment (Cheng et al., 2021).

2.1.1. Flowability and Hopper Design

Flowability, in its most simple definition, is the ability of bulk solid material to flow. Flowing means a continuous failure of the bulk solid sample, where it is deformed plastically due to a shear force. In the 1950s, Jenike laid the foundation for the quantitative measurement of flowability. He developed a shear tester and introduced the yield locus to represent the flowability. Jenike's method remains the most widely used method for silo design.

Figure 2.1 shows a bulk solid sample. The sample is first placed in a hollow cylinder and is consolidated by a stress σ_1, the major principal stress or consolidation stress. The consolidation causes the sample to increase in density and strength. After consolidation, the cylinder is removed, and the sample is loaded with compressive stress until failure. The stress at failure is the unconfined yield strength σ_c.

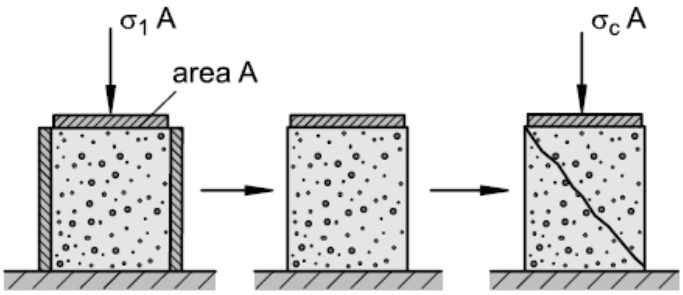

Figure 2.1: Uniaxial test (Schulze, 2007)

This procedure is repeated with different consolidation stresses, and a curve $\sigma_c(\sigma_1)$ is drawn; see Figure 2.2. This curve is called the flow function and represents the flowability of a material.

The flowability is defined as the ratio of σ_1 over σ_c. The higher the ratio, the better the flowability. As seen in Figure 2.2, the flowability depends on the consolidation stress and, thus, the stress history of the bulk solid material. Some bulk solids increase in strength when stored under compressive strength, e.g., time consolidation.

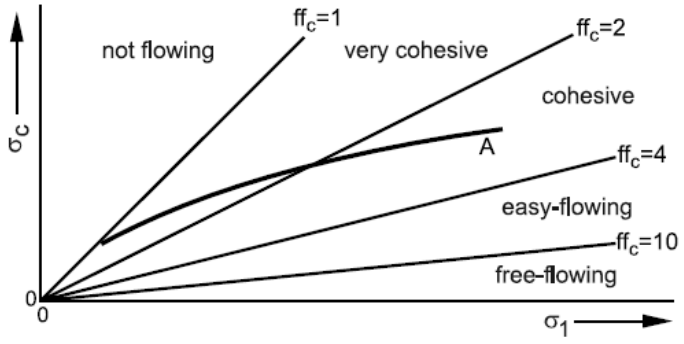

Figure 2.2: Flow Function (Schulze, 2007)

The bulk solid will flow when the applied stress exceeds the unconfined yield stress. In a hopper, the stress in the material is determined by gravity and is thus always roughly equal to the consolidation stress. The higher the flowability, the less strength the material gains under consolidation. This explains why a higher value of flowability means the material flows easier. Furthermore, a higher bulk density increases the flowability as well.

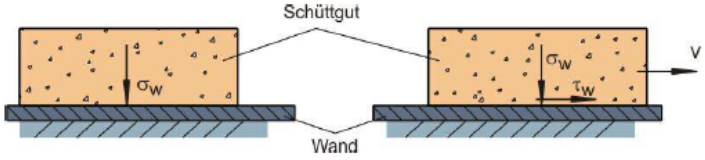

Figure 2.3: wall friction test (Schulze, 2007)

The material interacts with the environment, which the flowability alone does not capture. The wall friction defines the friction between the bulk solid and a surface, e.g., the hopper wall. The necessary shear stress to move the bulk solid across the wall material dependent on the normal stress plotted is the wall yield locus; an example is shown in Figure 2.4.

The flow function and wall yield locus, together with the dimensions of the hopper, are then used to determine the flow behaviour of the bulk solid in the hopper. Numerous design charts are available for equipment design when the values flow function, and wall yield locus are known. One must consistently execute the test at similar pressures as the final equipment.

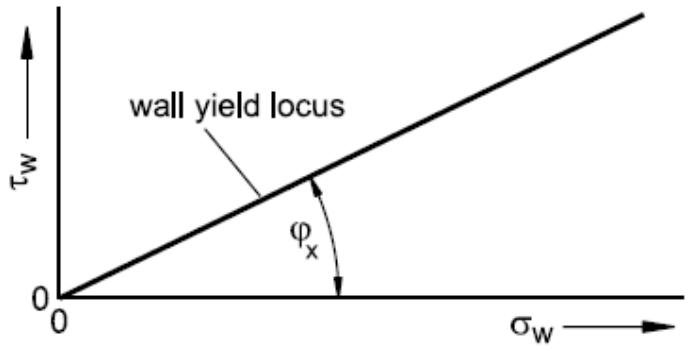

Figure 2.4: wall yield locus (Schulze, 2007)

2.2. Properties of BSM of Pellets

Stasiak et al. (2015) noted in their literature review that only a few papers addressed the flowability of granular biomass. Limiting the scope to the flowability of just pellets reduces the number of papers even further. The handling behaviour of biomass is complicated to predict because of the highly compressible and anisotropic material. However, pellets are much less compressible and isotropic, potentially resulting in more predictable flow behaviour. Table 2.1 provides an overview of the literature on the flowability of pellets and provides the most important properties. More literature on the characteristic of pellets exist, but most ignore the flowability, e.g., (Järvinen & Agar, 2014; Z. Liu et al., 2013; Mcmullen et al., 2005)).

2.2.1. Relationships of Bulk Solid Properties and Flowability

Many papers investigated the relationships between the properties of bulk solids and their flowability. The most studied effects on flowability are moisture content, size, size distribution and shape. There is no consensus on which parameter is the most important; this may differ with the chemical composition and order of the size of the bulk solid.

A higher moisture content generally decreases the flowability because liquid bridges form and increase the cohesive forces. Increasing moisture content further leads to a slight decrease in flowability until saturation. When the bulk solid is saturated, it becomes a suspension, and flowability increases dramatically (Schulze, 2021). The effect of moisture content on large particles is smaller than on small particles because the cohesive forces are small compared to the gravitational forces.

One must distinguish the difference between the inherent moisture content of a solid and surface moisture. Many particles cannot return to the same conditions by adding moisture after drying. Similarly, drying the sample differs from starting with a sample with a lower moisture content. Adding surface moisture has the biggest impact on the flowability, tremendously enhancing the liquid bridge formation. Studies addressing the effect of moisture content often consider external sources for moisturising of samples in question, e.g. by adding and mixing with water (Bernhart & Fasina, 2009; Hann & Strazisar, 2007; Lu et al., 2018; Massaro-Sousa & Ferreira, 2019). Similarly, Jensen et al. (2004) let the samples dry to investigate the effect. Another method is placing the solid in a warm, humid climate chamber for an extended period (Fasina & Sokhansanj, 1993). Fitzpatrick et al. (2004) investigated the effect of moisture content by comparing powders with inherent moisture contents.

Bernhart and Fasina (2009) found that for poultry litter, the flowability decreases with increasing moisture content. Hann and Strazisar (2007) concluded that the moisture content is one of the most critical parameters determining the flowability of limestone powder, and even a slight increase can significantly decrease the flowability. Lu et al. (2018) investigated the effect of moisture on the flowability of pulverised coal. They observed that the flowability decreases with increasing moisture content. For spent coffee beans, the powders' flowabilities were not significantly affected by the moisture content (Massaro-Sousa & Ferreira, 2019). Jensen et al. (2004) studied the effect of moisture content on the

Table 2.1: Properties of pellets

	Factor	Wu et al. (2011)	Stasiak et al. (2019)	Mattsson (1990)	Craven et al. (2015)	Hinterreiter et al. (2012)	Fasina and Sokhansanj (1993)	Schwedes and Schulze (2013)	Schwedes and Schulze (2022)	Miller (2013)
Pellet Type	-	Wood	Wood	Wood	Wood	Wood	Feed (Alfalfa)	Wood, straw	Waste Wood, RDF	Wood (A1)
Size	Diameter (mm)	6-12	6	12	6	7	6.7-10.1	6-8	8	8
	Length (mm)	10-20	8-30	15		18	5-15	-	10-25	3.15-40
Density	Bulk Density ($kg\,m^{-3}$)	500-650	-	-	650	773	580-670	-	550-615	600
	Particle Density ($kg\,m^{-3}$)	1100-1900	-	-	1260	-	-	-	-	-
	Compressibility (HR)	-	1.09	-	-	-	-	-	tested	-
	Moisture Content (% wb)	8-11	-	15	-	-	7-18	6-8	-	-
Flowability	FFc	-	-	-	6.12	-	-	-	-	-
	Angle of Internal Friction	33-43	26-30	-	35-40	-	23-27	-	-	-
	Effective Angle of Internal Friction	39-45	33-37	-	40-45	-	-	-	-	-
	Angle of Repose	32-41	-	35	-	-	27-34	-	33	-
Arching	Arching distance (mm)	-	-	30	-	29-35	-	-	-	-
	Arching Diameter	-	-	-	-	-	-	-	-	80
Wall friction	Tivar	11-13	-	-	15-18	-	-	-	-	-
	Steel	18-19	-	-	15-18	-	-	20-25	19-26	-
	Stainless steel	18-19	-	-	26-28	-	-	23-25	14-16	-

arching tendency of wood fuels made from tree residue and round wood. The authors discovered that increasing moisture content increases the tendency to bridge for most solid fuels. However, they found no significant correlation between the tendency to bridge and moisture content for solid fuels made from round wood. Similarly, Fitzpatrick et al. (2004) did not find a clear relationship between the moisture content of food powders and the flowability. Fasina and Sokhansanj (1993) observed that for feed pellets, AoR and angle of internal friction are increased with increasing moisture content. They found that the relationship between the angle of internal friction and moisture content is linear.

Among the studies in this field, the effect of particle size has seised the most attention. The Van der Waals forces are less dominant at larger particle sizes than gravity. Different authors, namely Bodhmage (2006), Hann and Strazisar (2007), Y. Liu et al. (2015), and Pachón-Morales et al. (2020), observed that a larger particle size increases the flowability of limestone powder, fine powders, biomass powder and pulverised coal, respectively. Craven et al. (2015) and Rezaei et al. (2016) found similar results with ground wood and wood chips, which have much larger particle sizes. In contrast, Fitzpatrick et al. (2004) did not find a clear relationship between the particle size of food powders and the flowability. Xu et al. (2019) showed that the AoR increases with an increasing particle size of torrefied biomass powder, indicating poorer flowability. In the study by Wu et al. (2011), increasing pellet diameter has no consistent effect on flowability.

Arching in the outlet of a hopper can develop due to two mechanisms: cohesive arching and mechanical arching. When cohesive arching is dominant, one would expect a larger particle size and, thus, better flowability to result in a smaller outlet diameter. However, when mechanical arching is dominant, an increase in particle size will most likely result in a larger required outlet diameter. In line with this, Hinterreiter et al. (2012) noted a positive relationship between the particle size and the tendency to bridge with materials such as wood chips, sawdust and pellets. The shape factor and length/diameter ratio are more important than the size, indicating that irregular, long and thin particles or pellets bridge more quickly. Jensen et al. (2004) found that the most critical indicator for the high arching tendency is the content of overlong (100mm+) particles.

Similarly, according to Mattsson (1990), the proportion of hooked, long and thin particles (high L/D ratio) mainly explains the tendency to bridge. A rule of thumb to prevent mechanical arching is to have an outlet diameter of 6-10x the maximum particle size for conical hoppers and 3-7x for wedge-shaped hoppers (Schulze, 2007). However, the results in the literature indicated a much smaller minimum outlet diameter for hoppers handling pellets. Ashour et al. (2017) determined that for pellet-like cylindrical particles, the long axis is oriented towards the centre of the outlet during flow. Therefore, the tendency to bridge is better explained by the diameter than the length of the pellets.

The particle size distribution also influences the flowability because a broader PSD results in more particle-particle contacts. Hann and Strazisar (2007) concluded that a tighter PSD improves flowability, even if that means a smaller mean particle size. They found that fines do not significantly impact up to 20% mass content. However, the influence increases steeply after that, with the mixture reaching similar unconfined yield strength as the fine fraction itself at about 40% fines content. Massaro-Sousa and Ferreira (2019) also noted the relatively poor flowability of mixtures containing more than 40% fines. Pachón-Morales et al. (2020) also found that wide PSDs can result in more cohesion because of the larger fraction of fine particles.

In contrast, Bodhmage (2006) found that small particles present in a powder could improve the flow. Sokhansanj (1996) found that the AoR increases with a higher fines content for feed pellets, indicating decreasing flowability. They found the relationship between the AoR and fines content is linear, with a fines concentration of 0 - 25%

The shape of particles is also an important factor in the flowability. Particle shape can be challenging to characterise. Popular metrics for pellets are the elongation or length/diameter ratio. Rezaei et al. (2016) found that the shape is more important in describing the flowability of ground wood than the size. In contrast, Bodhmage (2006), particle elongation and irregularity have less influence than particle size, but they agreed that longer and more irregular particles decrease flowability. According to Xu et al. (2019), the powder cohesion increases, and the flowability decreases when the aspect ratio deviates from 1 (elongated particles). Mellmann et al. (2014) and Pachón-Morales et al. (2020) also found that elongated powders are more cohesive and that the flowability for crushed grain products decreases as

the elongation increases, respectively. In contrast, Hann and Strazisar (2007) observed that particles with round edges, thus more regular particles, have poorer flowability because the particles have better contacts.

Not only the macroscopic shape of the particle is of influence, but the microscopic surface roughness also affects the flowability. Oshima et al. (1995) milled the same powder to the same mono-size with five different millers, allowing them to compare the shape and surface roughness. The surface roughness was more effective in explaining the flowability than the macroscopic shape. Guo et al. (2014) investigated the effect of surface roughness in biomass coal blends. The authors found that surface roughness was one of the most critical parameters in determining the AoR. Ray et al. (2020) measured surface roughness of corn stover samples and noticed significant variability. They hypothesised that increased surface roughness might lead to handling problems but emphasised that further research is required. Fitzpatrick et al. (2004) also noted that the influence of surface properties on flowability is interesting for further research.

The wall friction depends not only on the BSM but also on the wall material. Bernhart and Fasina (2009) found that the flow of poultry litter on a stainless steel surface was improved when the surface was mirror-finished or galvanised coated. Craven et al. (2015) and Wu et al. (2011) and Schwedes + Schulze measured the wall friction of pellets with different wall materials. The effect of the wall material is inconsistent. The friction with stainless steel was higher according to Wu et al. (2011) and Craven et al. (2015); however, according to Schwedes and Schulze (2013), the stainless steel wall material either had no effect on the wall friction or the friction decreased compared to normal steel. Furthermore, using a Tivar lining improved the wall friction in the tests of Wu et al. (2011), but it had no effect in Craven et al. (2015).

The ambient conditions, especially the relative humidity and temperature (and thus also the temperature of the bulk solid), also affect the flowability. The temperature in large silos filled with wood pellets can reach 65-70 °C (Larsson et al., 2012). Teunou and Fitzpatrick (1999) investigated this effect for different food powders, e.g., flour, tea, and whey permeate. The flowability of flour increased with increasing temperature, while it decreased for the two other powders. The flowability of all powders decreases with increasing relative humidity. Other bulk solids, such as sulfur pellets, can show powerful time consolidation effects depending on the storage temperature (Schulze, 2007).

Many researchers do not use shear cell measurements to classify the flowability but instead use the AoR and HR, e.g., Al-Hashemi and Al-Amoudi (2018), Kalman (2021), and Massaro-Sousa and Ferreira (2019). However, how well these results correlate to shear test results is unclear. The idea is that a poorer flowing bulk solid has a higher AoR. The HR tests assume that the bulk solid is loose in poor-flowing solids because of the influence of interparticle adhesive forces. It assumes, therefore, that poor-flowing bulk solids are more compressible. Table 2.2 gives an overview of the flowability based on (Al-Hashemi & Al-Amoudi, 2018; Kalman, 2021; Schulze, 2007). Kalman (2021) compared the Hausner Ratio and flowability of spheres experimentally and found similar results to the table. No published material is addressing the comparison between the flowability, Hausner Ratio and repose angle for pellets yet.

Table 2.2: Descriptions of flowability based on the Angle of Repose, Flow Factor and Hausner Ratio

Description	Angle of Repose	Flow Factor	Hausner Ratio
Very free-flowing	<30°		1.00-1.11
Free-flowing	30-38°	>10	1.12-1.18
Fair	38-45°	4-10	1.19-1.25
passable			1.26-1.34
Cohesive	45-55°	2-4	1.35-1.45
Very cohesive	>55°	1-2	1.46-1.59
No flow		<1	>1.59

2.2.2. Effect of Pressurization of Lock-Hopper on Flowability

The pressure in the lock hopper is increased to obtain the same pressure as in the gasification reactor. First, the silo is filled with the BSM, then pressure is increased. The pressurization causes a pressure

gradient. The larger the pressurization rate, the larger the pressure gradient. The pressure gradient causes consolidation of the BSM, therefore, decreasing its flowability compared to a non-pressurized silo (Wiese & Schwedes, 1991). The consolidation is caused by the pressure gradient, not by the absolute pressure. Therefore, only the pressurization rate and not the final tank pressure influences the flowability (Shen et al., 2022).

Shen et al. (2022) found that for pulverized coal, the material is compressed when the silo is pressurized. However, for pulverized coal with a Sauter mean diameter greater than 45 um, the compression effect is significantly reduced.

Wiese and Schwedes (1991) investigated limestone and pulverized coal. They found that the stress in the incompressible limestone caused by pressurization is very similar to that of compressive strength. Thus, concluding that it led to the consolidation of the material. For compressible BSMs, such as coal, the inertial forces due to the particle motion also play an important role. They derived an equation, neglecting the inertial forces, to calculate the stresses caused by pressurization in incompressible bulk solids. In contrast to Shen et al. (2022), they noted increasing consolidation effects with higher gas pressure. They do agree that a lower pressurization rate and larger particle size decrease the consolidation effect.

Wiese and Schwedes (1993) presented a model to calculate the vertical stress acting during pressurization under the assumption that the porosity is constant.

Luo et al. (2023) measured the flowability of coal, flour and glass powders after no pressurization, 14kPa/s and 36kPa/s pressurization rates and found decreases in flowability of 10 to 25%, with the smallest decrease for the glass powder and largest for the compressible coal powder.

2.3. Predicting Flowability by Using Pellet and BSM Properties

The relationships between the bulk solid properties and their flowability may be used to predict flowability by only measuring other properties. This can be advantageous when the measurements of these properties are cheaper than directly measuring the flowability while maintaining sufficient accuracy. In the case of pellets, measurements of properties such as chemical composition, length, diameter, roughness, density and mechanical durability may be used to predict flowability.

2.3.1. Methods for Causal Analysis

To investigate a phenomenon, a scientist may vary an independent variable and measures the dependent variable while controlling all other variables. However, controlling all variables is not always possible. In the case of pellets, many confounding variables and parameters affect both the independent and dependent variables. For instance, changing the chemical compositions alters the surface roughness and the particle length distribution, and all three factors can affect the flowability.

Predicting flowability can be accompanied by a classification problem. For example, Sousa et al. (2022) and Valente et al. (2020) developed a computational model to classify the flowability of metal powder, given its particle-level physical properties. They used a decision tree to solve the classification problem. Classification is a classical problem in machine learning and data mining (Tsang et al., 2011), and due to its applicability, much research considering the problem has been published. Jain et al. (2000) presented a literature review on classifiers. Xiu et al. (2020) used the k-means clustering method alongside statistical multi-variable regression analysis to quantify the relation between flowability and particle geometry. Sandler and Wilson (2010) used partial least squares modelling to predict flowability based on size and shape distribution. Other models to divulge the patterns in the data comprise regression and various machine learning models.

A good workflow will have several models compared using cross-validation rather than relying on only one initially. It may sometimes be worth a slight tradeoff in cross-validation predicted accuracy for a better explanatory power while comparing two candidate models. However, any method will have difficulties when there are few samples relative to features (also called measurement, variable, and dimensionality (Foley, 1972)).

Table 2.3: Methods used in the literature investigating the flow behaviour of bulk solid materials

Paper	Materials	Samples	Features	Linear	Interactions	Method
Hann and Strazisar (2007)	1	58	4	No	No	Plots
Xu et al. (2019)	4	4*6	1	No	No	Plots
Y. Liu et al. (2015)	1	7	1	No	No	Plots
Oshima et al. (1995)	1	5	1	No	No	Plots
Fasina and Sokhansanj (1993)	4	4*4	1	No	No	Plots
Bodhmage (2006)	6	6	2	No	No	Plots
Fitzpatrick et al. (2004)	13	13	3	No	No	Plots
Pachón-Morales et al. (2020)	3	3*2	3	No	Yes	Power law
Rezaei et al. (2016)	2	7 (4+3)	2	No	No	Power law
Massaro-Sousa and Ferreira (2019)	1	21	2	No	No	Empirical Relationships
Jensen et al. (2004)	4	25	5	Yes	Yes	Linear Regression
Hinterreiter et al. (2012)	76	76	7	Yes	Yes	Linear Regression
Bernhart and Fasina (2009)	1	6	1	Yes	No	Linear Regression
Zafari and Kianmehr (2014)	1	29	4	No	Yes	Response Surface
Kamperidou (2022)	20	20	8	Yes	No	Pearson Correlation
Sandler and Wilson (2010)	3	73	4	Yes	Yes	Partial Least Squares

2.3.2. Improving the Sample-to-Feature Ratio

Insufficient samples can lead to the issue of overfitting. A commonly recommended guideline is to maintain a sample-to-feature ratio of at least ten (Hastie & Tibshirani, 2003; Wagner & Rondinelli, 2016). Achieving an appropriate sample-to-feature ratio can involve increasing sample size or decreasing the number of features. In fields like material sciences, where data can be scarce, there's often a limited number of samples available (Wagner & Rondinelli, 2016). Reducing the number of features is referred to as feature selection, with the initial step being rooted in the scientist's domain knowledge. Subsequently, various data-driven approaches exist to further pare down the features.

2.3.3. Methods of Causal Analysis in Flowability Research

The literature presented in this section on the relationships between material properties and flowability used different methods to analyse their data, including plotting the variables of interest and studying the results in this way or finding mathematical relationships by using, for example, regression.

Hann and Strazisar (2007) manually selected the features based on literature research in their analysis of limestone powder. They could vary one feature at a time while controlling the other variables and measuring the unconfined yield strength. They plotted the results in a 2D graph to study the effects. Xu et al. (2019) used a similar approach to analyse different biomass powders. Using a similar method, Y. Liu et al. (2015) sieved pulverised coal to obtain different mean sizes whereby investigating the effect of the particle size. They were thus able to reliably study the effect of the particle size on the flowability. Lu et al. (2018) sprayed pulverised coal with water to vary the moisture content. They then plotted the moisture content against different flow indicators. Oshima et al. (1995) grounded the same powder with different mills, resulting in different shapes, and plotted the effects of features such as circularity on the flowability. Fasina and Sokhansanj (1993) varied the moisture contents of different Alfalfa pellets and depicted the moisture content against the Angle of Repose. Linear fits were carried out to relate the AoR to moisture content.

Bodhmage (2006) pursued a similar approach of plotting the dependent and independent variables to study the relationship between features such as particle size (distribution), shape and flowability. They also selected the features based on a literature review. However, they used different powders to vary the features and thus could not control all other variables in the experiments. Therefore, their

graphs are a 2d projection of a higher dimensional graph and do not show all the information. This approach requires much interpretation by the author in explaining the results and is vulnerable to bias. Fitzpatrick et al. (2004) also plot different powders in the same graph to study the relationship between the moisture content, particle size and flowability. Outliers are present that may be caused by other variables, such as surface properties, that are not kept constant because of being a different powder.

Pachón-Morales et al. (2020) used power law equations to correlate particle characteristics (mean particle size, span of PSD, mean aspect ratio) to various flowability indicators. They found relationships consistent with the data but noted that not all potential influences of other particle properties and process conditions were assessed. Therefore, the relationships found probably do not generalize well to other powders. According to the authors, for example, torrification of the powder is likely to alter the surface properties of the powder. Rezaei et al. (2016) also chose a power-law relationship to fit the Hausner Ratio as a function of grinder screen size. The model parameters were determined using the Levenberg-Marquardt nonlinear regression method.

Massaro-Sousa and Ferreira (2019) used a one-way analysis of variance based on Tukey's test to verify whether there were any statistically significant differences between the means of the different bulk densities and flow properties. Empirical equations were fitted to the data using Excel.

Using the SAS statistical package, Jensen et al. (2004) used a multi-linear regression model to evaluate the impact of solid fuel characteristics on arching properties. The influence of other variables, such as moisture content and bed depth, is tested with linear regression. Hinterreiter et al. (2012) used a multi-linear regression model to evaluate the impact of solid fuel characteristics on the arching properties using the SAS statistical package. After testing the impact of different fuel characteristics, the most crucial input variables were included: bulk density, moisture content, particle size, mean LD, shape factor, RGHN and interquartile distance. All possible pairwise interactions were also considered.

Bernhart and Fasina (2009) tested variables for statistical significance using the analysis of variance in SAS statistical Software. Linear regression and the package's nonlinear Proc NLIN function were exercised to conduct regression analysis on the bulk density, tapped density, particle density, compressibility, equilibrium moisture and flow data. Zafari and Kianmehr (2014) analysed the factors affecting the mechanical properties of biomass pellets. They used a response surface methodology based on the Box-Behken design. Kamperidou (2022) investigated the relationships between pellet properties using (linear) Pearson correlation coefficients.

2.4. Conclusion

Extensive literature research was conducted to discover which factors influence the flowability of pellets. No research explicitly investigated this for pellets, therefore, we considered the literature of BSM flowability in general and found that the following factors are recognized as large influences on the flowability of the BSM:

- Moisture Content
- Particle Size (Distribution), including fines content
- Particle Shape
- Surface Roughness
- Pressurization rate in lock-hoppers
- Chemical Composition

Furthermore, HR and AoR are often used as an alternative to shear testing.

The literature that measures the BSM properties of pellets, including the flowability and arching tendency, focuses almost exclusively on wood pellets, thus ignoring RDF pellets. Furthermore, the studies do not investigate the effect of the aforementioned properties on the flowability of the pellets. For example, no studies have compared the surface roughness of pellets and their flowability yet. Also, no studies investigated the feasibility of using the HR and AoR as an alternative for shear testing for

pellets. Therefore, it is necessary to determine the pellet and BSM (flow) properties, including the AoR and HR, for WW, FW and RDF pellets.

3

Experimental Setup

In this chapter, we present the experimental setup and methodologies. Figure 3.1 reveals a flowchart and work breakdown concerning the design experiments, including setup and methods.

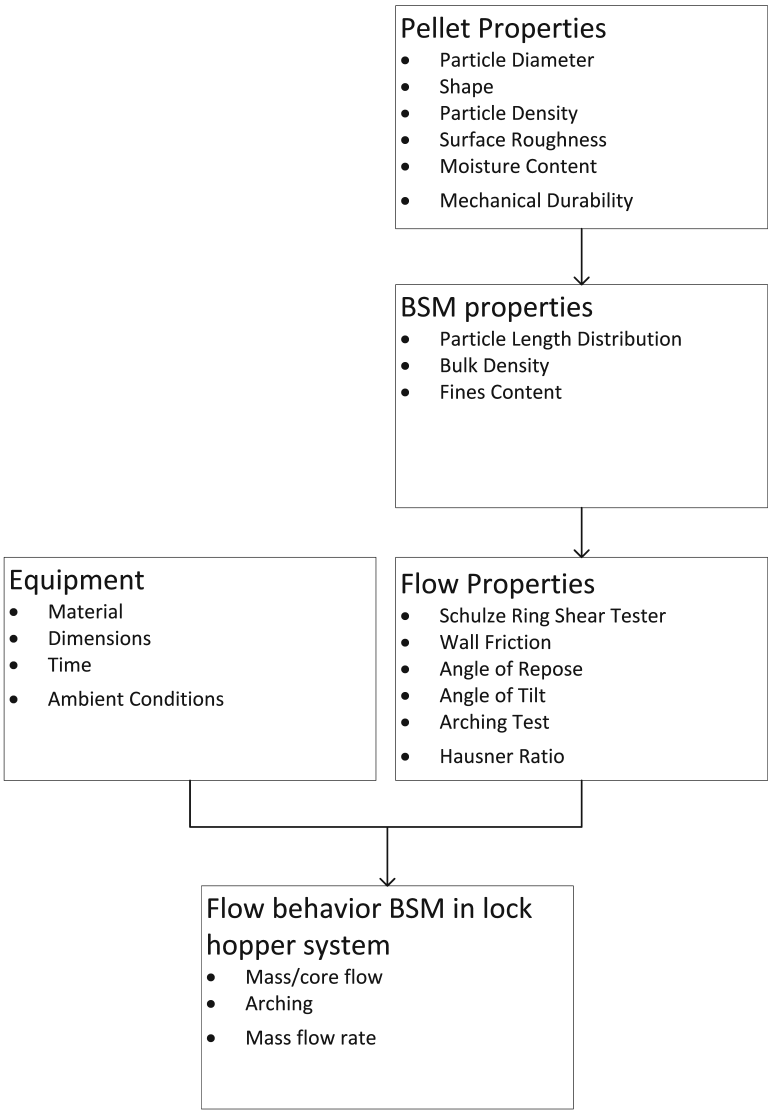

Figure 3.1: flowchart experimental setup

3.1. Methodology

To investigate the gap in the literature on the properties and flowability of different pellet types, we present an experimental plan to measure these properties. Not all factors identified in the previous chapter must be investigated because they are not relevant to the scope of HTW gasification material handling. Most notably, the investigation of the impact of moisture content on the flowability is unnecessary because the pellets are stored in environmentally-controlled atmospheres, thus the surface moisture content will never increase significantly.

Secondly, the effect of a varying particle length is not investigated due to time constraints. It is likely that this effect is minor because the difference in relative size is very small compared to, for example, powders.

The effect of PSD is very important due to the mechanical degradation of pellets during handling. The fines content can be varied while keeping all other variables constant. Measuring the flowability, and a range of flow indicators, such as AoR, AoT and HR, with varying fines contents allows the study of relationships between the flow indicators and flowability.

Many pellet properties are also measured, such as surface roughness and pellet density. Due to the (time) costs of sample collection, only a few samples can be collected during this research. Therefore, many models for casual analysis are unfeasible because they would overfit the data. It is also impossible to find relationships between the pellet properties and flowability when only studying three pellets because of the number of uncontrollable/confounding variables.

3.1.1. Methods for determining pellet properties

Determination of Pellet Diameter

The pellet diameters are measured according to ISO 17829. The diameter is measured perpendicular to the axis using a digital calliper with a resolution of 0.1 mm and a reported accuracy of ±0.2 mm. The test portion should be free of fines (<3.15 mm) and consist of at least ten pellets. In this research, the test portion consists of 20 pellets.

Figure 3.2: Tumbler 1000+ produced by Institut fuer Bioenergie with fines created by testing waste wood pellets

Determination of Mechanical Durability

The mechanical durability of pellets is determined according to ISO 17831-1 (EN 15210-1), using the tumbling can method. The device used is the Tumbler 1000+ produced by Institut fuer Bioenergie; see Figure 3.2. 500 ± 10 g of pellets are weighted accurately after being sieved by a 3.15 mm round hole sieve. This mass of pellets is called the mass before m_b. Following this, the sampled material is placed

in the tumbling can, which is rotated 500 times in 10 minutes. Afterwards, the sample is sieved and weighted to obtain mass after m_a. Finally, the mechanical durability is obtained using equation 3.1.

$$DU = \frac{m_a}{m_b} \times 100\% \tag{3.1}$$

Determination of Pellet Density

Pellets usually have one concave end and one convex end, Figure 3.3. In order to measure the volume accurately with a calliper, the concave and convex ends are first filed flat to obtain a cylinder, similar to Gilvari (2021). Then the particles are weighted using a scale with a resolution of 0.001 g and an accuracy of +-0.005 g. The calliper has an accuracy of ±0.2 mm. The accuracy of the pellet density is ±7% or about ±75 kg m^{-3}; see Equation 3.2 for an example calculation. Non-perfect cylindrical shapes of the pellets also reduce the accuracy of the volume determination.

$$\rho = \frac{m}{V} = \frac{m}{lD^2\frac{\pi}{4}} \tag{3.2}$$

$$\rho = \frac{891 \pm 1\%}{15.3 \pm 1\% * (8.1 \pm 2\%)^2 * \frac{\pi}{4}} \tag{3.3}$$

$$\rho = 1130 \pm 7\% kg/m^3 = 1130 \pm 76 kg/m^3 \tag{3.4}$$

Figure 3.3: Pellets with their convex and concave ends, and one filed flat

Figure 3.4: Determination of Particle Density

Determination of Surface Roughness

The surface roughness of pellets can be measured with a surface profilometer (Figure 3.5), namely the Rugosurf20 manufactured by Tesa. The Rugosurf20 measures the roughness according to the ISO 3274 and ISO 4287 standards. The Rugosurf20 traces a diamond tip along the surface and has a measurement range of 400 um in the z-direction. The roughness of the pellets can exceed this range with the presence of cracks or large particles present in the pellet.

The surface roughness is measured along the length of the pellet for at least 15 randomly selected pellets, similar to Kamperidou (2022). The surface roughness of a material cannot be characterized by a single parameter. Widely used parameters in studies concerning wood-based products are the Ra (arithmetic

average of profile height deviations from the mean), Rq (rms of profile height deviations from the mean) and Rz (mean peak-to-valley height) (Kamperidou, 2022). The precision of the measurement is in accordance with ISO 3274 class 1.

Figure 3.5: Determination of Surface Roughness

3.1.2. Methods for determining BSM properties

Determination of Bulk Density

The bulk density is determined based on ISO 17828. A 5 l stainless steel container is filled with pellets from a height of 200 - 300 mm above the upper rim. The container is then dropped three times from a height of 150 mm on a wooden board to allow settling. Surplus material is removed before measuring the mass of the pellets. The procedure must be repeated three times. The accuracy is according to the standard ±2%. The result must be reported to the nearest 10 kg m^{-3}.

Determination of Pellet Length Distribution

The pellet lengths are determined according to the standard ISO 17829 using a digital calliper with a resolution of 0.1 mm. The length of 50 pellets is measured along their axis. The particles are distributed according to their length, which, assuming constant diameter and density, equals distribution according to mass. Alternative methods to determine the Pellet Length Distribution use cameras and software for automation (Gilvari, 2021; Toscano et al., 2022). This saves time compared to the manual method. However, in this research, the manual method is chosen because the potential time saving would probably not outweigh the time cost of setting up the automatic method. The accuracy of the measuring device is ±0.2 mm.

Determination of Particle Size Distribution Fines

The PSD of the fines is determined using sieves. The used sieve has square holes with sizes from 3.15 mm to 0.18 mm. According to ASTM C136, the size of the test samples is 300 g minimum. Here, a mechanical sieve shaker manufactured by Haver and Boecker is used. The mass in each sieve is measured with a laboratory scale with a resolution of 0.1 g.

3.1.3. Methods for determining BSM flowability

Different testers for measuring the flowability of bulk solids have been developed over the years. Most of these tests lack essential qualities in order to be considered as quantitative methods (Schulze, 2007). Only quantitative tests can be used to quantify the friction angles of the bulk solid and subsequently use the results for equipment design. Other tests are often called comparative tests. Comparative tests

are only useful to compare two bulk solids tested with the same test apparatus, e.g., periodic control of the feedstock.

A quantitative tester must have a consolidation procedure, where steady-state flow is reached with subsequent measurement of strength. The load direction during consolidation and strength measurement must be similar. Also, a quantitative tester requires the stresses in the failure plane to be known. Further, the stress distribution must be homogeneous so that the sample is consolidated equally. A good tester should also eliminate the influence of the operator with a well-described test procedure. (Schulze, 2007)

Determination of Flow Properties

The flow properties of the bulk material are evaluated with the *Schulze Ring Shear Tester* (RST), according to ASTM D6773-22 and according to the manuals belonging to the RST.

The RST, see Figure 3.6, contains the sample in an annular cell. The normal force is applied on the cell through a roughened lid. The sample is sheared by rotating the shear cell relative to the lid. The torque required for shearing is measured.

The sample is first presheared with a certain normal force and resulting torque. This procedure removes the stress history of the sample and consolidates it with the desired stress. Then the sample is sheared to failure, so a yield locus can be made.

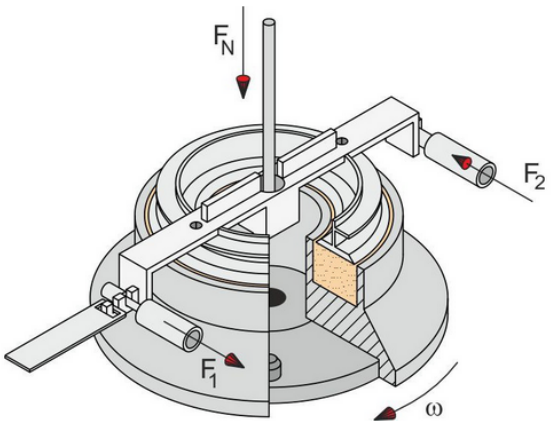

Figure 3.6: The Schulze Ring Shear Tester (Schulze, 2007)

The shear cell is overfilled with the pellets, and surplus pellets are removed using a blade. Any large holes created by digging pellets are filled up again. Then, the shear cell is weighted using a laboratory scale accurate to 0.1 g and placed on the machine. The lid must be placed gently onto the sample, and the hanger, counterweight, and tie rods must be attached. When the test has been completed, the shear cell is removed, and the fines content is measured.

After completion of the test, a yield locus can be approximated using either "straight-sections" or a regression line. Shear points that lie roughly on a straight line can be approximated by a regression line, but when the shear points show a curve, straight sections must be used.

There are a few indicators that the measured yield locus is unrealistic:

- The yield locus is bent upwards.
- The yield locus intersects the sigma-axis at positive values.
- Yield loci with different normal loads at preshear intersect.
- The preshear point is located above the yield locus.

In these cases, the test results should be discarded, and the measurement should be repeated.

For the measurements using the RST, the width of the annulus must be 20 times larger than the particle size according to the standards. When this requirement is not met, it may be inaccurate to consider the

particles as a continuum. In order to comply with this requirement, Craven et al. (2015) and Wu et al. (2011) used a large-scale annular shear tester. However, Stasiak et al. (2019) used a shear tester with an outer diameter of 195 mm and an inner diameter of 100 mm, which was too small. Their results do still seem reasonable. This agrees with Barletta et al. (2015), who found that for wood chips, the ring shear tester can be used to obtain accurate results on the flowability, even though the particles are officially too large for the tester. However, the wall friction results were lower than with the larger tester, which can result in under-designed equipment. Wang et al. (2022) investigated experimentally the effect of shear cell size on the flowability of powders and found that using a small shear tester could result in 15% higher FFc values, even with particle sizes substantially lower than the recommended values. Furthermore, they pointed out the poor reproducibility of the tests when the particles were large. ASTM D6773-08 notes that a smaller shear cell can result in higher measured shear strengths and, thus, somewhat larger unconfined yield strengths. This results in a more conservative design.

Determination of Wall Friction

The wall friction of the bulk material is evaluated with the Schulze Ring Shear Tester, according to ASTM D6773-22 and according to the manuals belonging to the RST. The wall material is cold-rolled steel, as recommended by Schwedes + Schulze in their report.

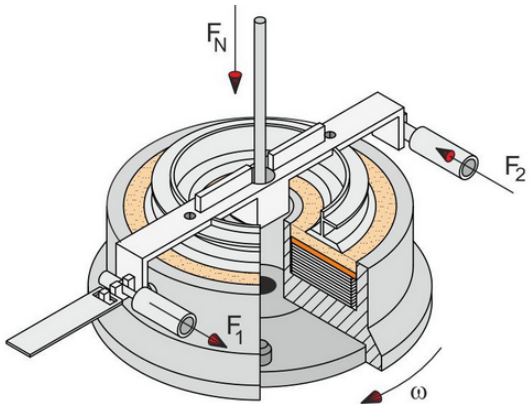

Figure 3.7: The Schulze Ring Shear Tester for Wall Friction (Schulze, 2007)

The test procedure for determining the wall friction is similar to the one used for assessing the flowability. Only the shear cell used for the wall friction test differs; see Figure 3.7. The wall specimen is below the bulk solid, just like the situation in a real hopper. This is important because, for segregating materials such as fines in pellets, the concentrations will be different at the top and bottom of the material.

The shear cell is filled with spacers, the wall material sample and the bulk solid material and a normal force is exerted on the material by the lid. The shear cell is rotated, the bulk solid is shifted across the surface of the wall material sample, and the torque is measured. After steady-state is achieved, the normal force is lowered so that the wall yield locus can be approximated.

The wall friction test is designed for particles up to 10 mm. The distance between the wall material sample and the lid must be 8 to 10 mm. Because the pellets are longer than 10 mm, larger distances between the sample and lid were experimented with. However, a larger distance between the lid and wall sample made the pellets move between the lid and the side of the shear cell, causing very large deviations in the results. Furthermore, the results obtained with a filling height of 8 mm are closer to the results reported by Schwedes + Schulze using the same pellets and wall material. It is still possible with a filling height of 8 mm that pellets accumulate in certain parts of the cell or get stuck between the lid and side wall. Therefore, the shear cell must be visually inspected after each test, and any tests showing these issues must be discarded and repeated.

Determination of Angle of Repose

The angle of repose test is a popular comparative test because of its simplicity and the ease of interpretation of the results. Different AoR test procedures exist; see Figure 3.8. The measured AoR

depends on the chosen test procedure, which is why it is not a material property. During these tests, the bulk solid is not consolidated; thereby offering little insight into the flow within the silo. Hinterreiter et al. (2012) found that the angle of repose was not very sensitive to the fuel properties and that the variation between laboratories was higher than the variation between the angle of repose values for fine and coarse wood chips.

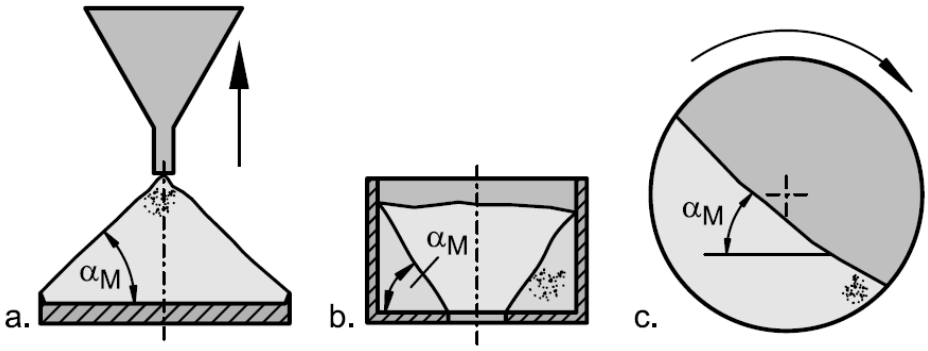

Figure 3.8: Angle of Repose test (Schulze, 2007)

The angle of repose is affected by three mechanisms (Kalman, 2021); see Figure 3.9. First, the wall sliding of the particles along the bottom wall is affected by the wall friction. Secondly, local avalanches are caused by individual particles rolling down the heap. Lastly, unstable shear surfaces within the heap which is affected by the internal friction of the material.

Only the last mechanism is of interest for the flowability of the material. Therefore, the AoR test uses edges on the bottom of the box to eliminate particles sliding along the bottom wall. The effect of local avalanches cannot be eliminated, but as recommended by Kalman (2021), we always take the largest angle in the heap to minimize the effect of recent local avalanches.

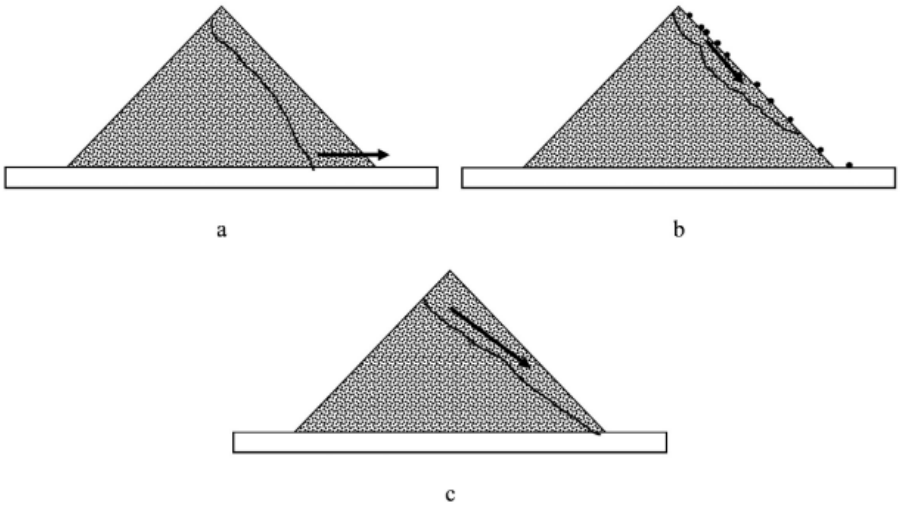

Figure 3.9: Mechanisms affecting the angle of repose (Kalman, 2021)

The angle of repose depends on the distance between the sides of the box, because of the formation of arches between the walls. A numerical investigation showed that the angle of repose no longer depends on the depth when the depth is at least 13 times the particle size (Zhou et al., 2001). We compared the AoR with a box depth of 50 mm and a depth of 120 mm. The top of the heap was steeper for the smaller box depth, likely caused by arching behaviour. The angle of the lower part of the heap is virtually identical. Therefore, a box depth of 120 mm is used for the experiments. This is more than 13 times the pellet diameter but much less than 13 times the maximum pellet length.

Determination of Angle of Tilt

A second angle of repose test is called the angle of tilt test (Figure 3.10). Kalman (2021) describes the angle of tilt test in detail. A box is placed on a tilting plane and filled to the brim with pellets. The angle at which a significant flow of material occurs is defined as the tilting angle. The tilting angle is not affected by wall sliding and local avalanches, making it theoretically superior to the angle of repose in predicting flowability. However, the material is not consolidated.

Figure 3.10: Angle of tilt test device. Left no flow, right flow

The inclinometer has an accuracy of 0.3°. A greater source of inaccuracy is the determination of the moment flow starts. The operator of the test must discern between local avalanches and flow due to unstable shear surfaces.

Determination of Hausner Ratio

Compressibility tests are also popular tests to define the flowability of bulk materials. Similar to the AoR and AoT tests, compressibility tests are performed under very low stresses and without consolidation. Therefore, the test is comparative.

The bulk density depends on the particle packing. The void ratio is the ratio of empty space, usually air, to solid in a bulk solid. A tighter packing of the material will result in a lower void ratio and, thus, a higher bulk density. The compressibility tests assume that in poor-flowing solids, the bulk solid has a relatively large void ratio because of the influence of interparticle cohesive forces. Therefore, after initial filling, the void ratio can be reduced significantly by tapping the container. The Hausner Ratio is a measure of the compressibility of a bulk solid and is calculated with Equation 3.5, where ρ_t is the tapped bulk density and ρ_b the untapped or loose bulk density.

$$HR = \frac{\rho_t}{\rho_b} \tag{3.5}$$

Igathinathane et al. (2010) measured the tapped bulk density of pellets using glass beakers. The beakers were dropped 50 times on a wooden surface from a height of 20 mm. This resulted in a stable, settled state of pellets. The measurements were repeated five times. Stasiak et al. (2019) determined the tapped bulk density of pellets by tapping a cylinder with another cylinder vertically 180 times.

In this research, a 1000 ml plastic measuring cylinder, shown in Figure 3.11, is used. The bulk solid is poured in from a height of approximately 100 mm above the brim of the cylinder. The filled cylinder is weighted with a laboratory balance accurate to 0.1 g (Kern EMS). The volume is read to the nearest 5 ml. Then the cylinder is placed on a mechanical sieving device, where it is vibrated with an amplitude of 3 mm during a period of 1 minute. Salehi et al. (2019) also used a vibrating sieve shaker for the HR

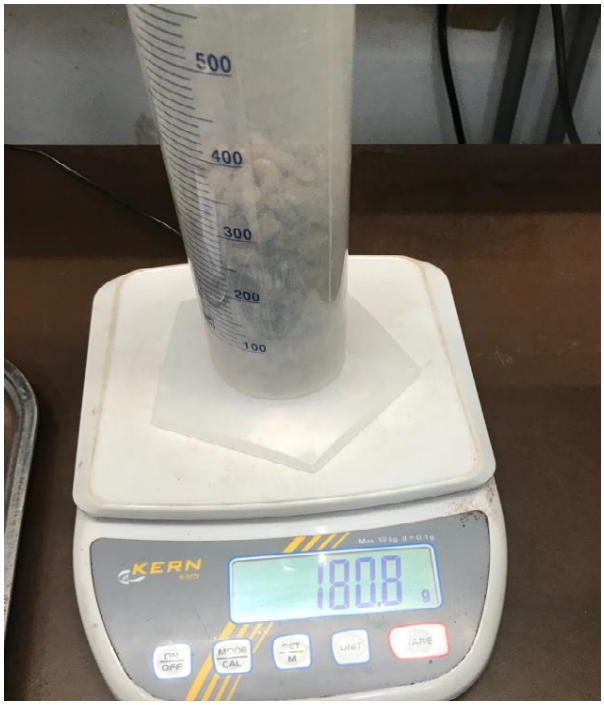

Figure 3.11: Tapped Density Test Setup

test. This results in a volume that cannot be reduced further by tapping or dropping the cylinder. This method is much more consistent than manually dropping the cylinder.

The accuracy of the determination of the volume is ±10 ml. This leads to an accuracy of the HR ratio of about ±2% or 0.03, see Equation 3.6.

$$HR = \frac{\rho_t}{\rho_b} = \frac{1000 \pm 10}{800 \pm 10} = \frac{1000 \pm 1\%}{800 \pm 1\%} = 1.25 \pm 2\% = 1.25 \pm 0.03 \tag{3.6}$$

Determination of Arching Diameter

The arching or bridging test is a relatively popular test for evaluating biomass bulk solids. Two types of arching tests exist; see Figure 3.12. The first test is a funnel test where the outlet diameter is increased until the bulk material flows. Often, the mass flow is measured, too. The second test uses a widening slot that increases the arching distance until flow of the BSM is achieved. Typically, the outlet diameter of a conical hopper is about twice as large as the outlet of a wedge-shaped hopper (Schulze, 2007).

Arching tests cannot be used to quantify the flowability of the bulk solid. They can only give a comparative statement about the arching distance. The arching distance depends significantly on the filling height. An increase in filling height generally leads to increased opening width (Mattsson, 1990). Therefore, the arching test filling height must correspond to the actual conditions. The flow regime may also affect the measurement (Schulze, 2007). Since the flow regime is a function of the solid and equipment, such as wall material and angle, a quantitative statement about the arching distance can only be made if the wall material and hopper angle are equal to the final product. A tester with filling height, wall material, and hopper angle equal to the final product is thus not feasible.

The arching tester used in this research consists of plastic cylinders with a round hole, the "outlet", in the middle. The outlets vary from 30 to 110 mm with 10 mm intervals. The pellets are placed in a hollow cylinder and placed on top of the outlet. A thin plastic sheet is placed between the outlet and cylinder and quickly removed to simulate the opening of the outlet.

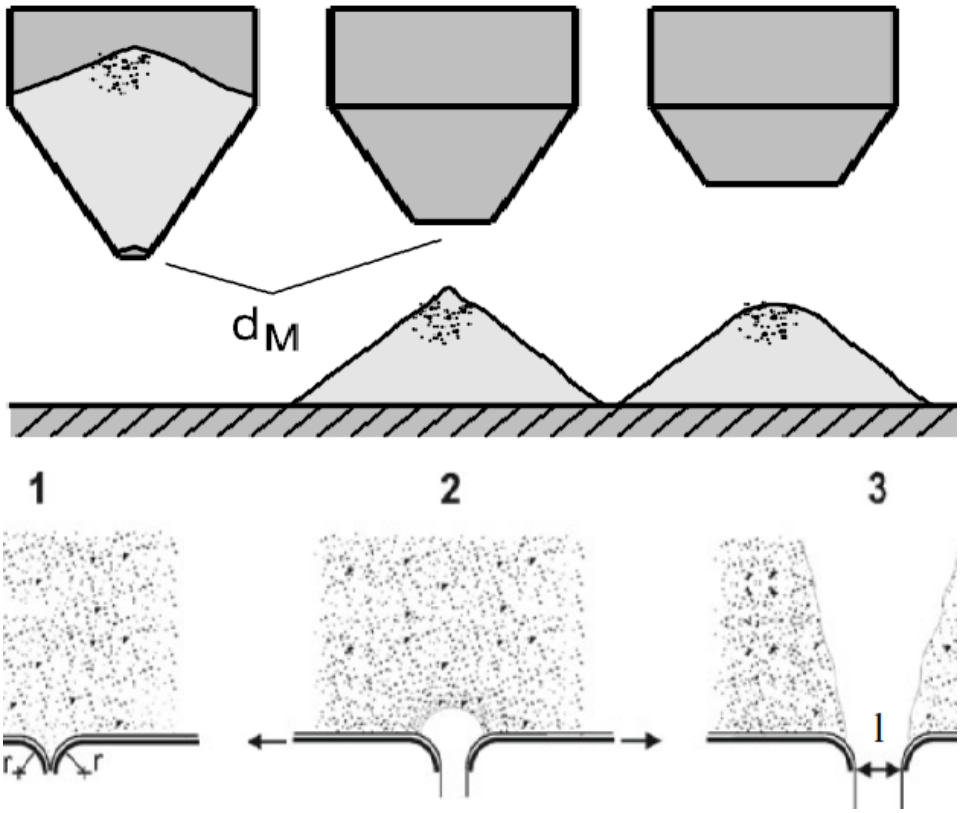

Figure 3.12: Two different arching tests (Schulze, 2007)

3.1.4. Methods for calculating BSM flow behaviour in lock hopper

Calculation of stresses in silo

The stresses in the silo depend on the silo geometry, wall material, and the bulk solid material. The silo geometry depends on the bulk solid material, wall material and the stresses in the hopper. This relationship between the stresses, geometry and bulk solid makes designing a silo an iterative process.

The stresses in a hopper differ during the filling state and discharging state. The filling state prevails when an empty silo has been filled, while the discharging state prevails when the material has been discharged (possibly during filling). During the discharge state, the material flows out in a convergent flow zone and is thus compressed horizontally. As a result, the larger stresses are oriented horizontally, and the material is supported more by the silo walls, resulting in higher wall normal stress and a lower vertical stress.

Most methods used to calculate stresses in silos divide the silo into horizontal slices. For each slice, a force equilibrium is considered, which comprises of the forces acting on the top and bottom of the slice, between the slice and the wall, and the weight of the slice. Alternative methods of calculating stresses are Finite Element Methods or DEM.

Janssen came up with the equation to calculate the stresses in the vertical part of the silo in 1895 (Janssen, 1895). These formulas are still used today, for example, in the European code EN1991-4 on the structural design of silos and tanks. Janssen considered a slice with an infinitesimal height dz; see Figure 3.13. He assumed that the vertical force acting on the slice is constant across the surface and that the bulk density rho is constant in the slice. Force equilibrium in the z-direction gives Equation 3.7:

$$\sigma_v A + g\rho_b dz = (\sigma_v + d\sigma_v)A + \tau_w U dz \tag{3.7}$$

Using the wall friction angle and the lateral stress ratio, this can be rewritten as Equation 3.8.

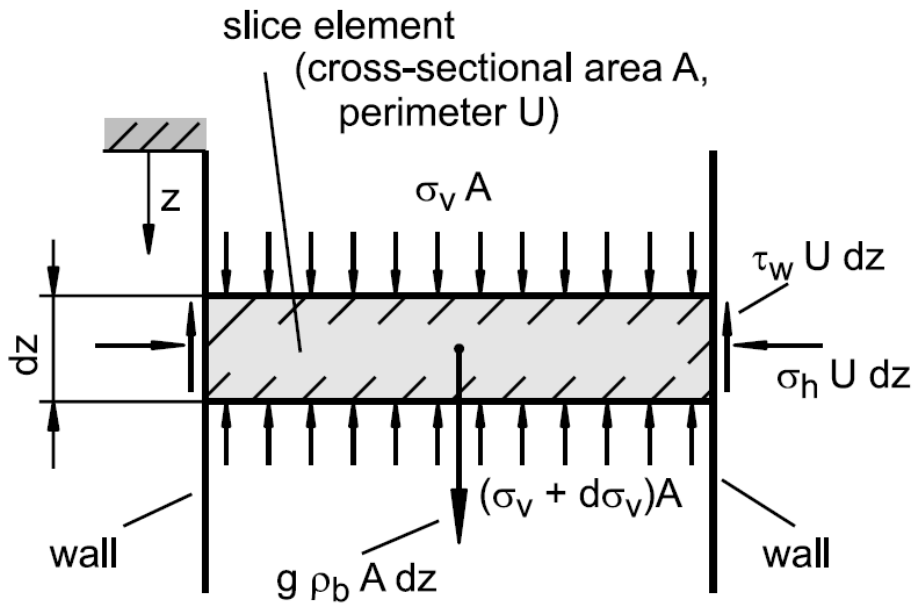

Figure 3.13: Force equilibrium of the slice used in Janssen's calculation (Schulze, 2007)

$$\sigma_v A + g\rho_b dz = (\sigma_v + d\sigma_v)A + K\sigma_v \tan\phi_x U dz \tag{3.8}$$

This can be simplified to obtain the differential Equation 3.9.

$$g\rho_b = \frac{A d\sigma_v}{dz} + K\sigma_v \tan\phi_x \frac{U}{A} \tag{3.9}$$

The stresses in the hopper during the filling state can be calculated as described by Motzkus (Motzkus, 1974).

The procedure of calculating the stresses in the hopper during the emptying state was derived by Jenike. Using design charts, the flow factor of the hopper is determined based on the angle of internal friction, wall friction and bulk density. The flow factor and the hopper flow factor are plotted. The intersection point gives the stress at the outlet and the minimum diameter. If there is no intersection, which is likely with a free-flowing solid such as pellets, the diameter of the outlet must be determined based on desired flow or to avoid mechanical arching. The stresses can then be determined.

The Silo Design Tool developed by Schulze automates these calculations and will be used in this research. This tool provides estimates for the vertical stresses and the stresses at the wall at any height in the silo.

The major principle stress at the outlet axis during filling conditions is oriented practically vertically. The major principal stress at the outlet axis during discharge can be estimated by assuming steady-state flow and by assuming that the horizontal and vertical stresses are the principal stresses. The stress ratio between the principle stresses is given by equation 3.10.

$$K_0 = \frac{\sigma_2}{\sigma_1} = \frac{1 - \sin\phi_e}{1 + \sin\phi_e} = \frac{\sigma_v}{\sigma_h} \tag{3.10}$$

Determination of Critical Outlet Diameter to Prevent Arching

The bulk solid will flow when the pressure in the hopper exceeds the unconfined yield strength, Equation 3.11.

$$\sigma_{1'} > \sigma_c \tag{3.11}$$

A stable arch in a hopper (Figure 3.14) is only possible when the stress in the arch does not exceed the unconfined yield strength. The stress in a stable arch is given by Equation 3.12, where m = 1 for conical hoppers.

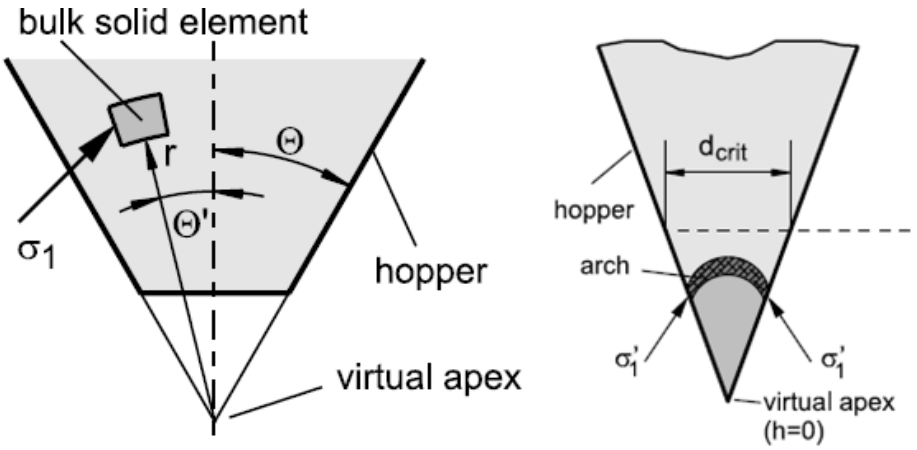

Figure 3.14: Hopper Coordinates and Stable Arch (Schulze, 2007)

$$\sigma_{1'} = \frac{2r \sin\theta g \rho_b}{1+m} \tag{3.12}$$

The flow factor depends on the hopper angle, bulk solid material and wall friction, and its intersection with the flow function gives the major stress in the arch, sigma1'. This critical value gives us the minimum outlet diameter by rearranging the previous equation.

$$d = 2r \sin\theta \tag{3.13}$$

$$d_{crit} = 2\frac{\sigma_{c,crit}}{g\rho_b} \tag{3.14}$$

Or, more exactly:

$$d_{crit} = H\frac{\sigma_{c,crit}}{g\rho_b} \tag{3.15}$$

Where H takes into account the hopper angle. The value of H can be looked up in design charts.

Fines content in lock hopper

During pellet handling, the pellets degrade physically. As a result, fines and dust are generated. Gilvari (2021) investigated the extent fines were found in handling equipment and found up to 15% fines in the bulk solid material. According to Ilic et al. (2018b), the fines content can even reach 25% in their installations. Even larger concentrations of fines may occur when segregation takes place. Mass flow is important to prevent segregation in silos.

After a certain amount of fines content in the BSM, the flowability is governed by the fines fraction. This is because the presence of pellets surrounded by fines has little influence (Schulze, 2007).

In the mechanical durability test, fines are defined as particles smaller than 3.15 mm. However, pellets do not only generate fines when handled but also lumps. Lumps are defined as particles larger than 3.15 mm and smaller than 5.6 mm (Gilvari, 2021). Figure 3.16 shows the difference between pellets, fines and lumps. The ratio of fines and lumps depends on the pellet type, especially the size of the material that is pressed into the pellet. Figure 3.15 shows the ratio for the pellets used in this research. Waste wood and fresh wood pellets comprise 1/3 lumps and 2/3 fines, while the RDF pellets break down

into 2/3 lumps and 1/3 fines. From here on, fine contents will refer to a mixture of fines and lumps according to the aforementioned ratios.

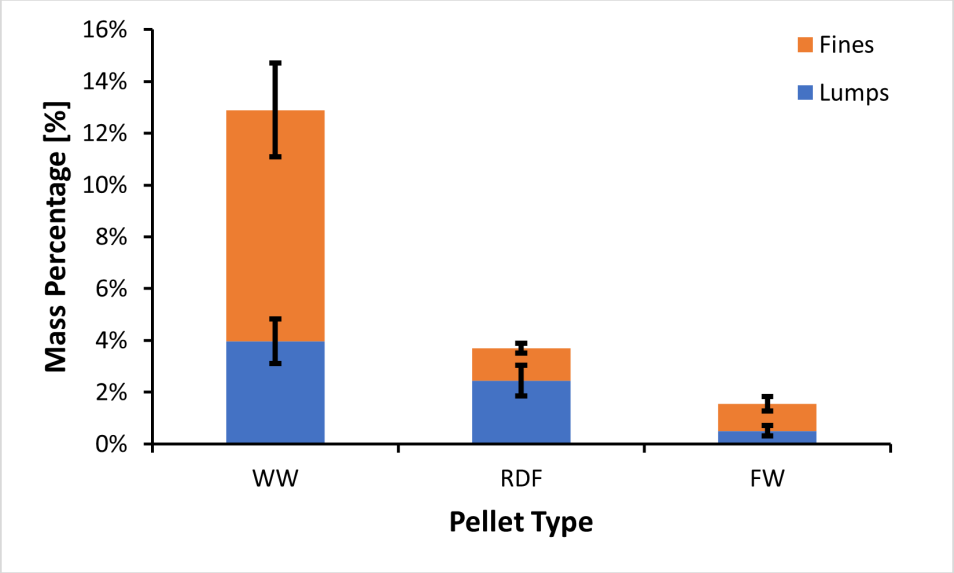

Figure 3.15: Ratio of Fines and Lumps Created by Mechanical Durability Test for the Three Pellet Types. Error Bars Show the Standard Deviation of the Measurements

All experiments are conducted at the following fines contents (fines + lumps): 0%, 10%, 20%, 30% and 100%. The tests at 100% fine content are expected to yield similar results to the 30% tests because the flowability is governed by the fines (Schulze, 2007).

The fines content is again measured after the test to account for the effects of potential segregation.

3.2. Experimental Plan

3.2.1. Material

Three pellets will be researched: fresh wood (Figure 3.22), waste wood (Figure 3.21) and refuse-derived fuel pellets (Figure 3.20). These pellets are realistic options for use in an HTW gasifier.

Due to the unreliability of waste streams, it is possible that not just one type of pellet is used but a mixture of 2 pellets. Therefore, the effect of mixing pellets on the flowability and wall friction is also investigated. Table 3.1 presents the mixtures. Figures 3.18 and 3.19 show the mixed pellets.

Table 3.1: The mass ratios of the mixtures of the three types of pellets investigated in this study

	RDF	WW	FW
Mixture 1	50%	50%	0%
Mixture 2	25%	75%	0%
Mixture 3	25%	0%	75%

Figure 3.16: From Left to Right: Waste Wood, RDF, Fresh Wood From Top to Bottom: Pellets, Lumps, Fines

Figure 3.17: Waste Wood, Fresh Wood and RDF Pellets at 30% Fines Content

Figure 3.18: Mixture of Fresh Wood and RDF Pellets

Figure 3.19: Mixture of Waste Wood and RDF Pellets

Figure 3.20: RDF Pellet

Figure 3.21: Waste Wood Pellet

Figure 3.22: Fresh Wood Pellet

3.2.2. Experimental Setup BSM properties and flowability

Table 3.2 presents an overview of the experimental plan. The samples are sieved before every experiment. After sieving, the desired amount of fines is added. After the experiments, the fines content is measured again.

Table 3.2: Experimental Plan

Experiment	Settings	Repetitions	Standard	Fine Content	Pellets
Pellet Properties					
Diameter	20 random pellets	1	ISO 17829	-	All
Density	-	10	-	-	All
Surface Roughness	-	15	ISO 3274/ISO 4287	-	All
Mech. Durability	500g, 500 rotations	3	ISO 17831-1	0%	No Mixture
Moisture Content	300g, 105°C, 24h	3	ISO 18134	0%	No Mixture
BSM properties					
PLD	50 random pellets	3	ISO 17829	0%	No Mixture
Bulk Density	5 l container	3	ISO 17828	0%	No Mixture
Shear Test	1250/10000 Pa Consolidation	2	ASTM D6773-22	0, 10, 20, 30, 100%	All, mixture only at 0% fines
Wall Friction Test	800/4400/8000 Pa Normal Stress	3	D6773-22	0, 10, 20, 30, 100%	All, mixture only at 0% fines
AoR	Ledge Test, 120 mm depth	3	-	0, 30%	No Mixture
AoT	-	3	-	0, 30%	No Mixture
HR	1000 ml plastic measuring cylinder	3	-	0, 30%	No Mixture
Arching Test	-	3	-	0%	No Mixture

4

Test Results

4.1. Introduction

This chapter presents the test results, providing an overview of the properties of the pellets and the bulk solid material. First, we show the pellet properties. Then we show and discuss the flow properties and the influence of fines.

4.2. Results and Discussion

All tests were conducted in the same laboratory. The ambient temperature varied from 17 to 24°C during the experiments. The relative humidity varied from 30 to 60%.

4.2.1. Pellet and bulk Properties

Table 4.1 presents the measured pellet properties.

Table 4.1: Properties of the pellets used in this research with the 95% CI where applicable

Sample	Diameter (mm)	Mean Length (mm)	L/D ratio (-)	Mechanical Durability (%)	Surface Roughness Rq (um)	pellet density ($kg\,m^{-3}$)	Bulk Density ($kg\,m^{-3}$)
RDF	6.27±0.06	10.0±1.0	1.6	97.9±0.25	21.7±4.7	962±36	470
Waste Wood	8.37±0.10	10.8±0.7	1.3	88.2±1.24	7.7±1.1	1112±37	620
Fresh Wood	6.15±0.03	16.1±1.5	2.6	98.8±0.0	9.3±2.5	1146±20	650

4.2.2. Pellet Length and Particle Size Distribution

Figures 4.1 until 4.6 show the PLD and PSD of the pellets. The different colours show the repetitions of the experiment. All pellets show similar distributions.

Notably, the FW Fines contain almost no particles smaller than 0.15 mm, while WW fines do. The base materials used to make the pellets influence the PSD. Sawdust is likely smaller than the ground wood used for FW pellets.

The maximum pellet lengths in these samples are 33.4, 21.1, and 20.0 mm for Fresh Wood, RDF and Waste Wood pellets, respectively. To avoid mechanical bridging, the maximum pellet length is vital for the outlet diameter design. The rule of thumb is to design the outlet diameter ten times larger than the maximum particle size. However, as Schwedes and Schulze (2022) mentioned, this can be on the safe side because most of the pellets are shorter than the maximum length. Therefore, looking at the D90 pellet size is also interesting; see Table 4.2.

Table 4.2: The Maximum, 90% Largest and Mean Pellet Lengths

	Max	D90	D50
RDF	21.1 mm	15.3 mm	10.0 mm
WW	20.0 mm	16.7 mm	10.8 mm
FW	33.4 mm	24.7 mm	16.1 mm

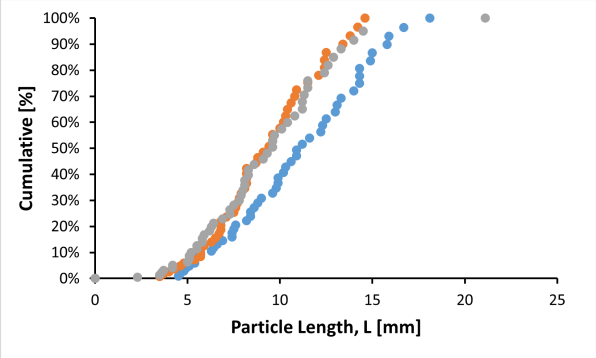

Figure 4.1: Particle Length Distribution for RDF Pellets. Three repetitions are shown.

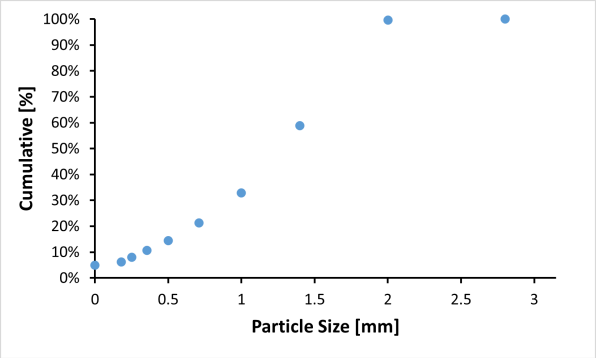

Figure 4.2: Particle Size Distribution for RDF Fines. No repetitions.

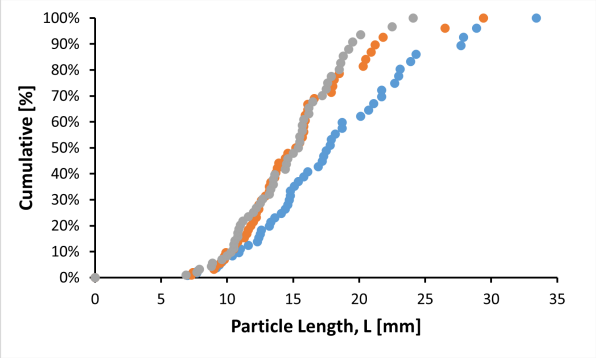

Figure 4.3: Particle Length Distribution for Fresh Wood Pellets. Three repetitions are shown.

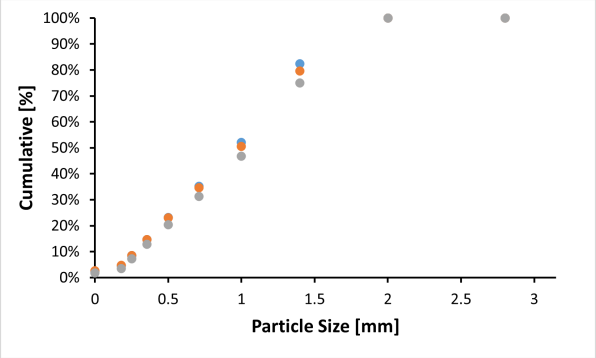

Figure 4.4: Particle Size Distribution for Fresh Wood Fines. Three repetitions are shown.

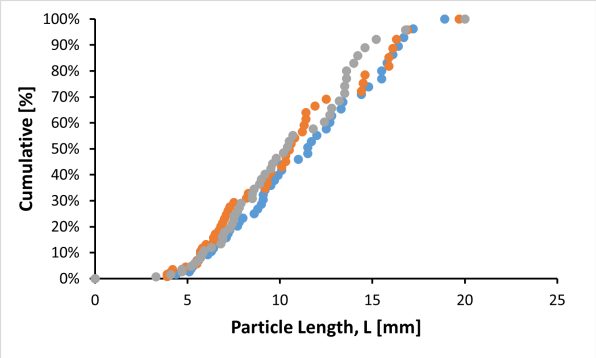

Figure 4.5: Particle Length Distribution for Waste Wood Pellets. Three repetitions are shown.

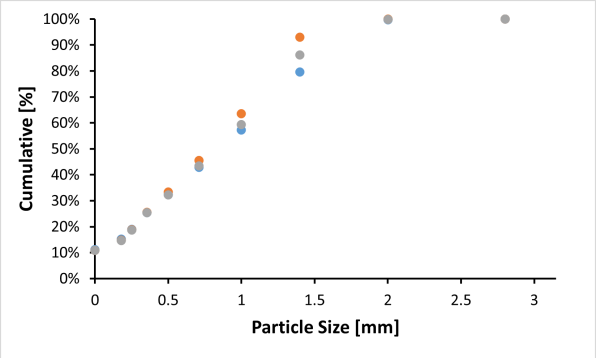

Figure 4.6: Particle Size Distribution for Waste Wood Fines. Three repetitions are shown.

Table 4.3: Void Ratio Based on the Bulk Density and Pellet Density Measurements

Sample	Bulk Density	Pellet Density	Void Ratio
RDF	470	962±36	0.51±0.02
WW	620	1112±37	0.44±0.01
FW	650	1146±20	0.43±0.01

4.2.3. Density of BSM of Pellets

The void ratio or porosity is the void volume ratio to the total volume (including all voids). We can determine the void ratio of the BSMs using the pellet density and the bulk density. A typical value of the porosity is 0.4 for a coarse dry BSM with close to spherical particles (Schulze, 2007). Table 4.3 shows the void ratios of the pellet BSMs. The wood pellets show a very similar void ratio, which is close to the typical porosity. However, the void ratio of the RDF pellets is significantly higher. A difference in cohesion cannot explain this because the flowability of RDF and WW is similar. The RDF pellets are built from larger pieces than the WW pellets; therefore, the surface roughness is much higher. As shown on the example pellet in Figure 3.20, the RDF pellets often have pieces of plastic sticking out. These irregularities in the pellets can explain the higher void ratio.

The bulk density was also determined by the RST and during the HR. The densities determined by the ring shear tester are inconsistent with those determined according to ISO 17828 and those derived during the HR test. Table 4.4 shows that the loose bulk density is lower than the bulk density, and the tapped density is higher. This makes sense because the container is only dropped three times during the bulk density test. Dropping the container three times allows the BSM to settle and reach a tighter packing than the loose density, but less densely packed than the tapped density during the HR test.

The RST density results in Figure 4.7 show that the bulk density remains roughly constant or even increases a little at 30% fines content compared to 0% content, even though the bulk density at 100% is significantly lower. The fines can occupy the voids between the pellets at low fines content, thus increasing the bulk density, especially at 10% fines content. At higher fines contents, the low bulk density and poor flowability of the fines negate the positive effect. Table 4.4 show the same effect for the bulk density measured during the HR test. The wood pellets increase in density when adding fines, especially the tapped density. Tapping allows the poor-flowing fines to occupy the voids. The effect is mainly present in the wood pellets and less in the RDF pellets. The RDF pellet fines contain a different mixture of fines and lumps (2/3 lumps and 1/3 fines instead of 1/3 lumps and 2/3 fines). The bigger lumps may have more trouble fitting in the voids, thus are unable to increase the bulk density similarly.

Figure 4.8 studies the effect of consolidation stress on bulk density. Under stress, the bulk density of the BSM increases, and the porosity decreases, since, usually, with compression of the BSM, the volume of the voids, but not the volume of the particles, decreases. The compression at 0% fines is similar for all pellets. The compressibility increases at higher fines contents, and a more significant difference between the pellets is observed. The RDF pellets show the greatest compressibility. The soft pieces of plastic lumps can deform easily under pressure to fill the voids. The FW pellets have the smallest compressibility, especially at 100% fines content. Schwedes and Schulze (2022) also investigated the effect of normal pressure on the bulk density of WW pellets at 0% fines content. They measured an increase of just 3% compared to our 5%.

4.3. BSM Flow Properties

First, the wall friction and flowability results are shown per pellet type. Later, mixtures are analysed, and finally, general conclusions are drawn.

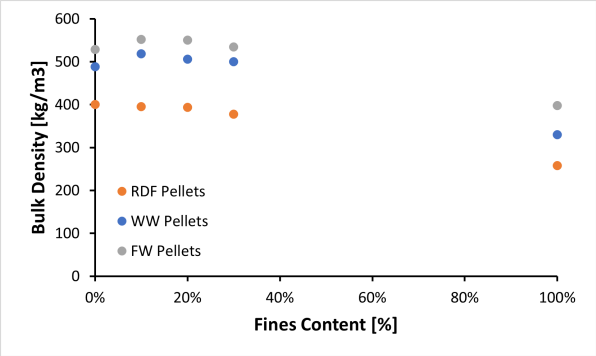

Figure 4.7: Effect of the Fines Content on the Bulk Density Measured by the RST at 1250 Pa Consolidation Stress

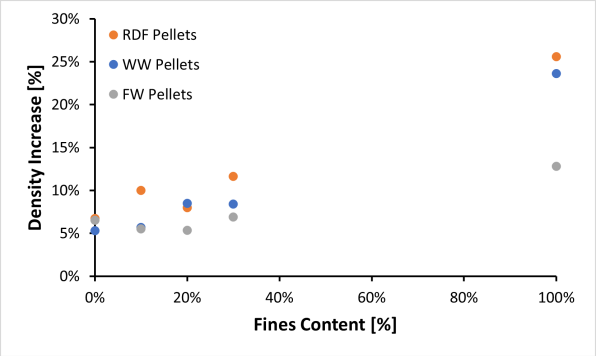

Figure 4.8: Density Increase Between 1250 Pa and 10000 Pa Consolidation Stress Measured by the RST

Table 4.4: The Loose and Tapped Bulk Densities at 0 and 30% Fines Content. Compared with the Bulk Density as Determined According to ISO 17828.

Sample	Fines Content	Bulk Density	Loose Density	Tapped Density
RDF	0%	470	438	508
	30%	-	426	501
WW	0%	620	587	682
	30%	-	582	705
FW	0%	650	620	691
	30%	-	653	792

4.3.1. Wall Friction

Wall Yield Loci

Figures 4.9, 4.11, and 4.13 show the wall yield loci of RDF, waste wood, and fresh wood on cold rolled steel, respectively.

The wall friction test results for all pellets showed that the shear stresses required to move the samples increased with increasing normal stress. Abou-Chakra and Zuk (1999) found that particles with a high surface roughness have a lower coefficient of friction. In these results, the RDF pellets show the highest wall friction angles while having the highest surface roughness. The unexpected combination of a high roughness and high wall friction angle may be caused by the plastic being softer than the wood and thus reaching a higher contact area. Comparing the two pellets made from wood, then, indeed, the pellet with the higher surface roughness, the fresh wood pellet, has the lower wall friction angle. The fresh wood pellets also appear harder, which can be partially substantiated by the better mechanical durability, and thus have an even smaller contact area.

A straight line through the measurements intersects the tau-axis at a positive, non-zero value, indicating adhesion. According to Rhodes (2008), a free-flowing material is unlikely to show adhesion in the wall friction test. The results in Schwedes and Schulze (2022) also showed no adhesion of RDF pellets with cold-rolled steel. However, they saw adhesion with carbon steel. Schwedes and Schulze (2013), who tested multiple pellets with carbon steel, found no adhesion with all pellets except with poor quality wood pellets with 50% fines content. Likely, these pellets are not free-flowing. Thus, some adhesion is expected. Barletta et al. (2015) did not measure a difference in adhesion measurement when comparing the larger wall friction tester with the ring shear tester.

Effect of Fines Content

Figures 4.10, 4.12, and 4.14 show the effect of the fines content on the wall friction angle for RDF, waste wood, and fresh wood on cold rolled steel, respectively. The influence of the fines content on the wall friction angle is minor for RDF. The wall friction angle for waste wood pellets decreases sharply when fines are added and is steady after 10% fines content. For fresh wood pellets, the wall friction increases

sharply when fines are added, reaching the maximum after only 10% fines content.

Schwedes and Schulze (2013) investigated the effect of fines content by comparing the wall friction of poor quality wood pellets at 20% and 50% fines. They found a minor increase only at 500 Pa normal stress. All other stress levels showed equal wall friction. Their results at 20% showed no adhesion, and at 50%, minor adhesion.

The results in this paper and the research of Schwedes and Schulze (2013) show that increasing the fines content initially influences the wall friction angle but quickly reaches a constant one. The fines content significantly impacts the wall friction angle at just 10% and remains the same until 100% fines. The fines govern the wall friction angle of a pellet fines mixture at just a 10% fines content. Intuitively, the fines may behave as a thin layer between the pellets and the wall materials already at relatively low content. Furthermore, due to the orientation of the wall friction test, where the wall material is below the bulk solid material, the fines content is higher than average at the wall-solid interface due to segregation. The higher relative concentration at the wall due to segregation is not a problem, as in a hopper, the fines content will also be higher at the walls due to segregation.

Abou-Chakra and Zuk (1999) found that the fines dominate the frictional assembly behaviour when the fines are smooth, and the coarse particles are rough. The smooth fines will increase the wall friction angle compared to 100% rough particles. The FW pellets are a case where adding fines increases the wall friction. This means that the FW fines are smoother than the FW pellets. In contrast, with WW the fines decrease the wall friction angle. The WW pellets are smoother than the FW pellets, and the fines are smaller. Here the fine fraction acts as a lubricant for the smooth pellets and decrease the wall friction.

To measure the wall friction of pellets for the design of a hopper, one can measure the wall friction of just the fines when the fines content in the hopper is expected to be at least 10%. Measuring the fines is cheaper because a smaller shear tester is required. However, this can be risky when the fines content drop below 10%. As Figure 4.12 shows, the wall friction of the pellets can be higher than the wall friction of the fines. Thus, designing a hopper based on the wall friction of the fines can lead to flow problems when the fines content drops below 10%.

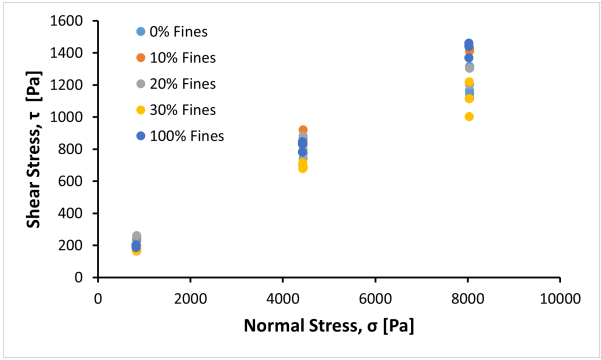

Figure 4.9: Effect of Normal Stress on Shear Stress in Wall Friction Test for RDF Pellets with Varying Fines Contents

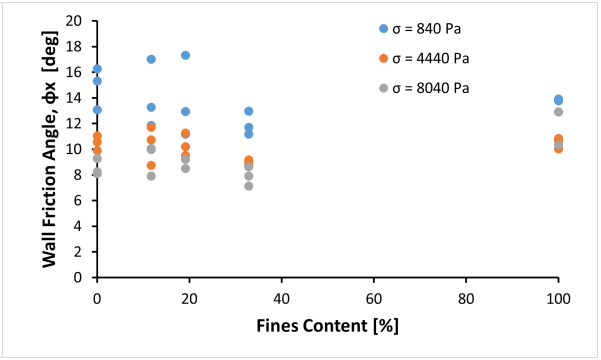

Figure 4.10: Effect of Fines Content on Wall Friction Angle in Wall Friction Test for RDF Pellets

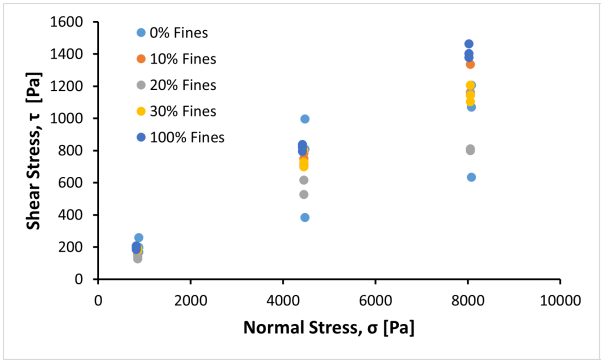

Figure 4.11: Effect of Normal Stress on Shear Stress in Wall Friction Test for Waste Wood Pellets with Varying Fines Contents

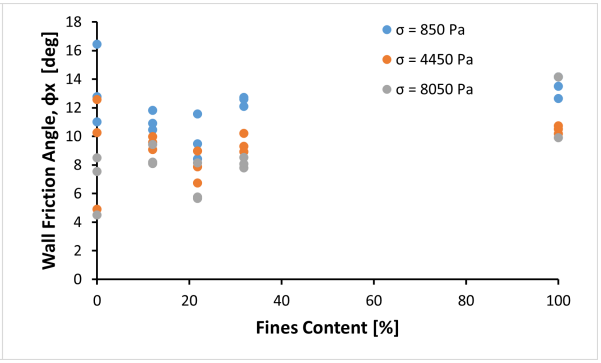

Figure 4.12: Effect of Fines Content on Wall Friction Angle in Wall Friction Test for Waste Wood Pellets

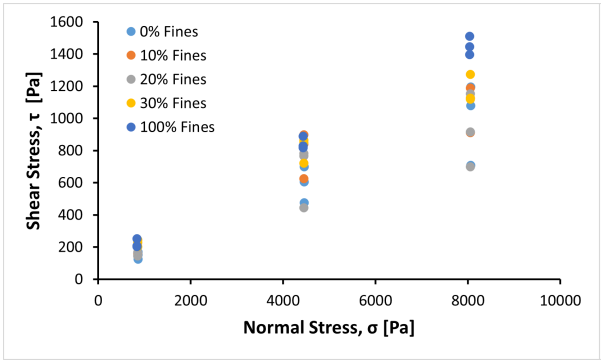

Figure 4.13: Effect of Normal Stress on Shear Stress in Wall Friction Test for Fresh Wood Pellets with Varying Fines Contents

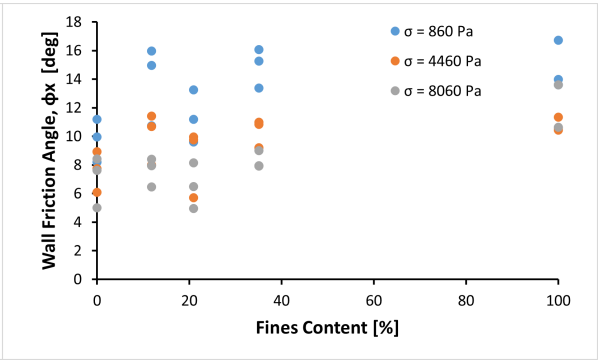

Figure 4.14: Effect of Fines Content on Wall Friction Angle in Wall Friction Test for Fresh Wood Pellets

4.3.2. Flowability

Effect of Consolidation Stress

Figures 4.15 until 4.20 show the effect of the consolidation stress on the flowability and the effective angle of internal friction. Together with the wall friction angle, these two values are of great importance in designing a mass flow hopper.

The flowability at high consolidation stresses is greater than at low consolidation stresses. This behaviour is expected. The effective angle of internal friction decreases slightly at higher consolidation stresses for RDF and WW. The ϕ_e stays the same for FW pellets. Craven et al. (2015) also found that the FFc increases with increasing consolidation stress while the effective angle of internal friction stays roughly equal.

Thus, the flowability and ϕ_e show favourable behaviour at higher consolidation stresses, illustrating the importance of evaluating the flowability and ϕ_e at the low consolidation stress at the hopper outlet. Measuring at high consolidation stresses will result in the under-design of the equipment.

The absolute spread of the flowability is larger at high consolidation stresses. However, the difference is that flowability is relative, e.g., a BSM with a flowability of 4 flows twice as well as a BSM with a flowability of 2. Furthermore, it is expected that the Schulze Ring Shear Tester shows a larger spread with free-flowing materials, which the materials are at higher consolidation stresses Schulze (2007). In contrast, the spread in ϕ_e is lower at high consolidation stresses. In general, the ring shear tester is more accurate at high consolidation stresses as absolute measurement inaccuracies of the sensors have a much smaller effect.

Effect of Fines Content

Figures 4.21 until 4.26 show that the fines content hurts the flowability. Similarly, they show that the effective angle of internal friction increases slightly with increasing fines content.

These results show that it is crucial to consider the fines content when designing a hopper. Only measuring the flowability and effective angle of internal friction will result in the under-design of the equipment.

The flowability decrease approaches the flowability at 100% fines with increasing fines content. The curve gets less steep with increasing fines content, indicating a non-linear relationship between the flowability and fines content. This agrees with Schulze (2007), who stated that at $1/3$ mass fraction of fines, the flowability is governed by the fines. Hann and Strazisar (2007), who tested the effect of fines in limestone powders, found that fines do not have a significant impact up to 20% mass content. However, after that, the influence increases steeply, with the mixture reaching similar unconfined yield strength as the fine fraction itself at about 40% fines content. Extrapolating our results, it will also be around 40-50% fines content where the flowability of the pellet-fine mixture reaches the flowability of the fines itself.

In contrast to Hann and Strazisar (2007), we already see a sharp decrease in flowability at 10% and 20% fines content for RDF and fresh wood pellets. The waste wood pellets are an outlier, where the flowability first increases at 10% fines, is similar to 0% at 20% fines content and only starts decreasing at 30% fines content. The WW pellets also showed that the small fines could act as a lubricant for the pellets in the wall friction tests.

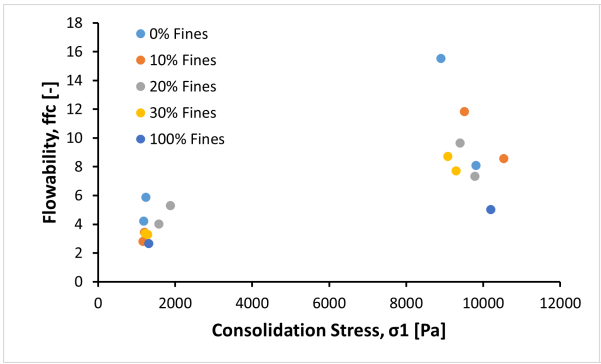

Figure 4.15: Effect of Consolidation Stress on Flowability for RDF Pellets with Varying Fines Contents

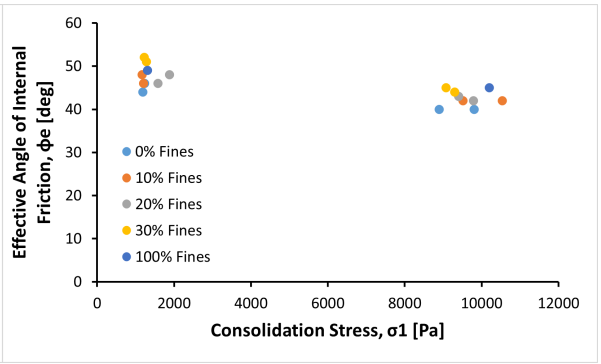

Figure 4.16: Effect of Consolidation Stress on Effective Angle of Internal Friction for RDF Pellets with Varying Fines Contents

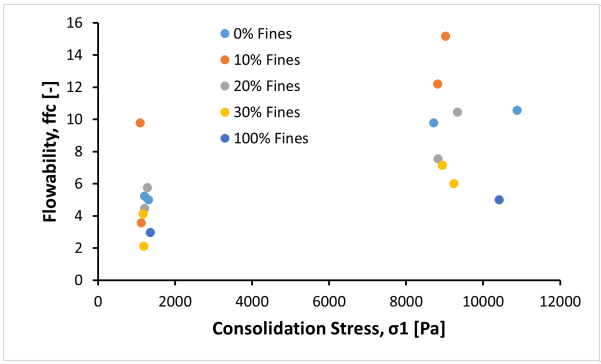

Figure 4.17: Effect of Consolidation Stress on Flowability for Waste Wood Pellets with Varying Fines Contents

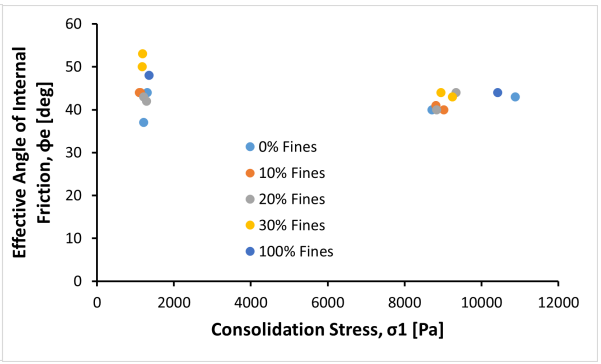

Figure 4.18: Effect of Consolidation Stress on Effective Angle of Internal Friction for Waste Wood Pellets with Varying Fines Contents

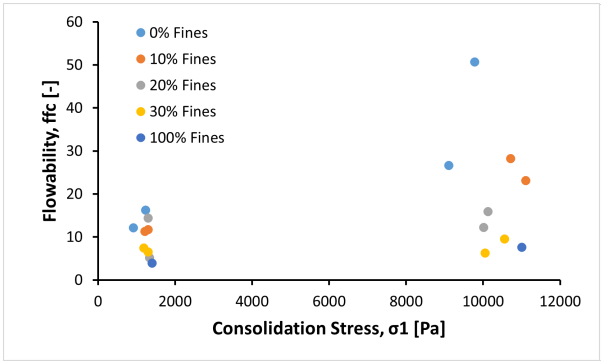

Figure 4.19: Effect of Consolidation Stress on Flowability for Fresh Wood Pellets with Varying Fines Contents

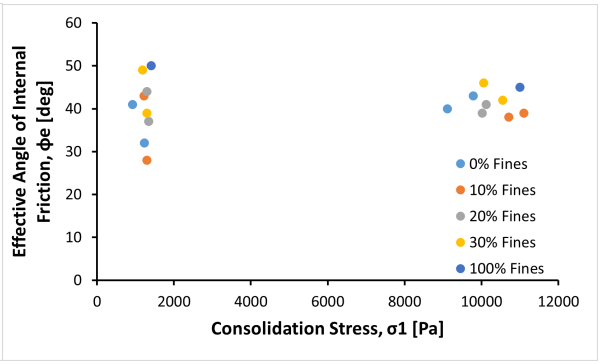

Figure 4.20: Effect of Consolidation Stress on Effective Angle of Internal Friction for Fresh Wood Pellets with Varying Fines Contents

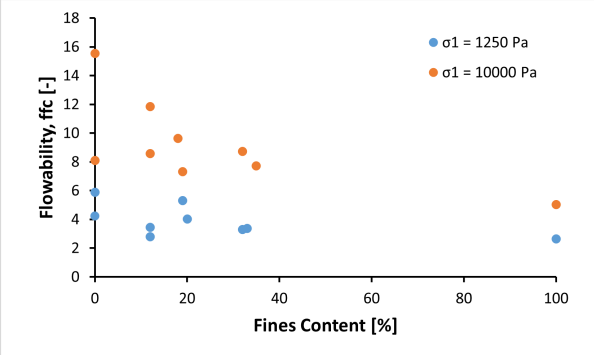

Figure 4.21: Effect of Fines Content on Flowability for RDF Pellets

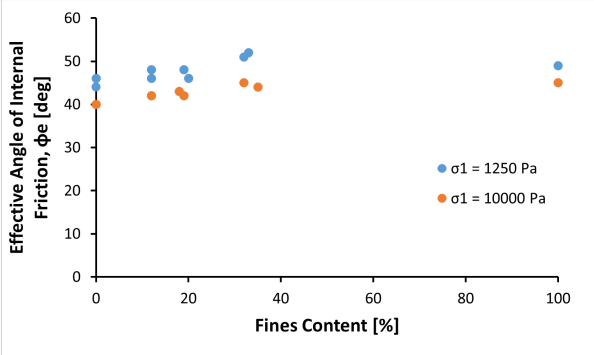

Figure 4.22: Effect of Fines Content on Effective Angle of Internal Friction for RDF Pellets

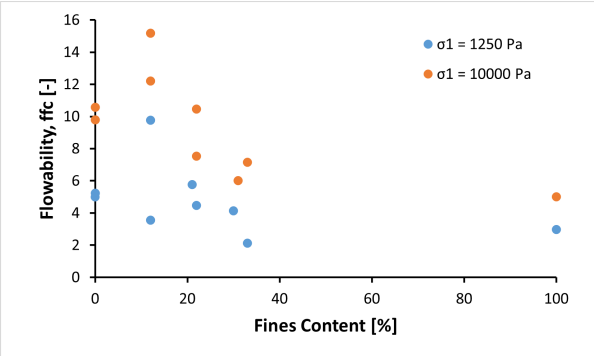

Figure 4.23: Effect of Fines Content on Flowability for Waste Wood Pellets

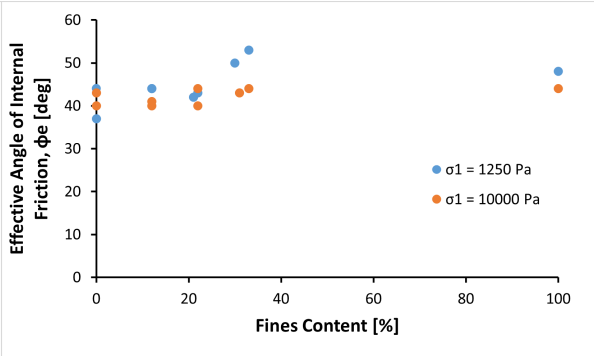

Figure 4.24: Effect of Fines Content on Effective Angle of Internal Friction for Waste Wood Pellets

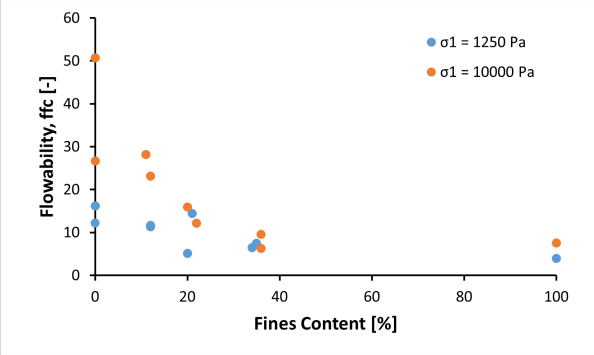

Figure 4.25: Effect of Fines Content on Flowability for Fresh Wood Pellets

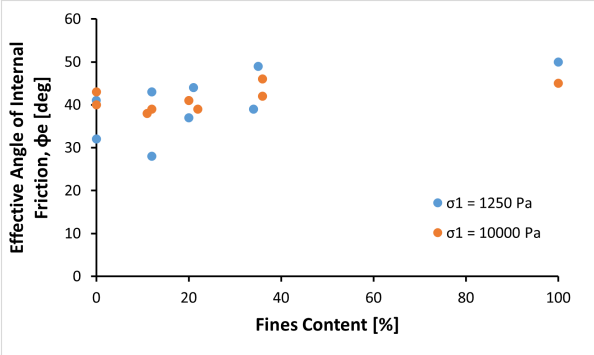

Figure 4.26: Effect of Fines Content on Effective Angle of Internal Friction for Fresh Wood Pellets. 0% on the x-axis corresponds to 100% RDF

4.3.3. Flowability and Wall Friction of Mixtures of Pellet Types

The effect of mixing pellets on the flowability and wall friction was investigated. Figure 4.27 shows the flowability of all pellets and mixtures. The mixtures show no unexpected flowability. Figure 4.28 shows the mixture ratio on the x-axis. It shows that the flowability of the mixture is consistent with the individual materials.

Figures 4.29 and 4.30 show the wall yield loci of the individual pellets and the mixtures. It shows that the material with the greatest ratio governs the wall friction. Thus, adding a small percentage of a material with a higher wall friction does not negatively impact the mixture's wall friction. Figure 4.30 shows that the wall friction of a 50/50 mixture is approximately the average of the individual pellets.

Schwedes and Schulze (2022) also investigated the effect of mixing RDF and Waste Wood pellets on the wall friction. They tested 100% Waste Wood pellets and a mixture of 80% Waste Wood and 20% RDF. Unfortunately, they did not report any results of 100% RDF pellets. They found that the wall friction angle for cold-rolled steel increases by 1 to 2° when adding RDF to the mixture.

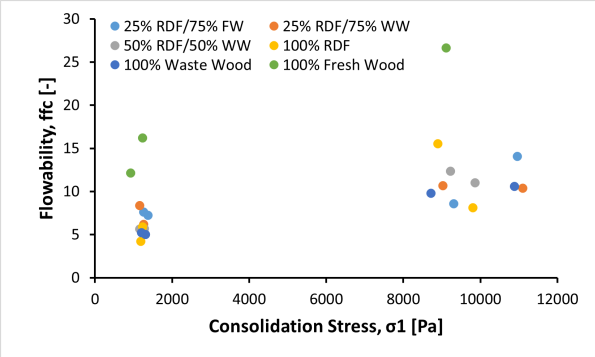

Figure 4.27: Flowability of the Pellets and Mixtures at 0% Fines Content

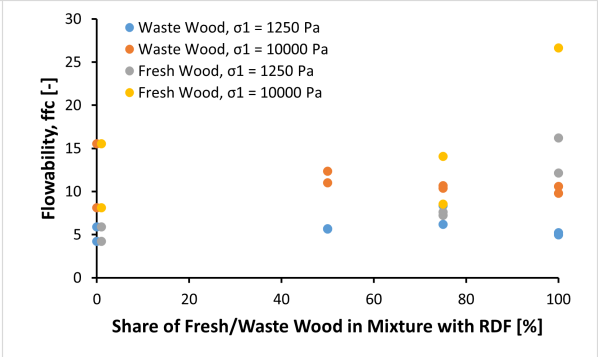

Figure 4.28: Effect of Mixing Pellets on Flowability. X-axis shows the mixture ratio, where 0% corresponds to 100% RDF pellets, and 100% corresponds to 100% WW/FW Pellets

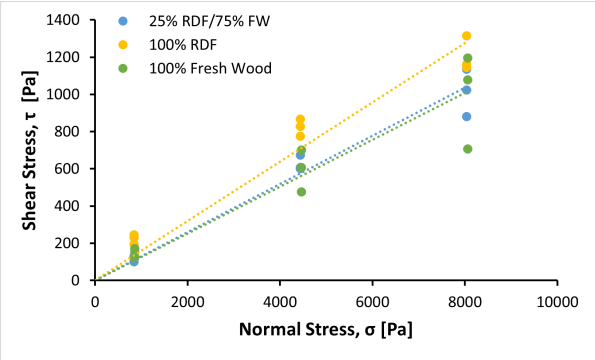

Figure 4.29: Wall Yield Loci for Fresh Wood and RDF Mixtures

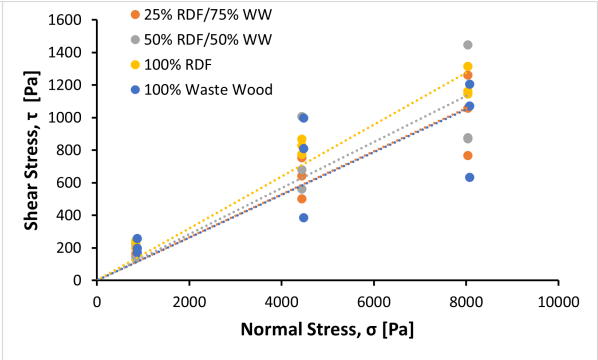

Figure 4.30: Wall Yield Loci for Waste Wood and RDF Mixtures

4.4. Conclusion

An extensive measurement plan was carried out to measure the pellets and BSM properties under different conditions and compositions. The pellets were tested at 0, 10, 20 and 30% fines content, and WW/RDF and FW/RDF mixtures were evaluated.

The most important conclusions of these measurements are:

- The bulk density is barely affected by the fines. Although the bulk density of 100% fines is much lower than the bulk density of the pellets, the fines occupy the voids between the pellets and thus do not lower the bulk density.

- The RDF and WW pellets have a shorter mean and maximum length than the FW pellets but a similar shape of the distribution. Their higher mechanical durability partially explains this.
- The difference in particle size between fines can be attributed to the base materials used.
- The fines content substantially impacts the wall friction angle, already at just 10% fines content. The wall friction angle of WW pellets is decreased with the addition of fines, while the wall friction angle of FW pellets is increased. The contradicting effects of the fines on the wall friction can be caused by differences in the roughness of the pellets and the fines, and the PSD of the fines.
- Higher consolidation stresses show improved flowability and have a moderate effect on the effective angle of internal friction. The fines content hurts flowability, with flowability approaching that of 100% fines at about 30% fines content.
- The analysis of pellet mixtures revealed that the flowability of the mixtures was consistent with the individual materials. The most prevalent material mainly determined the wall friction of the mixtures.

The results presented in this chapter will be used in Chapter 6 to design a mass flow hopper. Furthermore, the flowability results will be compared to other flow indicators, namely the AoR, AoT and HR, in Chapter 5 to see if more straightforward tests can be used to predict the flowability of pellets.

5

Predicting the Flowability with AoR, AoT and HR

5.1. Introduction

This chapter presents the relationships between the flow indicators and the flowability of pellets. The AoR, AoT and HR were measured for all three pellet types at 0% and 30% fines content. These are the fines content with the highest difference in flowability. Thus, the potential relationships will also show up most easily with these fines contents. The relationships may be used to determine the flowability of the pellets without requiring shear testing, thus speeding up the silo design process.

One of the critiques of these methods is, as discussed in Chapter 3, that they evaluate the bulk solid material at very low consolidation stresses. The results may thus not apply to the material at higher consolidation stresses. Therefore, we plot the flowability at 1250 and 10,000 Pa consolidation stress in the graphs. The trendlines are exponential functions.

Table 5.1 shows the relationships between the Angle of Repose, Hausner Ratio and flowability from the literature. Table 5.2 shows the mean values of the measurements used in this chapter.

Table 5.1: Descriptions of flowability based on the Angle of Repose, Flow Factor and Hausner Ratio

Description	Angle of Repose	Flow Factor	Hausner Ratio
Very free-flowing	<30°		1.00-1.11
Free-flowing	30-38°	>10	1.12-1.18
Fair	38-45°	4-10	1.19-1.25
passable			1.26-1.34
Cohesive	45-55°	2-4	1.35-1.45
Very cohesive	>55°	1-2	1.46-1.59
No flow		<1	>1.59

Table 5.2: Mean Values of the Flowability and Flow Indicators

Fines Content	Pellet	FFc [-] 1250 Pa	FFc [-] 10 kPa	AoR [°]	AoT [°]	HR [-]
0%	WW	5.1	10.2	47	57	1.16
	RDF	5.0	11.8	48	59	1.16
	FW	14.2	38.7	44	50	1.11
30%	WW	3.1	6.6	67	60	1.21
	RDF	3.3	8.2	68	64	1.18
	FW	6.9	7.9	58	53	1.21

5.2. Relationships between flowability and AoR, AoT and HR

5.2.1. Flowability and Angle of Repose

Figure 5.2 demonstrates the relationship between the AoR and flowability. It shows the expected pattern, where a higher AoR indicates poorer flowability. However, the relationship is weak and does not work across fines contents. The test can only discriminate the pellets according to flowability at the same fines content. Interestingly, the AoR is very good at classifying the fines content: all measurements around 45° belong to 0% fines content, and all measurements above 55° belong to 30% fines content measurements. Fines content has a more significant impact on the AoR than the flowability. why?

The data presented in Table 5.1 do not correspond to the abovementioned findings. This discrepancy can be attributed to variations in the AoR measurement setup. The AoR of pellets measured by other researchers is 32-41°(heap) Wu et al., 2011, 35°Mattsson, 1990, 27-34°Fasina and Sokhansanj, 1993, and 33°(heap) Schwedes and Schulze, 2022. Heap means that the AoR is measured by forming a heap of material by dropping the BSM from a certain distance. Schwedes and Schulze, 2022 also measured the draw-down AoR, where the material is at rest and a hole is opened. This test is more similar to the ledge test used in this paper. They found an AoR of 60°with this test. Hence, it becomes evident that it is crucial to calibrate the AoR test setup before concluding the flowability of the BSM. However, even with proper calibration, the AoR performs poorly in accurately determining flowability. Therefore, we cannot recommend relying on the AoR as a reliable indicator for assessing flowability.

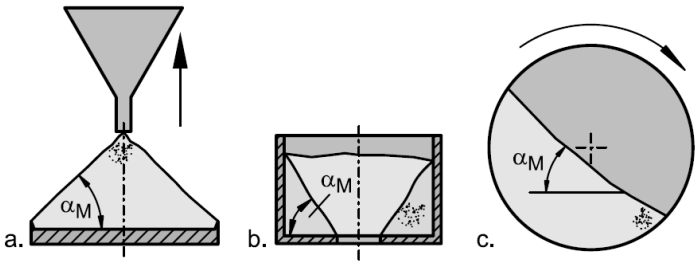

Figure 5.1: Angle of Repose Measurement Tests: Heap test (A) and draw down test (B) (Schulze, 2007)

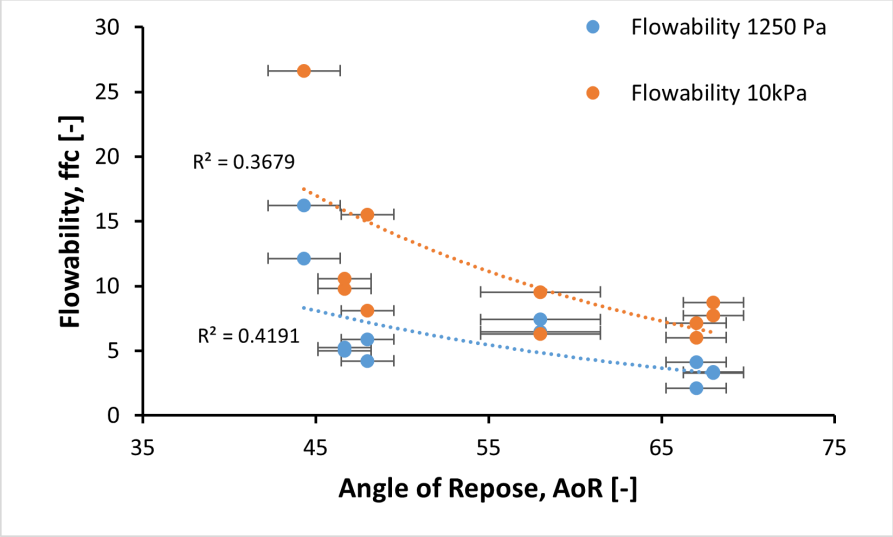

Figure 5.2: The relationship between the Angle of Repose and Flowability for the Tested Pellets. The error bars represent the standard deviation of the results.

5.2.2. Flowability Angle of Tilt

Figure 5.3 depicts the relationship between the AoT and flowability. According to Kalman (2021), the AoT is unaffected by local avalanches and solely determined by unstable shear surfaces, making it a potentially more accurate predictor of material flowability than the AoR. However, our experiments observed that local avalanches still occur during tilting, particularly when pellets start rolling. The local avalanches during tilting create challenges in precisely determining the moment of flow initiation due to an unstable shear surface.

The results show a strong correlation between the AoT and the flowability, particularly at 1250 Pa consolidation stress. Better performance at lower consolidation stresses is expected because the AoT test is also conducted at very low consolidation stresses. The relative spread in the measurements is large, mainly because of the small range of AoT measurements and the difficulty for the operator to determine the angle when flow occurs due to an unstable shear surface.

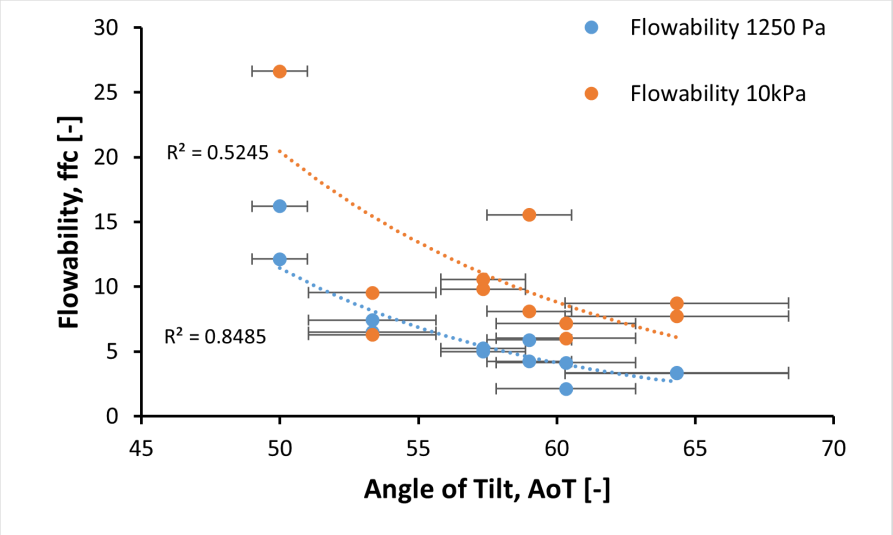

Figure 5.3: The relationship between the Angle of Tilt and Flowability for the Tested Pellets. The error bars represent the standard deviation of the results.

5.2.3. Flowability and Hausner Ratio

Figure 5.4 shows the relationship between HR and flowability. The test can identify the FW pellets' higher flowability at 0% fines content but surprisingly attributes the best score to the RDF pellets at 30% fines content. The HR test has the greater predictive quality of flowability values at the highest consolidation stress. This is unexpected because the BSM is not consolidated during the HR test. The performance at predicting the flowability at high consolidation stresses is only better than at low consolidation stresses due to the RDF results at 30% fines, which show high flowability and low HR. The low HR of RDF at 30% fines content compared to the wood pellets may also be explained by the different compositions of the fines, where the RDF sample contains more lumps.

Initially, the loose density of all pellets is similar at 0% and 30% fines content. For the wood pellets, the tapped density at 30% fines is significantly higher than at 0% fines. However, the tapped bulk density does not increase for the RDF sample, which explains the low HR. The lumps may have difficulty occupying the voids between the pellets than the fines. Thus at 30% fines content, the RDF sample's tapped density remains relatively low compared to the wood samples. This effect is not explained by the flowability but by the PSD of the fines and thus explains the outlier result of the RDF pellets. Salehi et al. (2019) also noted that BSMs with a higher fines content could fill the voids between larger particles and allow the attainment of larger space-filling during tapping. They also noted that a low density and high interparticle friction of biomass might reduce the effect of tapping, resulting in lower HR values.

This effect, where the RDF BSM is not as compressible by tapping at 30% content during the HR as the

wood pellets, is not observed in the RST, where it is compressed under normal force. Figure 4.8 shows that RDF is the most compressible of all BSMs at 30% fines content. The soft pieces of plastic lumps can deform easily under pressure to fill the voids. The FW pellets have the smallest compressibility, especially at 100% fines content.

The HR test also makes a clear split between the samples with 0% and 30% fines contents: all results with an AoR of >1.18 belong to 30% fines content samples, <1.16 belong to samples with 0% fines content.

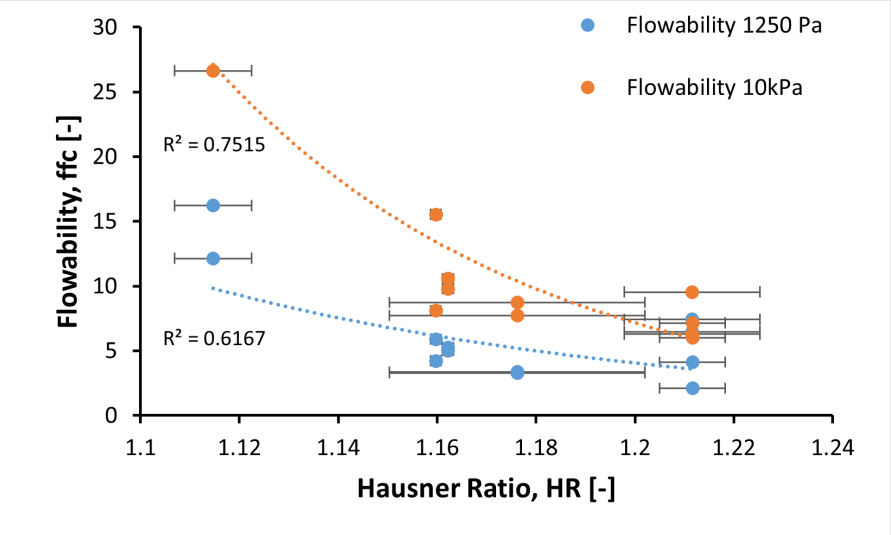

Figure 5.4: The relationship between the Hausner Ratio and Flowability for the Tested Pellets. The error bars represent the standard deviation of the results.

5.2.4. Discussion

Xu et al. (2018) also investigated the relationship between AoR, HR and flowability for powders. They fitted the AoR and flowability with a linear fit but noted that this may not be the best fit. An exponential fit was used when plotting HR and flowability. They also found large deviations between the measurement points and fitting lines, which were attributed to the differences in consolidation.

Xu et al. (2018) and Geldart et al. (2006) found a strong relationship between the AoR and HR for powders. Our results do not show strong relationships between any of the flow indicators. However, the ranges in the results of Geldart et al. (2006) and Xu et al. (2018) are much larger, with the HR ranging from 1.1 to 1.9. For the tested pellets in this research, the range is much smaller (1.1 to 1.2), thus the influence of (absolute) measurement errors and uncertainty is greater.

5.3. Conclusion

Measurements were carried out to measure the BSM flow properties and the flow indicators AoR, AoT and HR for all three pellet types at 0 and 30% fines content. The most important conclusions are:

- All three descriptors show the expected trend of decreasing flowability with an increasing AoR, AoT and HR.
- None of the relationships are accurate enough to predict the material's flowability and thus cannot be used in silo design.
- The fines content is a much more significant influence on the AoR than the flowability.
- The HR results are also heavily influenced by the fines content.
- The AoT is the most accurate, and the results depend mostly on flowability.

6

Hopper Design

6.1. Introduction

In this chapter four silos are designed based on our measurements. The design process is automated for ease of use in industry and the considerations and equations in the automated design tool are discussed.

6.2. Design Procedure

The design procedure proposed by Jenike (Jenike, 1964) has been successfully used for over 50 years (Schulze, 2007). The design procedure for conical hoppers determines the angle to ensure mass flow and the minimum outlet diameter to prevent cohesive arching and ratholing. The procedure is as follows:

- Estimate the effective angle of friction, bulk density, and wall friction at the outlet
- Determine the hopper slope using the design charts
- Read the flow-factor of the hopper from a chart
- Plot flow-function, flow-factor, and
  - If there is an intersection between the flow-function and flow-factor, read the critical stress at the intersection point from the graph. Then, read the value of H from the graph.
  - If there is no intersection, and the flow-function lies above the flow-factor, there will be flow always.
  - If there is no intersection, and the flow-function lies below the flow-factor, there will be no flow.
- Determine H
- Determine minimum outlet diameter

Using this design procedure, we will deisgn four silos in this chapter. All must comply with the specification given in Table 6.1.

- Conservative silo design compatible with three tested pelelts and potential future pellets
- WW pellet silo
- FW pellet silo
- RDF pellet silo

First, a hopper is designed for use with all pellet types. Here, we illustrate the design methods and considerations used. An extensive sensitivity analysis is presented to substantiate the conservative design. Finally, the process is automated in an Excel spreadsheet and three hopper designs are generated based on our measurements.

Table 6.1: The lock hopper specification used in the design in this chapter

	Lock-Hopper
Capacity (ton)	5
Diameter (m)	2
Mass flow rate (t/h)	10
Wall Material	Cold-rolled steel

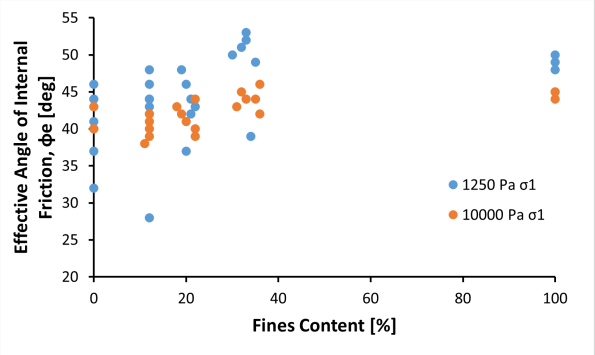

Figure 6.1: Graph of Effective Angle of Internal Friction for all Pellet Types used for Determining the Worst-Case Angle

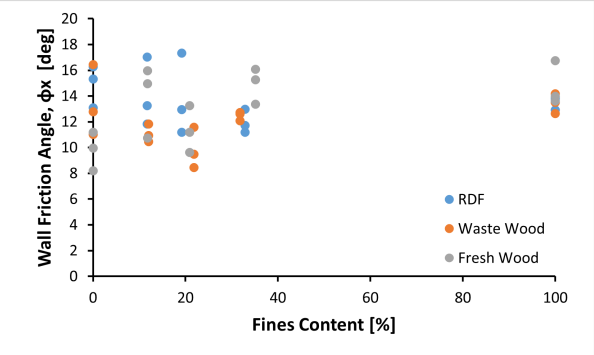

Figure 6.2: Graph of Wall Friction Angle for all Pellet Types used for Determining the Worst-Case Angle

6.3. Conservative Hopper Design

6.3.1. Hopper Cone Angle

Figure 6.1 is used to estimate the effective angle of internal friction at the outlet. The consolidation stress is 1250 Pa because the pressure at the outlet is low during discharge. The least favourable effective angle of internal friction is 53 degrees at a fines content of 30%, measured with waste wood pellets.

Figure 6.2 is used to estimate the wall friction angle at the outlet. The least favourable wall friction angle is 18° at a fines content of 19%, measured with RDF pellets.

The bulk density at low pressures (at the outlet) can be taken from the bulk density tests and ranges between 650 kg m^{-3} for 100% fresh wood pellets and 300 kg m^{-3} for 100% fines. At 30% fines, the density is about the same as the density at 0% fines.

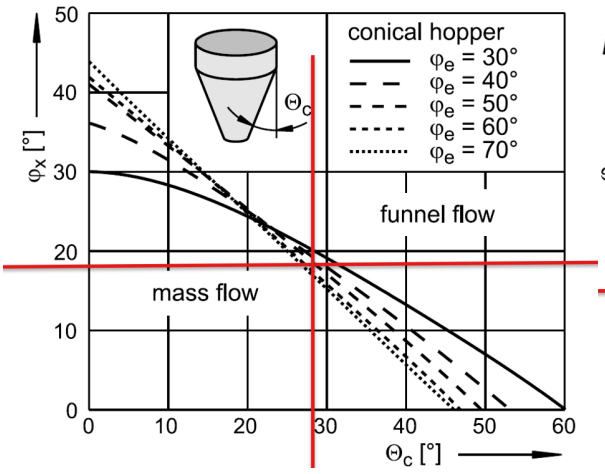

Figure 6.3: Mass Flow Diagram for Determining the Hopper Cone Angle

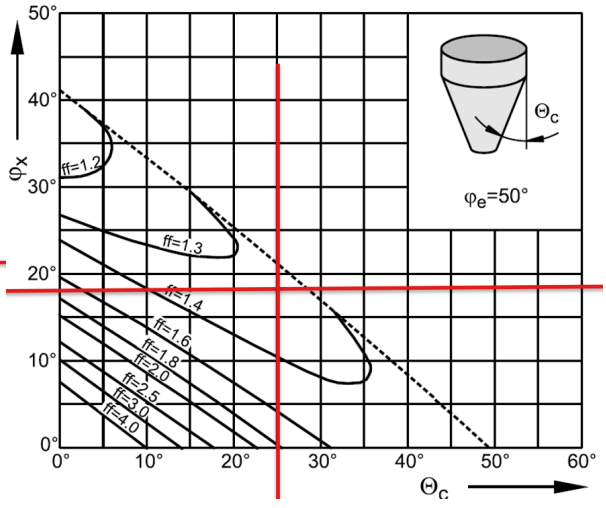

Figure 6.4: Flow Factor, ff, for Conical Hoppers

Then, Figure 6.3 is used with the estimated wall friction angle and angle of internal friction at the outlet. The resultant hopper cone angle from the graph is estimated to be 28° to ensure mass flow. Schulze (2007) advices a safety factor of 3°, resulting in a final hopper cone angle of 25°.

6.3.2. Minimum Outlet Diameter to Prevent Cohesive Arching

Figure 6.4 is used to determine the flow factor of the hopper. The flow factor is determined to be 1.35

Figure 6.5 is used to study the intersection between the flow factor and flow function. In our measurement range, there is no intersection. However, the results can be extrapolated. A worst-case linear extrapolation of the highest unconfined yield strengths at 1250 and 10000 Pa results in a $\sigma_c, crit$ of about 450 Pa. However, this is unrealistic. The flow function usually has a steeper slope at lower consolidation stresses resulting in a lower $\sigma_c, crit$. Fitzpatrick et al. (2004) also noted that linear extrapolation of the flow function can result in conservatively high outlet diameters "because the real flow function will most likely curve downwards more towards the origin in the extrapolated region and thus produce a smaller [outlet diameter]."

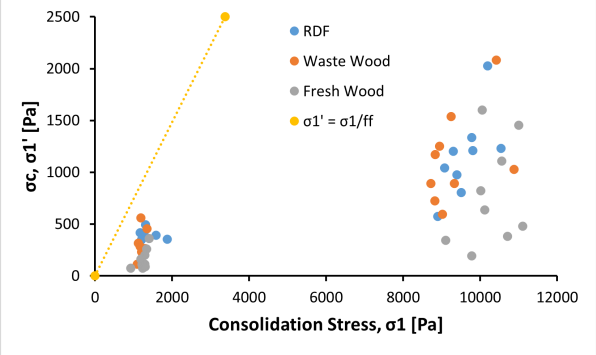

Figure 6.5: Plot of Flow Factor and Flow Function

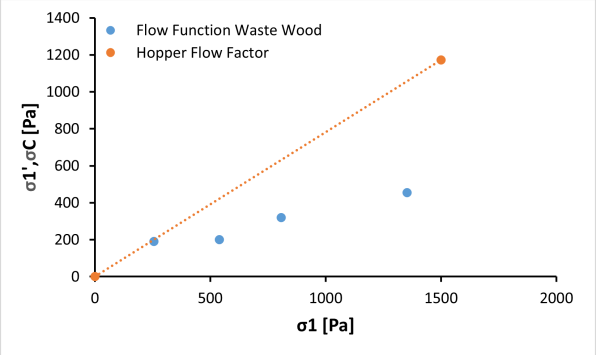

Figure 6.6: Plot of Flow Factor and Flow Function for 100% Waste Wood Fines

To obtain a more reasonable estimate, waste wood fines were tested at lower consolidation stress (Figure 6.6). 100% fines content was chosen because the results are more reliable due to the smaller particle size, especially at lower stresses. It can now be seen that $\sigma_c, crit$ is 200 Pa.

Figure 6.7 is then used to obtain the value of H, which is used to determine the minimum outlet diameter to prevent cohesive arching, Equation 6.1. Calculating with H = 2.35, ρ = 500 kg m^{-3} and $\sigma_c, crit$ = 200 Pa gives $d_c rit$ = 0.094 m.

$$d_c rit = H \frac{\sigma_c, crit}{g \rho_b, crit} \tag{6.1}$$

6.3.3. Minimum Outlet Diameter to Prevent Mechanical Arching

The outlet diameter to prevent cohesive arching is thus about 0.1 meter. However, the outlet diameter to prevent mechanical arching should also be considered. According to Schulze (2007), the rule of thumb to prevent mechanical arching is to take 6-10 times the maximum particle size for conical hoppers and 3-7 times the maximum particle size for wedge-shaped hoppers. Table 6.2 shows the maximum particle sizes. So according to the rule of thumb, an outlet diameter of 0.334 m should be chosen. However, this is most likely a large overestimation of the required particle size. Schwedes and Schulze (2022) note that most particles are much smaller than the maximum particle size; thus, the outlet diameter is "on the safe side." Mattsson (1990) and Hinterreiter et al. (2012) also found that a slot of about 2 times the pellet length is enough to prevent arching. They note that the arching distance for pellets is minimal compared to other biomass. Finally, Miller (2013) experimentally found a minimum outlet diameter of 0.08 m. The maximum pellet length is unknown, but the quality was A1 which specifies a maximum length of 40 mm according to the ENPlus Pellet Quality Requirements.

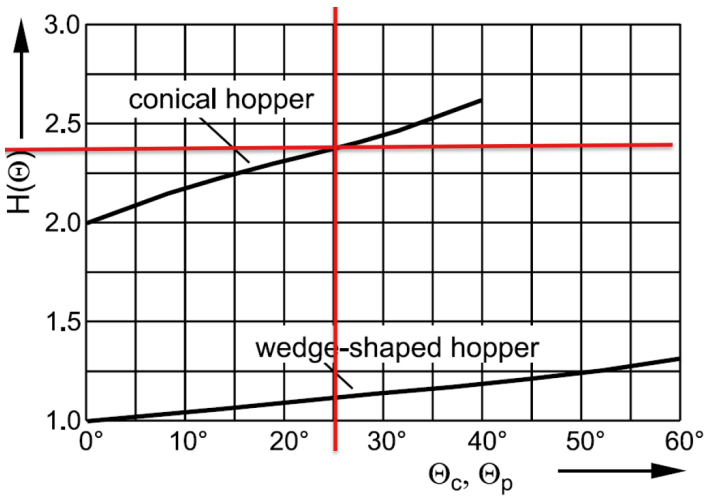

Figure 6.7: Function H

Table 6.2: The Maximum and 90% Largest and Mean Pellet Lengths Used to Determine the Minimum Outlet Diameter of the Hopper

	Max	D90	D50
RDF	21.1 mm	15.3 mm	10.0 mm
WW	20.0 mm	16.7 mm	10.8 mm
FW	33.4 mm	24.7 mm	16.1 mm

Ashour et al. (2017) investigated the mechanical arching of pellet-like cylindrical particles. They found that during discharge, the long axis of the pellets is oriented to the centre of the outlet. The possibility of clogging increases when particles are elongated with constant volume. However, for particles with an aspect ratio below 6, which is the case for all pellets used in this study, the comparison with spheres of a similar cross-section area in the rotation axis (not volume) is reasonable. This would indicate that the diameter may be a better metric instead of considering the maximum pellet length.

Table 6.3 compares the relationship between the diameter, outlet, and length and outlet. The table shows the mean length instead of the maximum length because the maximum length is not reported in the literature. It is clear that even for the mean length, the rule of thumb overestimates the outlet diameter for pellets. This effect is much greater when using the maximum particle length, which is often about twice the mean (as seen in Table 6.2). The table also shows that using the diameter instead of the particle length is much closer to the rule of thumb but on the upper limit for 3 of the six pellets. However, for the pellets tested in this report (FW, WW and RDF), the arching distance is much better predicted by the diameter than the length, thus confirming the finding of Ashour et al. (2017).

Table 6.3: Comparison of the relationship between the arching distance, pellet diameter, and mean pellet length. All research used a flat bottom silo, except for Miller, who used a cone with an angle.

	Mattsson (1990)	Hinterreiter et al. (2012)	Miller (2013)	FW	WW	RDF
Pellet Diameter [mm]	12	7	8	6	8	6
Mean Pellet Length [mm]	15	18	3.15-40	16	11	10
Slot Distance [mm]	30	35	-	-	-	-
Outlet Diameter [mm]	-	-	80	60	70	70
Length/outlet [-]	2.0	1.9	-	3.75	6.4	7
Diameter/outlet [-]	2.5	5	10	10	8.75	10

The mechanical arching depends on the particle size and shape. In general, pellets are found to be unlikely to show mechanical bridging. The rule of thumb of 6-10 times the maximum particle size is very safe. Therefore, we can safely take the lower side of this range, and instead of the maximum pellet

length, we will consider the D90 size, as most of the pellets are much smaller. This results in a minimum outlet diameter of 0.15 m for FW pellets. Larger pellets exist, which often also have a larger aspect ratio and, thus, a larger tendency to bridge. Therefore, a safety factor of 1.5 is used to obtain a minimum outlet diameter of 0.23 m. The minimum outlet diameter to prevent arching does not necessarily equal the minimum outlet diameter to reach the desired mass flow rate.

6.3.4. Minimum Outlet Diameter for the Mass Flow rate

It is impossible to predict the mass flow rate exactly, but an estimation based on an analogy to the outflow of liquids can be made (Schulze, 2007). The Torricelli equation states that the velocity, w, of a liquid, leaving a hole of distance, h, from the water surface, follows Equation 6.2.

$$w = \sqrt{2gh} \tag{6.2}$$

In a hopper, the outlet pressure is proportional to the outlet opening d; thus, the equation can be rewritten to Equation 6.3.

$$w \propto \sqrt{gd} \tag{6.3}$$

Multiplying the velocity by the outlet's area and the solid's bulk density results in mass flow. For a circular outlet and coarse-grained bulk solid, the fitted Equation 6.4, derived by Beverloo and the British Materials Handling Board, can be used.

$$\dot{m} = 0.58\rho_b\sqrt{g}(d - kx)^{2.5}k_\theta \tag{6.4}$$

Where k is 2.5 for non-spherical particles and $k_\theta = tan(\theta_c)^{-0.35} = 1.3$. Ashour et al. (2017) found that for particles with an aspect ratio lower than 4, the flow rate can indeed be approached by equivalent spheres of equal volume by Beverloo's formula. Furthermore, comparing the results obtained with Beverloo's formula with the experimental results of Miller (2013) in Table 6.4 shows a good correspondence. As recommended by Ashour et al. (2017), the x was chosen so that the spheres obtain an equivalent volume: x = 10 mm.

Table 6.4: Comparison of Experimentally Measured and Theoretical Mass Flow Rates for Wood Pellets with a Diameter of 8 mm and Mean Length of 10 mm

Outlet Diameter	Miller (2013) (Experimental)	Beverloo's Equation (Theoretical)
55	1.4 t/h	0.9 t/h
63	1.6 t/h	1.4 t/h
83	5.7 t/h	4.6 t/h
154	36.4 t/h	34.1 t/h
247	95.1 t/h	132.6 t/h

To achieve the minimum flow rate of the hopper of 10 t/h, an outlet diameter of about 0.105 m must be used. Adding a safety factor of 2, and thus designing for 20 t/h capacity, the outlet diameter must be 0.13 m.

6.3.5. Automated Hopper Design

Jenike's design procedure is first automated to ease the analysis of the sensitivity of the hopper design on the measurements. Using Excel, the design charts are converted to formulas taken from Oko et al. (2010). Interpolation is done using Lagrange interpolating polynomials. In addition to Oko et al. (2010), we also converted the determination of H into formulas for a more accurate outlet diameter determination. The mass flow rate is determined using Equation 6.4.

The spreadsheet results are compared with the manual results described in the previous section in Table 6.5. The Excel Model corresponds closely with the manual calculations.

Table 6.5: Comparison of Manual and Automated Hopper Design

	Manual Method	Spreadsheet
Cone Angle [deg]	25	24.9
Flow Factor [-]	1.35	1.28
SigmaC,crit [Pa]	200	206
Outlet Diameter [m]	0.094	0.098
Mass Flow Rate [t/h]	5.34	6.23

The model was also run for further validation with the inputs of Oko et al. (2010), and the outputs were compared in Table 6.6. The results are identical, except for the outlet diameter and mass flow rate. Our more accurate determination of H explains the outlet diameter difference. This also impacts the mass flow rate. The formula used by Oko et al. (2010) for the mass flow rate is also unknown, just like the particle size.

Table 6.6: Validation of Spreadsheet Method

	Spreadsheet	Oko et al. (2010)
Cone Angle [deg]	27.83	27.83
Flow Factor [-]	1.84	1.83
SigmaC,crit [Pa]	837	837
Outlet Diameter [m]	0.157	0.162
Mass Flow Rate [t/h]	18.71	23.86

A final addition to Oko et al. (2010)'s model is a linear interpolation of the flow function instead of the Lagrange polynomial interpolation. The linear interpolation is more robust under certain circumstances. The user can choose which interpolation method obtains the most realistic results.

6.3.6. Sensitivity Analysis and Considerations for Conservative Hopper Design

The properties of three types of pellets were evaluated. Due to the inconsistency and unpredictability of the biomass and waste markets, different pellets may be used in the future. These pellets likely have similar flow characteristics but may also show less favourable properties. Therefore, the sensitivity of the hopper design on the BSM properties is investigated. If the hopper design is sensitive to specific properties, it is advisable to over-design the hopper so mass flow is guaranteed with worse flowing pellets.

Wall Friction Angle and Effective Angle of Internal Friction

The wall friction angle and effective angle of internal friction are two of the most important properties when designing a hopper. It is, therefore, interesting to see what a change in these properties means for the design of the hopper.

In the results, we saw that for the different pellets with 0% fines content, the maximum wall friction angle could range from 12° (fresh wood) to 17° (waste wood). When also considering the fines, the upper end of the range increases to 18°. Similarly, the effective angle of internal friction at 1250 Pa ranges from 40° to 55°.

In the sensitivity analysis, we consider the maximum wall friction angle and the effective angle of internal friction with a reasonable range around it.

In Figure 6.8, the combined effect of the wall friction angle and effective angle of internal friction on the hopper cone angle is studied. The effective angle of internal friction has a negligible impact on the cone angle. The wall friction angle has a significant impact on the cone angle. When a pellet with just a 3° higher wall friction angle is used, the cone angle must be decreased to 21°.

The hopper cone angle is mainly affected by the wall friction angle. In literature, a large range of wall friction angles can be found, ranging from 14-28°. The wall friction angle also depends significantly on the wall material. We recommend conducting wall friction tests when facing new pellets with significantly different properties (roughness, composition, hardness) than those in this research. The highest measured ϕ_x is 19°; designing a hopper for a BSM with a ϕ_x of 23° results in a hopper angle of 19°. The hopper will still empty completely in the unlikely scenario of a pellet with even higher wall friction.

The combined effect on the outlet diameter is studied in Figure 6.9. The effect of both the effective angle of internal friction and wall friction on the outlet diameter is negligible.

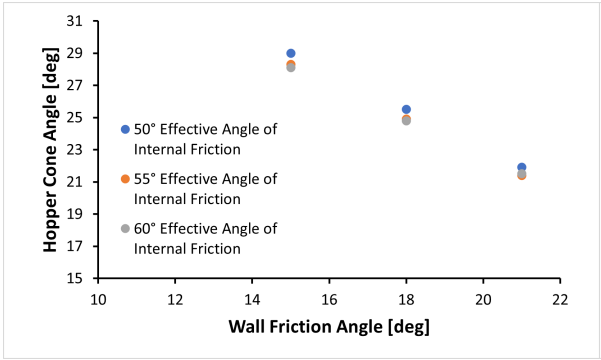

Figure 6.8: Effect of the Wall Friction Angle on the Cone Angle of the Hopper

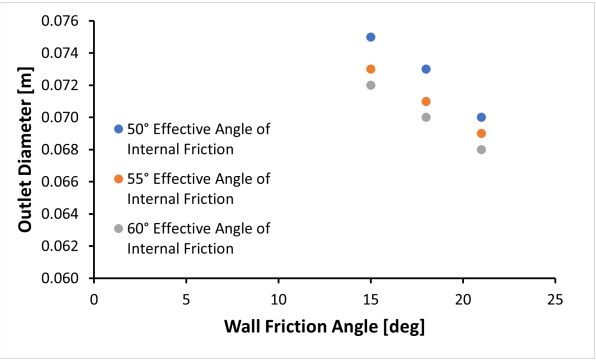

Figure 6.9: Effect of the Wall Friction Angle on the Outlet Diameter of the Hopper

Flowability

Another important material property in the design of a hopper is flowability. The flowability is used to draw the flow function, and its intersection with the hopper flow factor determines the size of the outlet. We shift the flow function by increasing the unconfined yield strength at every consolidation stress. This approach is shown graphically in Figure 6.10. In this Figure, 100% flowability represents the base scenario. 200% flowability means that the flowability is improved by a factor of two; in other words, at every consolidation stress, the unconfined yield strength is halved. 50% flowability represents a much worse flowing BSM, where the unconfined yield strength is doubled at every consolidation stress.

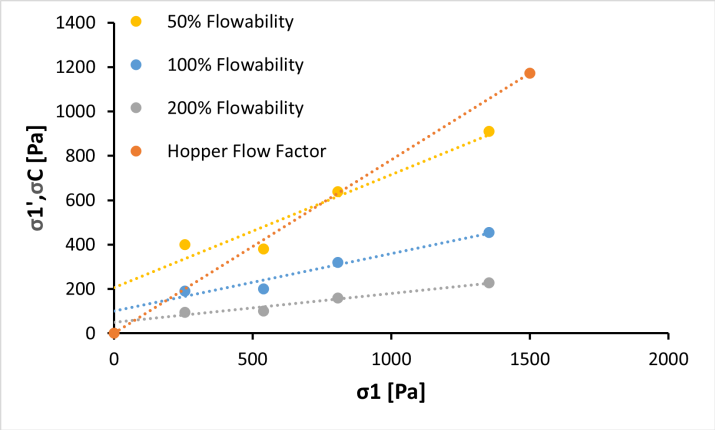

Figure 6.10: Graphical Representation of the Change in Input Used in Determining the Sensitivity of the Hopper Design on the Flowability of the BSM

Figure 6.11 shows the sensitivity of the outlet diameter when changing the flowability. It must be stressed that the 100% scenario is based on our measurements with 100% WW fines and thus already represents the worst-case scenario with respect to the flowability. The flowability of any pellets with any fines content is unlikely to be two times worse. However, the bulk density is taken at 30% fines. The bulk density is also varied in Figure 6.12. A bulk density of 300 kg m^{-3} is the bulk density of 100% fines, while a bulk density of 700 kg m^{-3} corresponds to a dense wood pellet bulk material.

Flowability has a large effect on the minimum outlet diameter. When the flowability is halved, the outlet diameter must be three times larger. Therefore, it is essential to take a sufficiently large safety factor in the design of the outlet diameter. The bulk density also has a significant influence on the minimum outlet diameter.

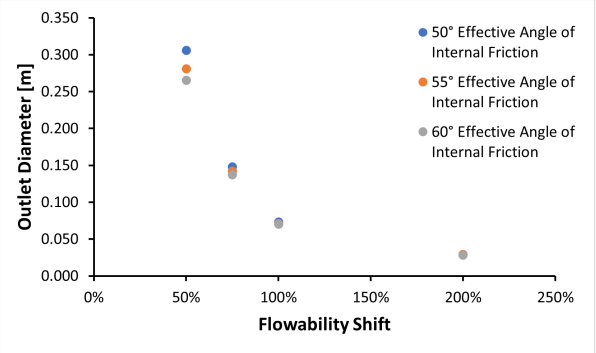

Figure 6.11: Effect of the Flowability on the Minimum Outlet Diameter

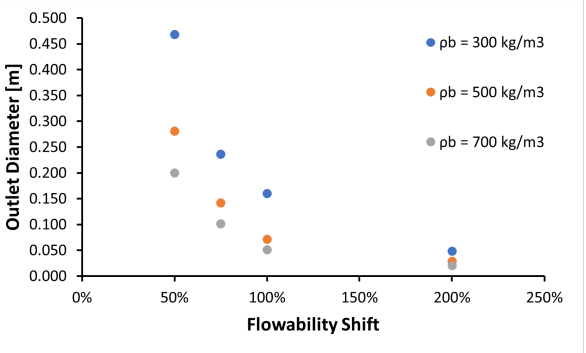

Figure 6.12: Effect of Flowability and Bulk Density on the Minimum Outlet Diameter

Mass Flow Rate

Table 6.4 shows that the mass flow rate of a hopper depends significantly on the outlet diameter. The mass flow rate also depends on the ρ_b, particle size, and hopper cone angle.

The bulk density has a linear relationship with the mass flow rate. Figure 6.13 shows the effect of the particle size and hopper angle on the mass flow rate. The particle size is the equivalent diameter of a sphere of equal volume, as discussed before. A steeper hopper cone results in a slightly increased mass flow rate. The mass flow rate is more sensitive to the particle size. A particle with an equivalent sphere diameter of 0.015 (e.g., a 20 mm long and 10 mm diameter pellet) loses about a quarter of the mass flow rate compared to a pellet of 11 mm long and 8 mm diameter. A mass flow rate of 10 t/h is assumed. If we again consider a bulk density of 300 kg m^{-3} and a particle with a diameter of 10 mm and a mean length of 20 mm, the required outlet diameter to reach double the required mass flow rate is 0.18 m. The Beverloo equation used to determine the mass flow rate works for free-flowing BSM. BSM with pellets and a high fines content are not free-flowing. It is unknown how the mass flow rate is affected.

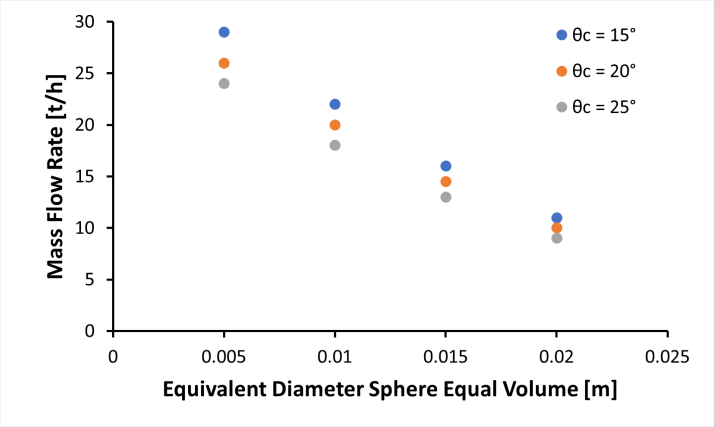

Figure 6.13: The Effect of the Particle Size and Hopper Angle on the Mass Flow Rate

6.3.7. Final Design of Conservative Hopper

The final design of the conservative hopper is presented in Figure 6.14. This hopper follows the diameter (2 m) and capacity (5 ton) presented in Table 6.1.

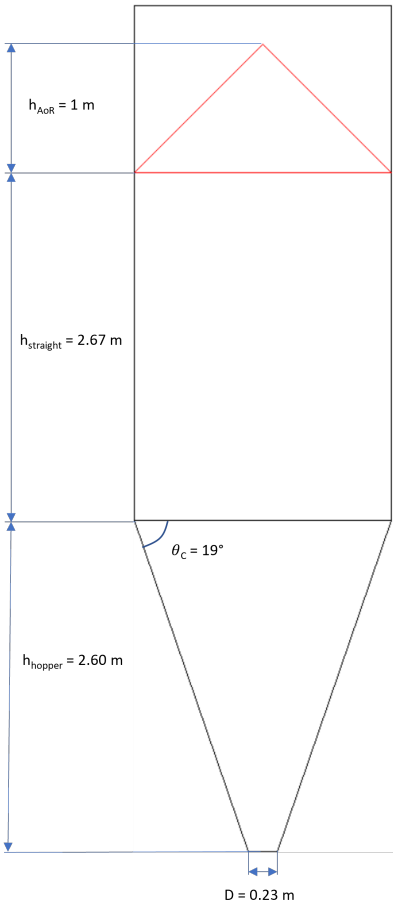

Figure 6.14: Conservative Silo Design.

6.4. Hopper Design with the Silo Design Tool

An Excel tool was developed based on the Spreadsheet method discussed before, and a lookup table with the measurement results and elementary geometry. The excel tool is able to determine silo dimensions based on the flow properties of the BSM to be stored. Combined with the Silo Stress Tool by Schulze, this tool can also give insights into stress levels in the silo and thus help with structural design.

6.4.1. Inputs and Outputs

The model can either work in an automatic or manual method. The inputs of the automatic method are:

- Pellet type
- Fines content
- Silo wall material
- Required capacity silo
- Diameter silo
- Minimum mass flow rate

If the pellet type is not present in the database, the user must input the pellet properties manually. The additional inputs of the manual method, and thus also the information of the pellets that is stored in the database, are as follows:

- Flow function/flowability
- Effective angle of internal friction
- D90 pellet length
- Bulk density
- Sphere of equivalent volume diameter
- Wall friction angle
- Heap test AoR

Based on these inputs, the model will provide the following outputs:

- Silo Dimensions, including hopper angle, outlet diameter, silo height
- Mass flow rate

6.4.2. Model working

The first step of the model is identical to the spreadsheet model. This step determines the hopper angle and minimum outlet diameter to prevent cohesive arching based on Jenike's equations. The second step calculates the minimum outlet diameters required to prevent mechanical arching, based on the rule-of-thumb. The minimum outlet diameter to reach the required mass flow rate, based on Beverloo's formula, is then calculated. The largest outlet diameter of these three is critical and thus considered for the design.

Then, using the calculated hopper angle and outlet diameter, and the required capacity, silo diameter and the AoR of the material, all dimensions of the silo can easily be determined using basic geometry. The model then shows the final design to the user.

The model is connected to a database with our measurement results, thus measurements results for these pellets do not have to be entered by the user.

6.4.3. Final Design of Hopper Design for Individual Pellet Types

The Silo Design Tool is used to design a hopper for FW, RDF and WW based on our measurements. The fines content is taken according to the mechanical durability: 10% fines content for FW, 20% fines content for RDf and a 30% fines content for WW. During the design, a safety factor of 1.5 is used on the minimum outlet diameter for cohesive and mechanical arching. A safety factor of 2 is used on the minimum flowrate. The standard safety factor is used to determine the cone angle. The measured AoR was the draw down test, while the heap test AoR must be known in silo design. To estimate the heap test AoR, the measured draw down test AoR was devided by 1.5. This is the approximate ratio between the tests according to Schwedes and Schulze (2022).

The results are shown in Figures 6.15 untill 6.17. The critical constraint for the WW and FW outlet is the mechanical arching diameter, while the critical constraint for RDF is the minimum flow rate. This difference is explained by the low bulk density of the RDF pellets. This also explains the much higher required silo.

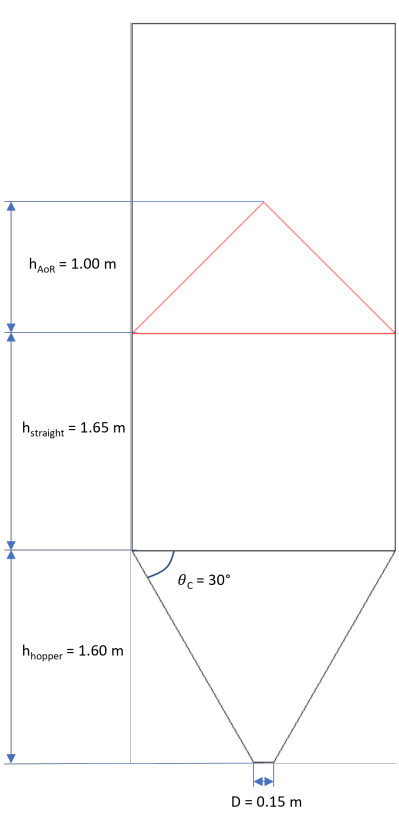

Figure 6.15: Silo Design for Waste Wood Pellets with 30% Fines Content. Flow rate is 27 t/h.

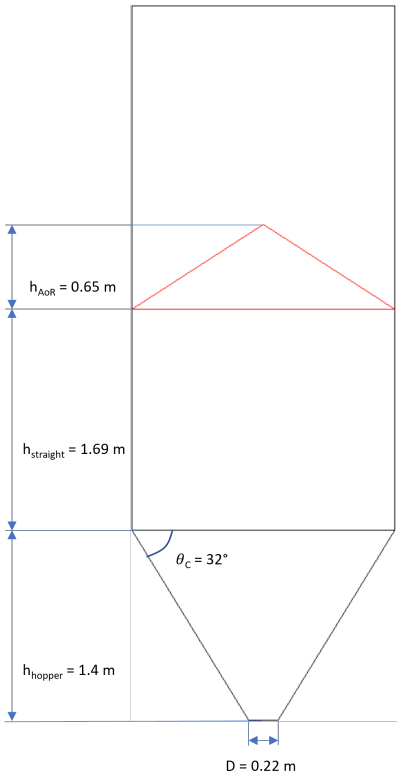

Figure 6.16: Silo Design for Fresh Wood Pellets with 10% Fines Content. Flow rate is 84 t/h.

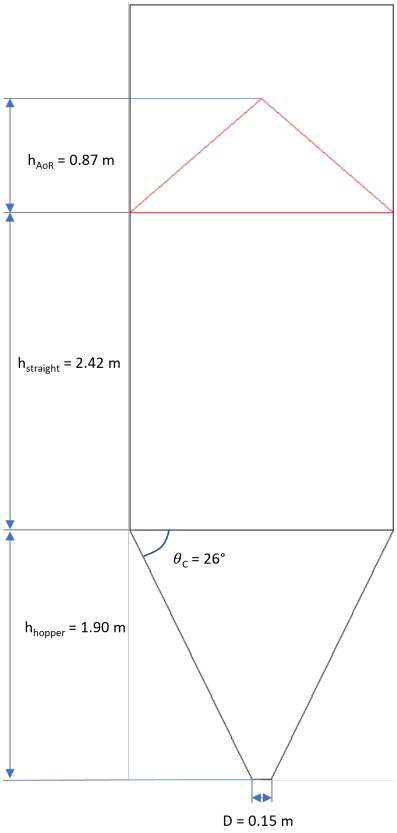

Figure 6.17: Silo Design for RDF Pellets with 20% Fines Content. Flow rate is 20 t/h.

6.5. Conclusions

The final design of the hoppers is presented in Table 6.7.

Table 6.7: Overview Design Parameters of the Four Silos

	Conservative	RDF	FW	WW
Capacity [ton]	5	5	5	5
Diameter [m]	2	2	2	2
Cone Angle [deg]	19	26	32	30
Outlet Diameter [m]	0.23	0.15	0.22	0.15
Total BSM Height [m]	6.27	5.19	3.74	4.25
Flow Rate [t/h]	-	20	84	27

In conclusion, the hopper design is mainly determined by a few BSM properties, which should thus be well-known before designing a hopper:

- The hopper cone angle is mainly affected by the wall friction angle.
- The cohesive arching, mechanical arching, and mass flow rate must be considered for the outlet sizing.
  - The flowability and the bulk density of the BSM determine the minimum outlet diameter for cohesive arching.
  - The mechanical arching depends on the particle size and shape.
  - The mass flow rate is mainly influenced by the BSM density and pellet size.
- The heap test AoR and density are important to determine the height of the silo.

Knowing these properties, the Silo Design Tool can be used to find the dimensions of a mass flow silo.

7

Conclusion and Recommendation

7.1. Conclusion

The use of biomass and waste-based pellets in the industry is growing, however, research on the flowability of pellets is scarce. In this thesis, we aimed to answer the following research question: "How can we use experiments to establish the pellet, BSM and flow properties of fresh wood, waste wood and refuse-derived fuel pellets to design a lock-hopper for material handling in gasification plants and to develop a quicker approach to establish the flow properties of pellets?"

A literature review is used to discover which factors influences the flowability of pellets, which may be used to predict the flowability. Due to a lack of literature on pellets, we considered the literature on BSM flowability in general and the following factors are recognized as large influences on the flowability of BSMs:

- Moisture Content
- Particle Size (Distribution), including fines content
- Particle Shape
- Surface Roughness
- Pressurization rate in lock-hoppers
- Chemical Composition

Furthermore, HR and AoR are often used as an alternative to shear testing. These may be more suitable in predicting the flowability than the aforementioned factors.

The literature that discusses the BSM properties of pellets, including the flowability and arching tendency, focuses almost exclusively on wood pellets, thus ignoring RDF pellets. Furthermore, the studies do not investigate the effect of the aforementioned properties on the flowability of the pellets. For example, no studies have compared the surface roughness of pellets and their flowability yet. Also, no studies investigated the feasibility of using the HR and AoR as an alternative for shear testing for pellets. Therefore, it is necessary to determine the pellet and BSM (flow) properties, including the AoR and HR, for WW, FW and RDF pellets.

An extensive measurement plan was based on various standards and previous research. Many pellet properties can be determined, such as the length distribution, diameter, density, surface roughness, mechanical durability and moisture content. The flowability and wall friction of the BSM can be determined using the Schulze Ring Shear Tester.

It was found that predicting the flowability based on the factors such as particle size, roughness and shape is unfeasible for this research, because of the time it takes to aquire the neccesary measurements. However, the fines content of the BSM can easily be varied to study the effect. The pellets were tested at 0, 10, 20 and 30% fines content, and WW/RDF and FW/RDF mixtures were evaluated.

The most important conclusions of these measurements are:

- The bulk density is barely affected by the fines. Although the bulk density of 100% fines is much lower than the bulk density of the pellets, the fines occupy the voids between the pellets and thus do not lower the bulk density up to 30% fines content.
- The RDF and WW pellets have a shorter mean and maximum length than the FW pellets but a similar shape of the distribution. Their higher mechanical durability partially explains this.
- The difference in particle size between fines can be attributed to the base materials used.
- The fines content substantially impacts the wall friction angle, already at just 10% fines content. The wall friction angle of WW pellets is decreased with the addition of fines, while the wall friction angle of FW pellets is increased. The contradicting effects of the fines on the wall friction can be caused by differences in the roughness of the pellets and the fines, and the PSD of the fines.
- Higher consolidation stresses show improved flowability and have a moderate effect on the effective angle of internal friction. The fines content hurts flowability, with flowability approaching that of 100% fines at about 30% fines content.
- The analysis of pellet mixtures revealed that the flowability of the mixtures was consistent with the individual materials. The most prevalent material mainly determined the wall friction of the mixtures.

Measuring the flowability, and a range of flow indicators, such as AoR, AoT and HR, at at 0 and 30% fines contents allows us to study the relationships between the flow indicators and flowability. The most important conclusions are:

- All three descriptors show the expected trend of decreasing flowability with an increasing AoR, AoT and HR.
- None of the relationships are accurate enough to predict the material's flowability and thus cannot be used in silo design.
- The fines content is a much more significant influence on the AoR than the flowability.
- The HR results are also heavily influenced by the fines content.
- The AoT is the most accurate, and the results depend mostly on flowability.

Finaly, four hoppers were designed:

- Conservative silo design compatible with three tested pelelts and potential future pellets
- WW pellet silo
- FW pellet silo
- RDF pellet silo

The Silo Design Tool was developed to automate the silo design process. The final design of the hoppers is presented in Table 7.1.

Table 7.1: Overview Design Parameters of the Four Silos

	Conservative	RDF	FW	WW
Capacity [ton]	5	5	5	5
Diameter [m]	2	2	2	2
Cone Angle [deg]	19	26	32	30
Outlet Diameter [m]	0.23	0.15	0.22	0.15
Total BSM Height [m]	6.27	5.19	3.74	4.25
Flow Rate [t/h]	-	20	84	27

A sensitivity analysis showed that the hopper design is mainly determined by a few BSM properties, which should thus be well-known before designing a hopper:

- The hopper cone angle is mainly affected by the wall friction angle.

- The cohesive arching, mechanical arching, and mass flow rate must be considered for the outlet sizing.
  - The flowability and the bulk density of the BSM determine the minimum outlet diameter for cohesive arching.
  - The mechanical arching depends on the particle size and shape.
  - The mass flow rate is mainly influenced by the BSM density and pellet size.
- The heap test AoR and density are important to determine the height of the silo.

Knowing these properties, the Silo Design Tool can be used to find the dimensions of a mass flow silo. Then the Silo Stress Tool can be used to determine the stresses in the silo for structural design.

7.2. Recommendations for Industry

It is wise for the industry to choose a conservative hopper design to ensure correct operation with potentially worse flowing pellets in the future. A conservative design is preferable, because slightly higher capitcal costs in the silo outweights the potential costs when flow problems cause a plant shutdown. The following properties are most important in determining whether the flow of material in the hopper will achieve mass flow:

- The **wall friction angle** of the BSM and the **hopper wall material** is most important in determining whether the BSM will achieve mass flow.
- **Flowability** and **density** are essential in determining the critical outlet diameter for cohesive arching.
- The **particle size** and **shape** are most important in determining the critical outlet diameter for mechanical arching.
- The **density** and **particle size** are most important for the mass flow rate.

Thus, of all BSM properties and interactions, the following are the most important:

- Wall Friction Angle
- Flowability
- Density
- Particle size and shape

The density and the particle size and shape are easy to determine. The flowability and wall friction angle tests require specialised equipment. Therefore, we investigated three methods of predicting flowability. Methods to predict the wall friction angle were not investigated. We do not recommend any of the three tests for use in silo design or when evaluating new pellets for use in the silo.

When confronted with a new pellet, we believe that the following points must raise the alarm, even when choosing the conservative silo design.

- Extremely low bulk densities (<350 $\mathrm{kg\,m^{-3}}$)
- Very large pellets or pellets with large aspect ratios (>6)
- Visually very poor flowing or very cohesive pellets (likely because of a high (>30%) fines content)

Unless a shear tester is available, it is difficult to say when a pellet's flowability is too poor for the chosen hopper design. If any of the abovementioned warning signs is observed, it is recommended to test the BSM with a shear tester. A safety factor is present in the proposed hopper design. Thus, a pellet must have a significantly worse flow characteristics than the RDF, WW and FW pellets tested.

If the operator of the gasification plant has any control over the properties of the pellets, the following properties are recommended:

- Small diameter (6 mm)

- Small aspect ratio (<2)
- Good mechanical durability to limit fines
- High density (>500 kg m^3)

It is still unclear which properties influence the wall friction angle. We recommend conducting wall friction tests when facing new pellets with significantly different properties (roughness, composition, hardness) than those in this research. However, even with pellets with much higher wall friction angles, the hopper will still empty completely; thus, we foresee no major issues in the plant operation.

7.3. Recommendations for Future Research

The shear tests conducted on pellets in this research were performed using a shear tester that does not meet the standards regarding size. The results should be verified using a larger shear tester. Also, the mixtures were only tested at 0% fines content. It is unknown what influences fines have in the mixtures. Furthermore, fines of different pellets can be added to other pellets. This way, it can be investigated if the difference in the effect of the fines in the wall friction for WW and FW is caused by the fines or by the pellets.

The effect of the pressure and pressurization rate of the lock-hopper on the flowability was not investigated experimentally. Literature suggests that the pressurization rate mainly effects BSMs with small particle sizes, suggesting that pellets may not be affected significantly. Also, the cohesive arching was not critical in any of our designs, thus (small) changes in the flowability do not influence the design. However, additional research is required to answer these questions with certainty, especially in situations with high fines contents because of the smaller particles.

It is still unclear which pellet properties influence the flowability and wall friction angle of the pellets in which ways. There are multiple ways in which this can be investigated further. It is possible to analyse many types of pellets and look for correlations, as done by Kamperidou (2022). Furthermore, an approach similar to Sousa et al. (2022) and Valente et al. (2020) in classifying metal powders can be used. Also, varying one variable at a time to test the effects can be used if these variables can be controlled during the production of the pellets.

The effects of segregation in the hopper were not considered in this research. For example, if a mixture of two pellets segregates, the wall friction may be dominated by the pellet ending up along the walls. The effects of segregation can be studied using DEM. The necessity of mass flow to prevent segregation can also be researched. If there is little segregation, mass flow may not be necessary, and less steep hopper angles can be used. DEM simulations can also provide insight into the effect of other material properties on the flow behaviour, such as the pellet length distribution. Finally, DEM can also be used to study the mechanical arching behaviour at the outlet.

Finally, the mass flow rate was only investigated at 0% fines content. The Beverloo formula is applicable then when the material is non-cohesive. The addition of fines reduces the flowability of the BSM and thus reduces the accuracy of the mass flow rate prediction. It is unknown how the addition of fines influences the mass flow rate. The mass flow rate is likely influenced by the decreased bulk density, the decreased flowability and the change in particle sizes.

Bibliography

Abou-Chakra, H., & Zuk, U. T. (1999). *Coefficient of friction of binary granular mixtures in contact with a smooth wall part i: Direct shear box measurements of the effects of particle size ratio and particle surface roughness*.

Al-Hashemi, H. M. B., & Al-Amoudi, O. S. B. (2018). A review on the angle of repose of granular materials. *Powder Technology*, *330*, 397–417. https://doi.org/10.1016/j.powtec.2018.02.003

Ashour, A., Wegner, S., Trittel, T., Börzsönyi, T., & Stannarius, R. (2017). Outflow and clogging of shape-anisotropic grains in hoppers with small apertures. *Soft Matter*, *13*, 402–414. https://doi.org/10.1039/c6sm02374f

Barletta, D., Berry, R. J., Larsson, S. H., Lestander, T. A., Poletto, M., & Ramírez-Gómez, Á. (2015). Assessment on bulk solids best practice techniques for flow characterization and storage/handling equipment design for biomass materials of different classes. *Fuel Processing Technology*, *138*, 540–554. https://doi.org/10.1016/j.fuproc.2015.06.034

Basu, P. (2013). *Biomass gasification, pyrolysis and torrefaction* (2nd). Elsevier Inc.

Bell, D. A., Towler, B. F., & Fan, M. (2011). *Gasifiers*. Elsevier. https://doi.org/10.1016/b978-0-8155-2049-8.10004-x

Berghel, J., Ståhl, M., Frodeson, S., Pichler, W., & Weigl-Kuska, M. (2022). A comparison of relevant data and results from single pellet press research is mission impossible: A review. *Bioresource Technology Reports*, *18*. https://doi.org/10.1016/j.biteb.2022.101054

Bernhart, M., & Fasina, O. O. (2009). Moisture effect on the storage, handling and flow properties of poultry litter. *Waste Management*, *29*, 1392–1398. https://doi.org/10.1016/j.wasman.2008.09.005

Bhaskar, T., & Pandey, A. (2015). *Advances in thermochemical conversion of biomass-introduction*. Elsevier Inc. https://doi.org/10.1016/B978-0-444-63289-0.00001-6

Bodhmage, A. (2006). *Correlation between physical properties and flowability indicators for fine powders*.

Bradley, M. S. (2016). *Biomass fuel transport and handling*. https://doi.org/10.1016/B978-1-78242-378-2.00004-3

Cheng, Z., Leal, J. H., Hartford, C. E., Carson, J. W., Donohoe, B. S., Craig, D. A., Xia, Y., Daniel, R. C., Ajayi, O. O., & Semelsberger, T. A. (2021). Flow behavior characterization of biomass feedstocks. *Powder Technology*, *387*, 156–180. https://doi.org/10.1016/j.powtec.2021.04.004

Craven, J. M., Swithenbank, J., & Sharifi, V. N. (2015). Investigation into the flow properties of coarse solid fuels for use in industrial feed systems. *Journal of Powder Technology*, *2015*, 1–12. https://doi.org/10.1155/2015/786063

Dai, J., Cui, H., & Grace, J. R. (2012). Biomass feeding for thermochemical reactors. *Progress in Energy and Combustion Science*, *38*, 716–736. https://doi.org/10.1016/j.pecs.2012.04.002

Dooley, J. H., Lanning, C. J., Yi, H., & Puri, V. (2020). Overview of doe flowability measurement and modeling project at forest concepts and penn state university. *ASABE 2020 Annual International Meeting*. https://doi.org/10.13031/aim.202000080

Energy, G. (2022). *Htw - high temperature winkler technology*. https://www.gidara-energy.com/htw

Fasina, O. O., & Sokhansanj, S. (1993). *Effect of moisture content on bulk handling properties of alfalfa pellets*.

Fitzpatrick, J. J., Barringer, S. A., & Iqbal, T. (2004). Flow property measurement of food powders and sensitivity of jenike's hopper design methodology to the measured values. *Journal of Food Engineering*, *61*, 399–405. https://doi.org/10.1016/S0260-8774(03)00147-X

Foley, D. H. (1972). Considerations of sample and feature size. *IEEE Transactions on Information Theory*, *18*, 618–626. https://doi.org/10.1109/TIT.1972.1054863

Geldart, D., Abdullah, E. C., Hassanpour, A., Nwoke, L. C., & Wouters, I. (2006). Characterization of powder flowability using measurement of angle of repose.

Gilvari, H. (2021). Degradation of biomass pellets during transport, handling and storage an experimental and numerical study. https://doi.org/10.4233/uuid:aecd60c9-f7f9-416a-92ff-80261d7c954c

Guo, Z., Chen, X., Liu, H., Guo, Q., Guo, X., & Lu, H. (2014). Theoretical and experimental investigation on angle of repose of biomass-coal blends. *Fuel*, *116*, 131–139. https://doi.org/10.1016/j.fuel.2013.07.098

Hann, D., & Strazisar, J. (2007). Influence of particle size distribution, moisture content, and particle shape on the flow properties of bulk solids. *Instrumentation Science and Technology*, *35*, 571–584. https://doi.org/10.1080/10739140701540453

Hastie, T., & Tibshirani, R. (2003). *Expression arrays and the p n problem*.

Hinterreiter, S., Hartmann, H., & Turowski, P. (2012). Method for determining bridging properties of biomass fuels-experimental and model approach. *Biomass Conversion and Biorefinery*, *2*, 109–121. https://doi.org/10.1007/s13399-012-0033-7

Igathinathane, C., Tumuluru, J. S., Sokhansanj, S., Bi, X., Lim, C. J., Melin, S., & Mohammad, E. (2010). Simple and inexpensive method of wood pellets macro-porosity measurement. *Bioresource Technology*, *101*, 6528–6537. https://doi.org/10.1016/j.biortech.2010.03.034

Ilic, D., Williams, K., Farnish, R., Webb, E., & Liu, G. (2018a). On the challenges facing the handling of solid biomass feedstocks. *Biofuels, Bioproducts and Biorefining*, *12*, 187–202. https://doi.org/10.1002/bbb.1851

Ilic, D., Williams, K., Farnish, R., Webb, E., & Liu, G. (2018b). On the challenges facing the handling of solid biomass feedstocks. *Biofuels, Bioproducts and Biorefining*, *12*, 187–202. https://doi.org/10.1002/bbb.1851

Jain, A. K., Duin, R. P., & Mao, J. (2000). Statistical pattern recognition: A review. *IEEE Transactions on Pattern Analysis and Machine Intelligence*, *22*, 4–37. https://doi.org/10.1109/34.824819

Janssen, H. (1895). Versuche uber getreidedruck in silozellen. *Z. ver. deut. Ing.*, *39*, 1045.

Järvinen, T., & Agar, D. (2014). Experimentally determined storage and handling properties of fuel pellets made from torrefied whole-tree pine chips, logging residues and beech stem wood. *Fuel*, *129*, 330–339. https://doi.org/10.1016/j.fuel.2014.03.057

Jenike, A. W. (1964). Storage and flow of solids. *Bulletin of the University of Utah*, *53*.

Jensen, P. D., Mattsson, J. E., Kofman, P. D., & Klausner, A. (2004). Tendency of wood fuels from whole trees, logging residues and roundwood to bridge over openings. *Biomass and Bioenergy*, *26*, 107–113. https://doi.org/10.1016/S0961-9534(03)00101-6

Kákonyi, M., Bárkányi, Á., Chován, T., & Németh, S. (2021). Modelling of refuse-derived fuel gasification reactor. *Chemical Engineering Transactions*, *88*, 211–216. https://doi.org/10.3303/CET2188035

Kalman, H. (2021). Quantification of mechanisms governing the angle of repose, angle of tilting, and hausner ratio to estimate the flowability of particulate materials. *Powder Technology*, *382*, 573–593. https://doi.org/10.1016/j.powtec.2021.01.012

Kamperidou, V. (2022). Quality analysis of commercially available wood pellets and correlations between pellets characteristics. *Energies*, *15*. https://doi.org/10.3390/en15082865

Kaza, S., Yao, L., Perinaz, B.-T., & Frank, v. W. (2018). *What a waste 2.0*. World Bank.

Klinghoffer, N. B., Themelis, N. J., & Castaldi, M. J. (2013). *Waste to energy (wte): An introduction*. Elsevier Ltd. https://doi.org/10.1533/9780857096364.1.3

Larsson, S. H., Lestander, T. A., Crompton, D., Melin, S., & Sokhansanj, S. (2012). Temperature patterns in large scale wood pellet silo storage. *Applied Energy*, *92*, 322–327. https://doi.org/10.1016/j.apenergy.2011.11.012

Liu, Y., Lu, H., Guo, X., Gong, X., Sun, X., & Zhao, W. (2015). An investigation of the effect of particle size on discharge behavior of pulverized coal. *Powder Technology*, *284*, 47–56. https://doi.org/10.1016/j.powtec.2015.06.041

Liu, Z., Liu, X., Fei, B., Jiang, Z., Cai, Z., & Yu, Y. (2013). The properties of pellets from mixing bamboo and rice straw. *Renewable Energy*, *55*, 1–5. https://doi.org/10.1016/j.renene.2012.12.014

Lopez, G., Artetxe, M., Amutio, M., Alvarez, J., Bilbao, J., & Olazar, M. (2018). Recent advances in the gasification of waste plastics. a critical overview. *Renewable and Sustainable Energy Reviews*, *82*, 576–596. https://doi.org/10.1016/j.rser.2017.09.032

Lu, H., Guo, X., Jin, Y., & Gong, X. (2018). Effect of moisture on flowability of pulverized coal. *Chemical Engineering Research and Design*, *133*, 326–334. https://doi.org/10.1016/j.cherd.2018.03.023

Luo, B., Wang, X., You, M., Liang, C., Liu, D., Ma, J., & Chen, X. (2023). Effect of gas permeation and consolidation stress evolution on powder flow properties in the gas pressurization process. *Granular Matter*, *25*. https://doi.org/10.1007/s10035-023-01315-0

Massaro-Sousa, L., & Ferreira, M. C. (2019). Spent coffee grounds as a renewable source of energy: An analysis of bulk powder flowability. *Particuology*, *43*, 92–100. https://doi.org/10.1016/j.partic.2018.06.002

Mattsson, J. E. (1990). Basic handling characteristics of wood fuels: Angle of repose, friction against surfaces and tendency to bridge for different assortments. *Scandinavian Journal of Forest Research*, *5*, 583–597. https://doi.org/10.1080/02827589009382641

Mcmullen, J., Fasina, O. O., Wood, C. W., & Feng, Y. (2005). *Storage and handling characteristics of pellets from poultry litter*.

Mellmann, J., Hoffmann, T., & Fürll, C. (2014). Mass flow during unloading of agricultural bulk materials from silos depending on particle form, flow properties and geometry of the discharge opening. *Powder Technology*, *253*, 46–52. https://doi.org/10.1016/j.powtec.2013.11.010

Miller, M. (2013). *Bestimmung des auslaufmassen-stroms von holzpellets in abhän-gigkeit des auslauf-durchmessers*. ThyssenKrupp Uhde GmbH.

Minglani, D., Sharma, A., Pandey, H., Dayal, R., Joshi, J. B., & Subramaniam, S. (2020). A review of granular flow in screw feeders and conveyors. *Powder Technology*, *366*, 369–381. https://doi.org/10.1016/j.powtec.2020.02.066

Motzkus, U. (1974). *Belastung von siloböden und auslauftrichtern durch körnige schüttgüter*. Technischer Universität Carolo-Wilhelmina.

Nobre, C., Longo, A., Vilarinho, C., & Gonçalves, M. (2020). Gasification of pellets produced from blends of biomass wastes and refuse derived fuel chars. *Renewable Energy*, *154*, 1294–1303. https://doi.org/10.1016/j.renene.2020.03.077

Oko, C. O. C., Diemuodeke, E. O., & Akilande, I. S. (2010). *Design of hoppers using spreadsheet* (2).

Oshima, T., Zhang, Y. L., Hirota, M., Suzuki, M., & Nakagawa, T. (1995). The effect of the types of mill on the flowability of ground powders. *Advanced Powder Technology*, *6*, 35–45. https://doi.org/10.1016/S0921-8831(08)60546-4

Pachón-Morales, J., Colin, J., Casalinho, J., Perré, P., & Puel, F. (2020). Flowability characterization of torrefied biomass powders: Static and dynamic testing. *Biomass and Bioenergy*, *138*. https://doi.org/10.1016/j.biombioe.2020.105608

Ray, A. E., Williams, C. L., Hoover, A. N., Li, C., Sale, K. L., Emerson, R. M., Klinger, J., Oksen, E., Narani, A., Yan, J., Beavers, C. M., Tanjore, D., Yunes, M., Bose, E., Leal, J. H., Bowen, J. L., Wolfrum, E. J., Resch, M. G., Semelsberger, T. A., & Donohoe, B. S. (2020). Multiscale characterization of lignocellulosic biomass variability and its implications to preprocessing and conversion: A case study for corn stover. *ACS Sustainable Chemistry and Engineering*, *8*, 3218–3230. https://doi.org/10.1021/acssuschemeng.9b06763

Rezaei, H., Lim, C. J., Lau, A., & Sokhansanj, S. (2016). Size, shape and flow characterization of ground wood chip and ground wood pellet particles. *Powder Technology*, *301*, 737–746. https://doi.org/10.1016/j.powtec.2016.07.016

Rhodes, M. (2008). *Introduction to particle technology* (2nd ed). Wiley.

Salehi, H., Berry, R., Farnish, R., & Bradley, M. (2019). A new uniaxial compression tester: Development and application. *Chemical Engineering Transactions*, *74*, 463–468. https://doi.org/10.3303/CET1974078

Sandler, N., & Wilson, D. (2010). Prediction of granule packing and flow behavior based on particle size and shape analysis. *Journal of Pharmaceutical Sciences*, *99*, 958–968. https://doi.org/10.1002/jps.21884

Schulze, D. (2007). *Powders and bulk solids*. Springer.

Schulze, D. (2021). *Powders and bulk solids*. Springer International Publishing. https://doi.org/10.1007/978-3-030-76720-4

Schwedes and Schulze. (2013). *Ermittlung von fließeigenschaften von biomasse und siloauslegung für massenfluss*. Schwedes + Schulze Schuettguttechniek GmbH.

Schwedes and Schulze. (2022). *Measurement of flow properties of waste-pellets and silo design for mass*. Schwedes + Schulze Schuettguttechniek GmbH.

Sharma, K. D., & Jain, S. (2020). Municipal solid waste generation, composition, and management: The global scenario. *Social Responsibility Journal*, *16*, 917–948. https://doi.org/10.1108/SRJ-06-2019-0210

Shen, Z., Guo, X., Wang, S., Lu, H., & Liu, H. (2022). Compression behaviour of pulverized coal under gas pressurization for the gasification process [article size plays an important role in compressionbehaviour. When the SMD of pulverized coal is greaterthan approximately 46m (HR < 1.25), there is no signif-icant compression under gas pressurization in the experi-mental rangerate more important than final pressureFinal pressure not of significant influence on the compression]. *International Journal of Energy Research*, *46*, 19064–19071. https://doi.org/10.1002/er.8509

Sokhansanj, S. (1996). *Effect of fines on storage and handling properties of alfalfa pellets*.

Sorrell, S. (2015). Reducing energy demand: A review of issues, challenges and approaches. *Renewable and Sustainable Energy Reviews*, *47*, 74–82. https://doi.org/10.1016/j.rser.2015.03.002

Sousa, B. C., Valente, R., Krueger, A., Schmid, E., Cote, D. L., & Neamtu, R. (2022). Investigating the suitability of tableau dashboards and decision trees for particulate materials science and engineering data analysis. *Minerals, Metals and Materials Series*, 691–701. https://doi.org/10.1007/978-3-030-92381-5_66

Stasiak, M., Molenda, M., Bańda, M., & Gondek, E. (2015). Mechanical properties of sawdust and woodchips. *Fuel*, *159*, 900–908. https://doi.org/10.1016/j.fuel.2015.07.044

Stasiak, M., Molenda, M., Bańda, M., Wiącek, J., Parafiniuk, P., Lisowski, A., Gancarz, M., & Gondek, E. (2019). Mechanical characteristics of pine biomass of different sizes and shapes. *European Journal of Wood and Wood Products*, *77*, 593–608. https://doi.org/10.1007/s00107-019-01415-w

Teunou, E., & Fitzpatrick, J. J. (1999). Effect of relative humidity and temperature on food powder flowability. *Food Engineering*. www.elsevier.com/locate/jfoodeng

Toscano, G., Stefano, S. D., Naspi, M., Goller, R., Masci, C., & Gasperini, T. (2022). Performance evaluation of a benchtop wood pellet length analyser based on visual imaging. *2022 IEEE Workshop on Metrology for Agriculture and Forestry, MetroAgriFor 2022 - Proceedings*, 1–6. https://doi.org/10.1109/MetroAgriFor55389.2022.9965188

Tsang, S., Kao, B., Yip, K. Y., Ho, W. S., & Lee, S. D. (2011). Decision trees for uncertain data. *IEEE Transactions on Knowledge and Data Engineering*, *23*, 64–78. https://doi.org/10.1109/TKDE.2009.175

Valente, R., Ostapenko, A., Sousa, B. C., Grubbs, J., Massar, C. J., Cote, D. L., & Neamtu, R. (2020). Classifying powder flowability for cold spray additive manufacturing using machine learning. *Proceedings - 2020 IEEE International Conference on Big Data, Big Data 2020*, 2919–2928. https://doi.org/10.1109/BigData50022.2020.9377948

Wagner, N., & Rondinelli, J. M. (2016). Theory-guided machine learning in materials science. *Frontiers in Materials*, *3*. https://doi.org/10.3389/fmats.2016.00028

Wang, C., Song, S., Gunawardana, C. A., Sun, D. J., & Sun, C. C. (2022). Effects of shear cell size on flowability of powders measured using a ring shear tester. *Powder Technology*, *396*, 555–564. https://doi.org/10.1016/j.powtec.2021.11.015

Wiese, N., & Schwedes, J. (1993). *The variation in the behaviour of bulk solids as a result of sudden pressure changes in the surrounding gas phase*.

Wiese, N., & Schwedes, J. (1991). Effects of sudden pressure changes in the surrounding gas phase on flow properties of bulk solids [Its distribution along the height resembles that of compressive strength. Therefore, the forces resulting from the pressure gradients are responsible for the consolidation of limestone.]. *Chemical Engineering Technology*, *14*, 53–59. https://doi.org/10.1002/ceat.270140108

Wu, M. R., Schott, D. L., & Lodewijks, G. (2011). Physical properties of solid biomass. *Biomass and Bioenergy*, *35*, 2093–2105. https://doi.org/10.1016/j.biombioe.2011.02.020

Xiu, H., Ma, F., Li, J., Zhao, X., Liu, L., Feng, P., Yang, X., Zhang, X., Kozliak, E., & Ji, Y. (2020). Using fractal dimension and shape factors to characterize the microcrystalline cellulose (mcc) particle morphology and powder flowability. *Powder Technology*, *364*, 241–250. https://doi.org/10.1016/j.powtec.2020.01.045

Xu, G., Li, M., & Lu, P. (2019). Experimental investigation on flow properties of different biomass and torrefied biomass powders. *Biomass and Bioenergy*, *122*, 63–75. https://doi.org/10.1016/j.biombioe.2019.01.016

Xu, G., Lu, P., Li, M., Liang, C., Xu, P., Liu, D., & Chen, X. (2018). Investigation on characterization of powder flowability using different testing methods. *Experimental Thermal and Fluid Science*, *92*, 390–401. https://doi.org/10.1016/j.expthermflusci.2017.11.008

Zafari, A., & Kianmehr, M. H. (2014). Factors affecting mechanical properties of biomass pellet from compost. *Environmental Technology (United Kingdom)*, *35*, 478–486. https://doi.org/10.1080/09593330.2013.833639

Zhang, Y., Cui, Y., Chen, P., Liu, S., Zhou, N., Ding, K., Fan, L., Peng, P., Min, M., Cheng, Y., Wang, Y., Wan, Y., Liu, Y., Li, B., & Ruan, R. (2019). *Gasification technologies and their energy potentials*. Elsevier. https://doi.org/10.1016/B978-0-444-64200-4.00014-1

Zhou, Y. C., Xu, B. H., Yu, A. B., & Zulli, P. (2001). Numerical investigation of the angle of repose of monosized spheres. *Physical Review E - Statistical Physics, Plasmas, Fluids, and Related Interdisciplinary Topics*, *64*, 8. https://doi.org/10.1103/PhysRevE.64.021301

A

Scientific Paper

Flow Behaviour of Pellets

Designing a Mass Flow Hopper for Biomass and Waste Pellets in Gasification Plant

Lars Markman, BSc; prof.dr.ir. D. Schott; E.M. Moghaddam, PhD; dr.ir. J.T. Padding
Mechanical Engineering, TU Delft

***Abstract*— Utilizing waste and wood pellets in gasification reactors is a promising solution to the waste and energy problem. However, plant shutdowns often occur due to failures in the feedstock handling systems. Unfortunately, research focusing on the flow properties and the impact of mechanical degradation on the flow properties of pellets is lacking. In this study, the flow properties of RDF, fresh wood pellets, and waste wood pellets with fines contents ranging from 0% to 30% were analyzed by Schulze Ring Shear Testing, angle of repose, angle of tilt, and Hausner ratio. The collected data was used to design a mass flow hopper and establish relationships between flowability and the angle of repose, angle of tilt, and Hausner ratio.**

Our findings revealed that the fines fraction significantly influenced wall friction at a fines content of just 10%. The fines could increase or decrease the wall friction angle depending on the material. Additionally, the fines content adversely affected the flowability, with flowability reaching the flowability of the fines fraction at 30% fines content. Mixtures of RDF with waste or fresh wood pellets showed consistent wall friction and flowability similar to the base materials. We observed that a higher angle of repose, angle of tilt, and Hausner ratio indicated lower flowability. However, their predictive accuracy was limited, and we do not recommend relying on them for hopper design.

I. Introduction

The global energy demand is rising and is primarily met by unsustainable and polluting fossil fuels (Sorrell, 2015). At the same time, the amount of municipal solid waste is rapidly growing due to economic and population growth (Kaza et al., 2018). Landfill space is limited and emits significant greenhouse gases (Kákonyi et al., 2021). Energy and waste management have long been challenging issues, but with the increasing awareness of environmental concerns, there is a growing demand for a solution (Klinghoffer et al., 2013). Waste gasification holds the potential to address energy and waste problems simultaneously.

Gasification is a thermochemical process that can convert an extensive range of feedstock, such as waste or biomass, into valuable gas. However, the feedstock must meet specific requirements for gasifier use. It must withstand high gasifier pressure and have below 15% moisture content. To achieve this, the solid fuel used in the gasifier undergoes a densification process, such as pelletization. Pelletization involves compressing the feedstock at high temperature (up to 100+°C) and pressure (20 bar) to force small particles to adhere to each other, resulting in larger, denser pellets (Gilvari, 2021).

In a gasification plant pellets must be transported into the reactor. Because of the elevated pressure, the feeding, bottom ash and dust removal systems have to be performed by lock hoppers. They are handled by a series of equipment; they end up in the pressurised lock-hopper handling systems, after which they enter the reactor. The gravity lock-hoppers are located above each other. First, the pellets enter the feed hopper. The feed hopper feeds the pellets to the lock hoppers through a chute. The lock hopper is pressurised to the desired pressure. Then, the pellets are fed to the charge bin, where they are finally transported to the gasifier using a star feeder and screw conveyors.

Plant shutdowns often occur due to failures in the handling systems for feedstock (Basu, 2013; Craven et al., 2015; Dooley et al., 2020). Problems such as flow obstructions, incomplete emptying, and segregation can arise during the discharge of solids from silos (Schulze, 2007). Another prevalent industrial problem in hoppers is arching, where particle cohesion or interlocking blocks the outlet, preventing material flow (Rezaei et al., 2016). Designing handling equipment for waste- and biomass-based pellets is particularly challenging because the materials do not have consistent specifications due to seasonal effects, long-term price fluctuations, and availability (Bradley, 2016). Additionally, pellets mechanically degrade during handling, which may increase the fines content beyond expected levels.

In order to ensure reliable flow and avoid arching, Jenike's design procedure can be used to predict the required hopper angle and minimum outlet diameter based on the hopper geometry, wall friction, flowability and effective angle of internal friction (Jenike, 1964).

Existing literature reviews on biomass flowability focus mainly on non-pelletized biomass (Cheng et al., 2021; Minglani et al., 2020; Stasiak et al., 2015). Literature on non-pelletized biomass, coal and powders identifies the most important properties that influence the flowability in BSM in general as the moisture content, the particle size (distribution), the particle shape, surface roughness, chemical composition and pressurization rate in lock-hoppers:

- A higher moisture content generally decreases the flowability because liquid bridges form and increase the cohesive forces (Bernhart & Fasina, 2009; Fasina & Sokhansanj, 1993; Hann & Strazisar, 2007; Lu et al., 2018).
- Liu et al. (2015), Pachón-Morales et al. (2020), and Rezaei et al. (2016) observe that a larger particle size increases the flowability for biomass powder, pulverized coal, and ground wood, respectively. Craven et al. (2015) had similar finding with wood chips, which had significantly larger particle sizes than the powders.
- A higher fines content dramatically influences the flowability because it results in more particle-particle contacts (Hann & Strazisar, 2007; Pachón-Morales et al., 2020; Sokhansanj, 1996).
- The pressurization rate is the main cause of a decrease in the flowability in lock-hoppers, however, this effect

TABLE I: Properties of Pellets in Literature

	Factor	Wu et al. (2011)	Stasiak et al. (2019)	Mattsson (1990)	Craven et al. (2015)	Hinterreiter et al. (2012)	Fasina and Sokhansanj (1993)	Schwedes and Schulze (2013)	Schwedes and Schulze (2022)	Miller (2013)
Pellet Type	-	Wood	Wood	Wood	Wood	Wood	Feed (Alfalfa)	Wood, straw	Waste Wood, RDF	Wood (A1)
Size	Diameter (mm)	6-12	6	12	6	7	6.7-10.1	6-8	8	8
	Length (mm)	10-20	8-30	15		18	5-15	-	10-25	3.15-40
Density	Bulk Density ($kg\,m^{-3}$)	500-650	-	-	650	773	580-670	-	550-615	600
	Particle Density ($kg\,m^{-3}$)	1100-1900	-	-	1260	-	-	-	-	-
	Compressibility (HR)	-	1.09	-	-	-	-	-	tested	-
	Moisture Content (% wb)	8-11	-	15	-	-	7-18	6-8	-	-
Flowability	FFc	-	-	-	6.12	-	-	-	-	-
	Angle of Internal Friction	33-43	26-30	-	35-40	-	23-27	-	-	-
	Effective Angle of Internal Friction	39-45	33-37	-	40-45	-	-	-	-	-
	Angle of Repose	32-41	-	35	-	-	27-34	-	33	-
Arching	Arching distance (mm)	-	-	30	-	29-35	-	-	-	-
	Arching Diameter	-	-	-	-	-	-	-	-	80
Wall friction	Tivar	11-13	-	-	15-18	-	-	-	-	-
	Steel	18-19	-	-	15-18	-	-	20-25	19-26	-
	Stainless steel	18-19	-	-	26-28	-	-	23-25	14-16	-

is most prevalant with powders with small particle sizes (Luo et al., 2023; Shen et al., 2022; Wiese & Schwedes, 1993; Wiese & Schwedes, 1991).

Table I presents an overview of the results from literature that focuses on pellet flow properties. The literature that measures the BSM properties of pellets, including the flowability and arching tendency, focuses almost exclusively on wood pellets, thus ignoring RDF pellets. Furthermore, these studies do not investigate the effect of the pellet properties on the flowability of the pellets. For example, no studies have compared the surface roughness of pellets and their flowability yet. Furthermore, although it is common to use the AoR and HR as an indicator for flowability in industrial environment and research due to speed and ease of use, no research has yet compared the AoR, HR and shear test results for pellets (Al-Hashemi & Al-Amoudi, 2018; Kalman, 2021; Massaro-Sousa & Ferreira, 2019; Salehi et al., 2019). For these reasons, it is necessary to determine the pellet and BSM (flow) properties, including the AoR and HR, for WW, FW and RDF pellets.

This paper aims to analyze the flow properties of three different biomass and waste pellets with four different testing methods (Schulze ring shear test, angle of repose, angle of tilt and Hausner ratio). The effect of mechanical degradation on the flowability was investigated by varying the fines content. The results from the four different testing methods were correlated to determine their predictive powers. It was found that predicting the flowability based on the factors such as particle size, roughness and shape is unfeasible for this research, because of the time it takes to aquire the neccesary measurements. Finally, a hopper was designed based on the flowability measurements and sensitivity analysis of Jenike's hopper design method.

II. Materials and methods

A. Materials

Waste wood (WW) and *refuse-derived fuel* (RDF) pellets were sourced from industry, while commercially available *fresh wood* (FW) pellets of A1 quality were obtained. The properties of these pellets are presented in Table II, and the *pellet length distribution* (PLD) is depicted in Figure 2. Measurements were taken using a calliper (ISO 17829) on the delivered material to determine the PLD before conducting mechanical degradation tests. Considering the unpredictability of waste streams, a mixture of two types of pellets may be utilized instead of a single pellet. Therefore, the impact of pellet mixing on flowability and wall friction is also examined in this study.

When pellets physically degrade, fines and lumps are formed, shown in Figure 1. Fines are particles that measure less than 3.15 mm, while lumps refer to particles ranging from 3.15 mm to 5.6 mm in size (Gilvari, 2021). The proportion of fines and lumps resulting from physical degradation varies depending on the pellet type, particularly the size of the material used in pellet production. Figure 3 presents the ratios determined for the pellets in this research, using the Tumbler 1000+ per ISO 17831-1 (EN 15210-1) standards. Henceforth, the term "fines contents" will encompass a mixture of fines and lumps, as determined by the ratios depicted in the figure. Different fines contents (fines + lumps) were examined throughout the experiments, specifically 0%, 10%, 20%, 30%, and 100%. Fines and

Fig. 1: From Left to Right: Waste Wood, RDF, Fresh Wood
From Top to Bottom: Pellets, Lumps, Fines

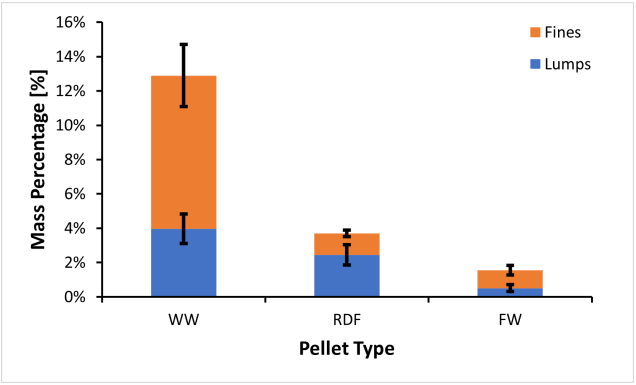

Fig. 3: The Mass Percentage of Fines (<3.15 mm) and Lumps (3.15<lumps<5.6 mm) Generated by the Mechanical Durability Test. The Error Bars Represent the Standard Deviation of the Results.

lumps were obtained by grinding the pellets in a blender and then sieving the material to obtain the fines and lumps.

B. Methods

1) Angle of repose and tilt: The *angle of repose* (AoR) depends on the chosen test procedure: thus, it is not a material property. The AoR is affected by three mechanisms (Kalman, 2021), illustrated in Figure 4. 1) Wall sliding of the particles along the bottom wall, which is affected by the wall friction. 2) Local avalanches are caused by individual particles rolling down the heap. 3) Unstable shear surfaces within the heap are affected by the internal friction of the material. Only the last mechanism is of interest for the flowability of the material. Therefore, we use the ledge test, where the bottom of the box eliminates particles sliding along the bottom wall with an edge. The box is filled with material, then one of the sides of the box is opened, and the material flows out. The angle is measured using a protractor on the transparent side of the box. The effect of local avalanches cannot be eliminated. Still, as Kalman (2021) recommends, we always take the largest angle in a heap to minimize the effect of recent local avalanches.

A second AoR test is the *angle of tilt* (AoT) test, which Kalman (2021) described in detail. A box is placed on a tilting plane and filled to the brim with pellets. The angle at which a significant material flow occurs is defined as the tilting angle. The tilting angle is unaffected by wall sliding and local avalanches, making it theoretically superior to the AoR at predicting flowability. The inclinometer has an accuracy of 0.3°. A more significant source of inaccuracy is determining the moment flow starts. The test operator must discern between local avalanches and flow due to unstable shear surfaces.

2) Hausner ratio: The *Hausner ratio* (HR) test assumes that the bulk solid has a relatively large void ratio due to interparticle adhesive forces in solids with poor flowability. Therefore, after initial filling, the void ratio can be reduced significantly by tapping the container. The HR is a measure of the compressibility of a bulk solid and is calculated with Equation 1, where ρ_t is the tapped bulk density and ρ_b the untapped, loose bulk density.

$$HR = \frac{\rho_t}{\rho_b} \tag{1}$$

In this research, a 1000 ml plastic measuring cylinder is filled with the bulk solid from approximately 100 mm above the brim of the cylinder. The filled cylinder is weighed with a laboratory balance accurate to 0.1 g (Kern EMS). The volume is read to the nearest 5 ml. Then the cylinder is placed on a mechanical sieving device until the volume is not reduced further by tapping or dropping the cylinder. This procedure is similar to the literature for biomass (Igathinathane et al., 2010; Salehi et al., 2019; Stasiak et al., 2019).

3) Schulze Ring Shear Tester: The bulk material's flow properties and wall friction are evaluated with the *Schulze Ring Shear Tester* (RST), according to ASTM D6773-22 and the manuals belonging to the RST. The material was

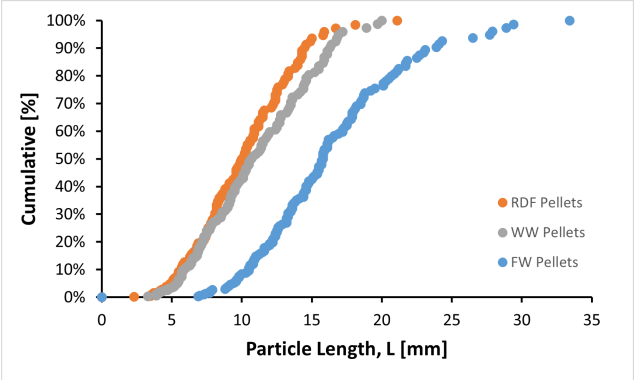

Fig. 2: Pellet Length Distribution of the Three Pellet Types

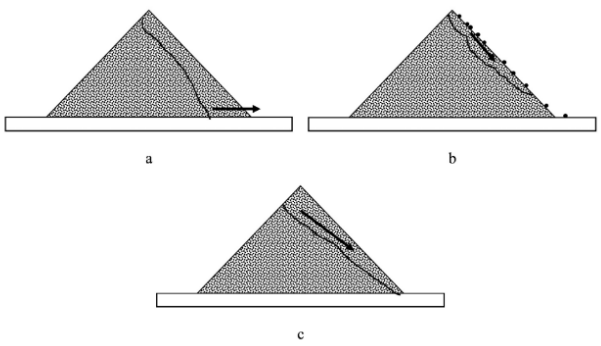

Fig. 4: Mechanisms affecting the angle of repose (Kalman, 2021)

TABLE II: Properties of the pellets used in this research with the 95% CI where applicable

Sample	Diameter (mm)	Mean Length (mm)	L/D ratio (-)	Mechanical Durability (%)	Surface Roughness Rq (um)	pellet density ($kg\,m^{-3}$)	Bulk Density ($kg\,m^{-3}$)
RDF	6.27±0.06	10.0±1.0	1.6	97.9±0.25	21.7±4.7	962±36	470
Waste Wood	8.37±0.10	10.8±0.7	1.3	88.2±1.24	7.7±1.1	1112±37	620
Fresh Wood	6.15±0.03	16.1±1.5	2.6	98.8±0.0	9.3±2.5	1146±20	650

tested at 1250 Pa and 10,000 Pa consolidation stresses. The wall friction was evaluated at 800 Pa, 4,400 Pa and 8,000 Pa normal stress on cold-rolled steel.

The standards outline that the width of the annulus must be 20 times the particle size when conducting measurements using the RST. Failure to meet this criterion may lead to inaccuracies because no defined sear plane may form. In contrast to the standard, Barletta et al. (2015) discovered that, despite wood chips being officially too large for the tester, the RST can still yield accurate results regarding flowability. However, the wall friction angles were lower than those obtained with a larger tester, potentially resulting in under-engineered equipment designs.

In a study by Wang et al. (2022), the effect of shear cell size on the flowability of powders was experimentally investigated. They found that employing a smaller shear tester could lead to 15% higher flowability values, even when dealing with particle sizes significantly smaller than the recommended values. Additionally, the researchers observed poor reproducibility of the tests when working with larger particles. According to ASTM D6773-08, using a smaller shear cell can result in higher measured shear strengths and, consequently, slightly larger unconfined yield strengths resulting in a more conservative design.

III. Results and Discussion

All tests were conducted in the same laboratory. The ambient temperature varied from 17 to 24°C during the experiments and the relative humidity varied from 30 to 60%.

A. BSM properties and the effect of fines

Figure 5 shows the effect of the fines content on the wall friction at 800 Pa normal pressure, which is close to the pressure at the outlet and thus critical for the design of the hopper. The influence of the fines content on the wall friction angle is minor for RDF. The wall friction angle for waste wood pellets decreases sharply when fines are added and is steady after 10% fines content. For fresh wood pellets, the wall friction increases sharply when fines are added, reaching the maximum after only 10% fines content.

The results in this paper and the research of Schwedes and Schulze (2013) show that increasing the fines content initially influences the wall friction angle but quickly reaches a constant one. The fines govern the wall friction angle of a pellet fines mixture at just a 10% fines content. A small number of fines may behave as a thin layer between the pellets and the wall materials. Furthermore, due to the orientation of the wall friction test, where the wall material is below the bulk solid material, the fines content is higher than average at the BSM-wall interface due to segregation. This is not a problem, as in a hopper, the fines content will also be higher at the walls due to segregation.

Abou-Chakra and Zuk (1999) discovered that wall friction is primarily and negatively influenced by fines when the fines are smooth and the coarse particles are rough. This finding can be applied to our scenario involving FW pellets, where the inclusion of fines increases the wall friction angle. Consequently, it can be inferred that the fines in FW pellets are smoother than the pellets themselves. In contrast, regarding WW pellets, the fines contribute to a decrease in the wall friction angle. In this case, the fines fraction appears to act as a lubricant for the smooth pellets, reducing wall friction.

The data presented in Figure 6 show the effect of the fines content on the effective angle of internal friction, indicating that an increase in fines leads to a higher angle of internal friction. Similarly, Figure 7 illustrates a decrease in flowability as the fines content increases. Notably, significant decreases in flowability are observed at 10% and 20% fines content for both RDF and FW pellets. Waste wood pellets show a different trend, where flowability initially increases at 10% fines content, remains similar to the flowability at 0% fines at 20% fines content, and only begins to decrease at 30% fines content. This behaviour aligns with the findings regarding wall friction, where WW pellets also demonstrate that fines can act as a lubricant for WW pellets.

Moreover, the decrease in flowability appears to approach the flowability observed at 100% fines content, suggesting that the fines govern the flow characteristics. This observation agrees with Schulze (2007), who stated that the fines primarily determine flowability when they constitute approximately one-third of the total mass. Additionally, Hann and Strazisar (2007) investigated the impact of fines in limestone powders and found that fines have a limited influence up to a 20% mass content. Beyond that threshold, however, the influence of fines increases significantly, with the mixture exhibiting an unconfined yield strength similar to that of the fines fraction itself at approximately 40% fines content. This is similar to our findings with WW pellets.

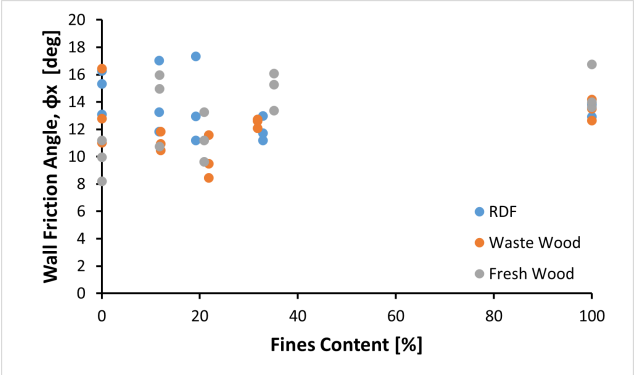

Fig. 5: The Effect of Fines on the Wall Friction Angle of the Three Pellets at 800 Pa Normal Pressure

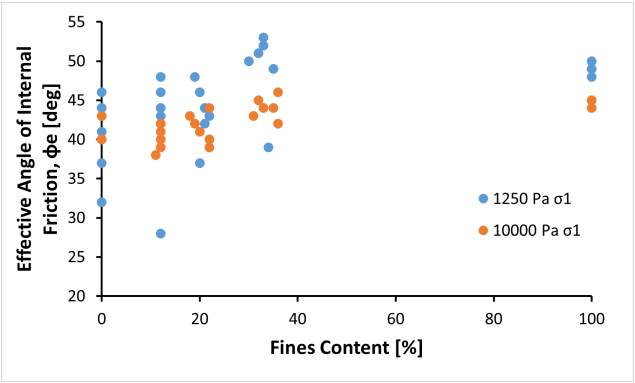

Fig. 6: The Effect of Fines on the Effective Angle of Internal Friction at Two Consolidation Stresses for all Pellets Combined

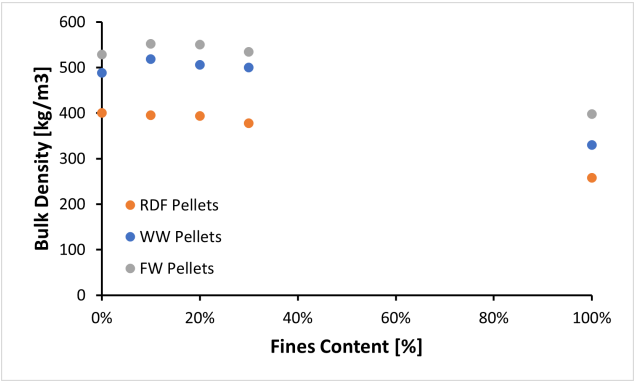

Fig. 8: Effect of the Fines Content on the Bulk Density Measured by the RST at 1250 Pa Consolidation Stress

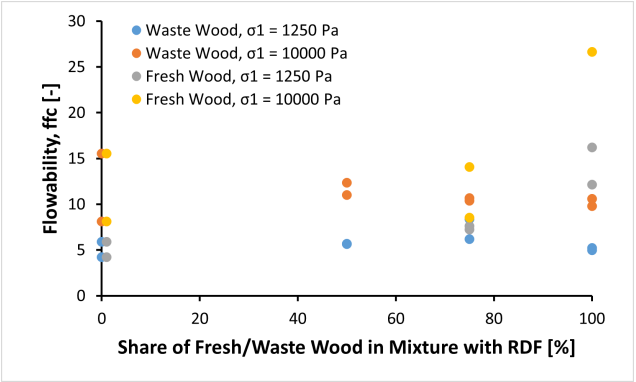

Fig. 9: Effect of Mixture Ratio on Flowability

B. Density

The bulk density of the pellets is measured using the standardized test according to ISO 17828, the tapped and loose bulk density is measured during the HR, and the bulk density is measured in the RST. Figure 8 shows the effect of the fines content as measured with the RST at 1250 Pa consolidation stress. The magnitude of the results is inconsistent with the bulk density and HR test, but there is no reason to believe the trend is incorrect. Furthermore, the HR bulk densities at 0% and 30% fines content confirm the trend.

The bulk density initially increases slightly with the addition of fines. The fines can occupy the voids between the pellets at low fines content, thus increasing the bulk density. This effect is most pronounced at 10% fines content. At higher fines contents, the low bulk density and poor flowability of the fines negate the positive effect.

C. Effect of mixtures on flowability and wall friction

We aimed to examine the impact of mixing pellets on both flowability and wall friction. Figure 9 presents the results, with the mixture ratio depicted on the x-axis. The data indicates that the flowability of the mixture aligns with the behaviour observed for the individual materials.

Figure 10 and Figure 11 display the wall yield loci of individual pellets and mixtures. The results indicate that the material with the highest ratio in the mixture primarily influences the wall friction. Consequently, the addition of a small percentage of a material with higher wall friction does not have a significant negative impact on the overall wall friction of the mixture. In particular, Figure 11 demonstrates that the wall friction of a 50/50 mixture approximates the average of the individual BSMs. This suggests the relative contributions of the individual materials determine the wall friction of the mixture. Schwedes and Schulze (2022) found that the wall friction angle of WW on cold-rolled steel increased by 1 to 2° when adding 20% RDF to the mixture.

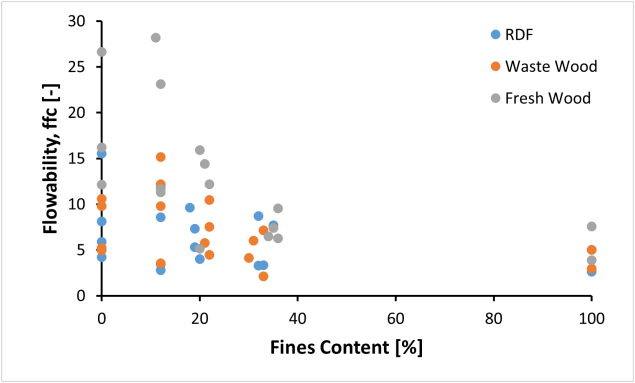

Fig. 7: The Effect of Fines on the Flowability of all Pellets for all Consolidation Stresses Combined

D. AoR, AoT and HR

The Angle of Repose (AoR) and Hausner Ratio (HR) are commonly employed to quantify flowability in place of shear testing. Table III presents the relationships between the Angle of Repose, Hausner Ratio, and flowability based on existing literature. Their relationship with flowability for pellets must still be investigated. Thus, we investigate the relationships between the flowability and the AoR, AoT and HR for pellets with 0% and 30% fines content. We explored

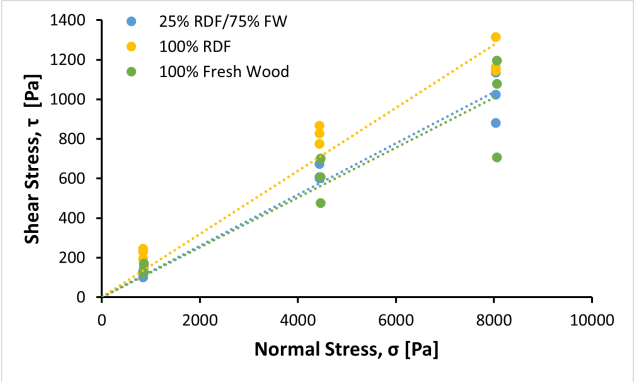

Fig. 10: Wall Yield Loci for Fresh Wood and RDF Mixtures

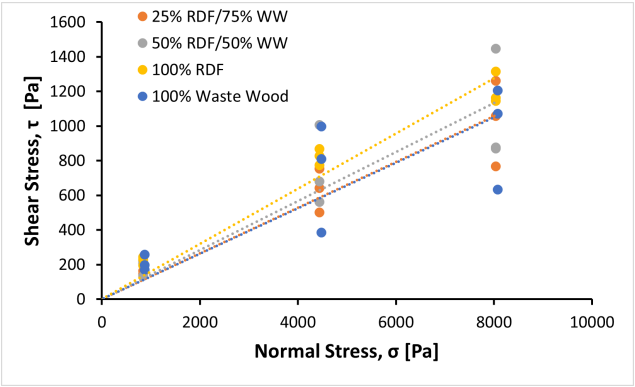

Fig. 11: Wall Yield Loci for Waste Wood and RDF Mixtures

TABLE III: Descriptions of flowability based on the Angle of Repose, Flow Factor and Hausner Ratio

Description	Angle of Repose	Flow Factor	Hausner Ratio
Very free-flowing	<30°		1.00-1.11
Free-flowing	30-38°	>10	1.12-1.18
Fair	38-45°	4-10	1.19-1.25
passable			1.26-1.34
Cohesive	45-55°	2-4	1.35-1.45
Very cohesive	>55°	1-2	1.46-1.59
No flow		<1	>1.59

the correlations between flowability and the AoR, AoT and HR for these pellets. Table IV shows the mean values of the measurements.

Figure 12 demonstrates the relationship between the AoR and flowability. It shows the expected pattern, where a higher AoR indicates poorer flowability, but the relationship is weak and does not work across fines contents. The test can only discriminate the pellets according to flowability at the same fines content. Interestingly, the AoR is very good at classifying the fines content: all measurements around 45° belong to 0% fines content, and all measurements above 55° belong to 30% fines content measurements. Fines content has a more significant impact on the AoR than it has on flowability.

The data presented in Table III do not correspond to the abovementioned findings. This discrepancy can be attributed to variations in the AoR measurement setup. In a study by Schwedes and Schulze (2022), a comparison was made between the AoR of WW pellets measured using the drawdown and heap methods, revealing that the drawdown test obtains values that are about 1.5 times higher than those obtained using the heap method.

The relationship between the AoT and flowability is depicted in Figure 13. According to Kalman (2021), the AoT is unaffected by local avalanches and solely determined by unstable shear surfaces, making it a potentially more accurate predictor of material flowability than the AoR. In

TABLE IV: Mean Values of the Flowability and Flow Indicators

Fines Content	Pellet	FFc [-] 1250 Pa	FFc [-] 10 kPa	AoR [°]	AoT [°]	HR [-]
0%	WW	5.1	10.2	47	57	1.16
	RDF	5.0	11.8	48	59	1.16
	FW	14.2	38.7	44	50	1.11
30%	WW	3.1	6.6	67	60	1.21
	RDF	3.3	8.2	68	64	1.18
	FW	6.9	7.9	58	53	1.21

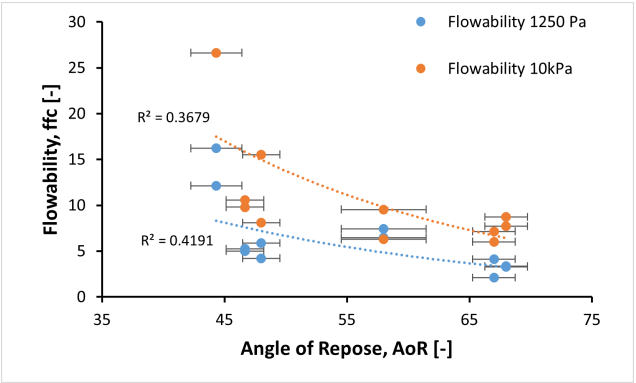

Fig. 12: The relationship between the Angle of Repose and Flowability for the Tested Pellets. The error bars represent the standard deviation of the results.

contrast, our experiments showed that local avalanches still occur during the tilting process, particularly when pellets start rolling. This creates challenges in precisely determining the moment of flow initiation due to an unstable shear surface.

The results do show a strong correlation between the AoT and the flowability, particularly at 1250 Pa consolidation stress. This is expected because the AoT test is also conducted at very low consolidation stresses. The relative spread in the measurements is large, mainly because of the small range of AoT measurements and the difficulty for the operator to determine the angle when flow occurs due to an unstable shear surface.

Figure 15 shows the relationship between HR and flowability. The test can identify the FW pellets' higher flowability at 0% fines content but surprisingly attributes the best score to the RDF pellets at 30% fines content. The HR test has greater predictive quality of flowability values at the highest consolidation stress. This is unexpected because the BSM is not consolidated during the HR test. This conclusion is only due to the RDF results at 30% fines, which show high flowability and low HR. The low HR of RDF at 30% fines content compared to the wood pellets may also be explained by the different compositions of the fines, where the RDF sample contains more lumps.

Initially, the loose density of all pellets is similar at 0% and 30% fines content. For the wood pellets, the tapped density at 30% fines is significantly higher than at 0% fines.

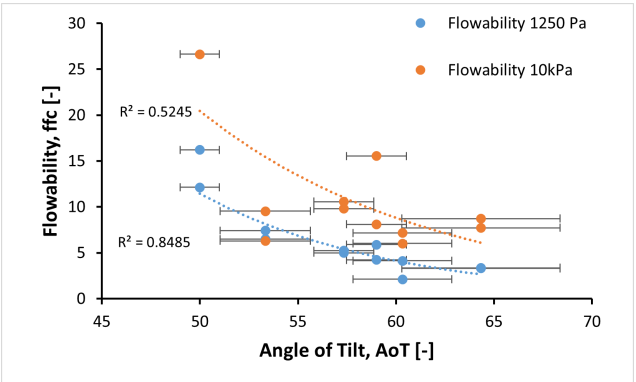

Fig. 13: The relationship between the Angle of Tilt and Flowability for the Tested Pellets. The error bars represent the standard deviation of the results.

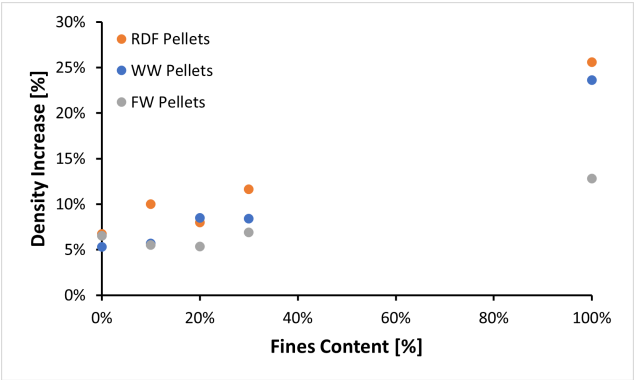

Fig. 14: Density Increase Between 1250 Pa and 10000 Pa Consolidation Stress Measured by the RST

However, the tapped bulk density does not increase for the RDF sample, which explains the low HR. The lumps may have difficulty occupying the voids between the pellets, compared to the fines, because of their larger size. Thus at 30% fines content, the RDF sample's tapped density remains relatively low compared to the wood samples. This effect is not explained by the flowability but by the PSD of the fines, and thus explains the outlier result of the RDF pellets. Salehi et al. (2019) also noted that BSMs with a higher fines content could fill the voids between larger particles and allow the attainment of larger space-filling during tapping. They also noted that a low density and high interparticle friction of biomass might reduce the effect of tapping, resulting in lower HR values.

This effect, where the RDF BSM is not as compressible by tapping at 30% content during the HR as the wood pellets, is not observed in the RST, where it is compressed under normal force. Figure 14 shows that RDF is the most compressible of all BSMs at 30% fines content. The soft pieces of plastic lumps can deform easily under pressure to fill the voids. The FW pellets have the smallest compressibility, especially at 100% fines content.

The HR test also makes a clear split between the samples with 0% and 30% fines contents: all results with an AoR of $>$1.18 belong to 30% fines content samples, $<$1.16 belong to samples with 0% fines content.

All three descriptors show the expected trend of decreasing flowability with an increasing AoR, AoT and HR. For the correct operation of the hopper, the predictive quality of the flowability descriptor at low consolidation stress is most important. None of the relationships are accurate enough to predict the material's flowability.

As Table IV shows, the AoR can rank the pellets in order of flowability at a single fines content. However, when looking at the AoR and flowability across fines content, the fines content is a much more significant influence on the AoR than the flowability. The HR ratio test results depend not only on the flowability but also on the composition of the fines. This makes it unsuitable. The AoT is the most accurate, and the results can be explained purely in terms of flowability. A drawback of the test is the difficulty to interpret the results due to local avalanches.

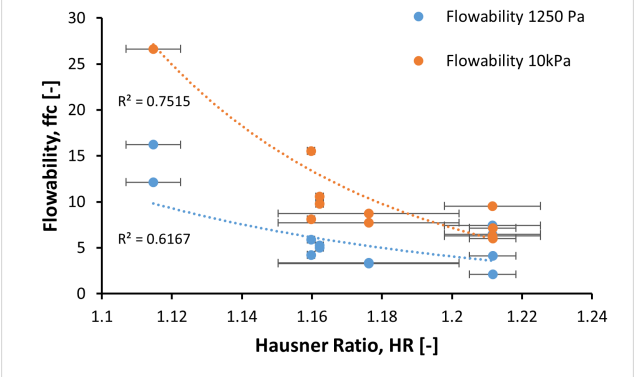

Fig. 15: The relationship between the Hausner Ratio and Flowability for the Tested Pellets. The error bars represent the standard deviation of the results.

TABLE V: Results of Jenike's Design Procedure and Comparison with Automated Hopper Design

	Jenike's Method	Spreadsheet
Cone Angle [deg]	25	24.9
Flow Factor [-]	1.35	1.28
$\sigma_c, crit$ [Pa]	200	206
Outlet Diameter [m]	0.094	0.098
Mass Flow Rate [t/h]	5.34	6.23

E. Hopper design

We use Jenike's design procedure to design a mass flow hopper for the evaluated pellet types and their fines contents. Figures 5 and 6 determine the worst-case wall friction angle and effective angle of internal friction. Furthermore, the yield locus for 100% waste wood fines is used to establish the minimum outlet diameter necessary to prevent cohesive arching (Figure 16). For these calculations, a bulk density of 500 $\mathrm{kg\,m^{-3}}$ at 30% fines content is assumed. Table V shows the results of the design.

Table V provides the minimum outlet diameter required to prevent cohesive arching. Next to cohesive arching, mechanical arching is a also significant concern, given the size of the pellets. The general guideline for preventing mechanical arching suggests using 6-10 times the maximum particle size for conical hoppers and 3-7 times the maximum particle size for wedge-shaped hoppers (Schulze, 2007). Table VI compares the relationship between pellet diameter and the outlet diameter, as well as pellet length (mean length, as maximum length is not reported) and the outlet diameter. It is evident that even when considering the mean length,

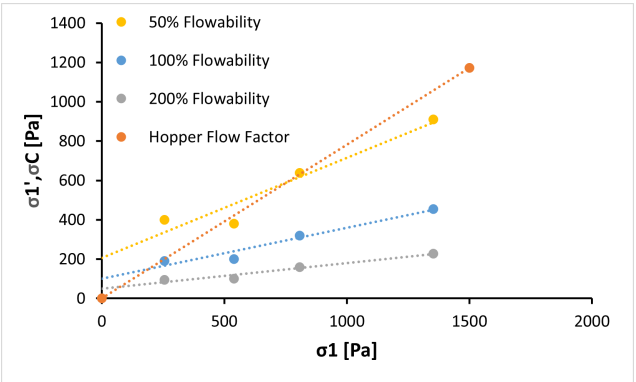

Fig. 16: Graphical Representation of the Change in Input Used in Determining the Hopper Design Sensitivity on the BSM Flowability. 100% flowability of WW Fines is used in Designing the Minimum Outlet Diameter to Prevent Cohesive Arching.

TABLE VI: Comparison of the relationship between the arching distance, pellet diameter, and mean pellet length. All research used a flat bottom silo, except for Miller, who used a cone with an angle. FW, WW and RDF results are from experiments at very small consolidation stresses.

	Mattsson (1990)	Hinterreiter et al. (2012)	Miller (2013)	FW	WW	RDF
Pellet Diameter [mm]	12	7	8	6	8	6
Mean Pellet Length [mm]	15	18	3.15-40	16	11	10
Slot Distance [mm]	30	35	-	-	-	-
Outlet Diameter [mm]	-	-	80	60	70	70
Length/outlet [-]	2.0	1.9	-	3.75	6.4	7
Diameter/outlet [-]	2.5	5	10	10	8.75	10

the rule of thumb tends to overestimate the outlet diameter for pellets. This overestimation would be even greater if we were considering the maximum particle length.

For the pellets investigated in this study (FW, WW, and RDF), the arching distance is better predicted by the diameter rather than the length. This observation is explained by the work of Ashour et al. (2017), who studied the mechanical arching of pellet-like cylindrical particles. They found that the pellets' long axis aligns towards the outlet's centre during discharge. The likelihood of clogging increases when particles are elongated while maintaining a constant volume. However, for particles with an aspect ratio below 6 (which applies to all the investigated pellets), comparing them to spheres with a similar cross-sectional area along the rotation axis (not volume) is reasonable. This suggests that, instead of focusing on the maximum pellet length, considering the diameter might be a more appropriate metric.

To determine the mass flow rate for a circular outlet and coarse-grained non-cohesive bulk solid, the Equation of Beverloo can be used (derived in Schulze (2007)). Calculating the theoretical mass flow rate for the pellets and comparing the results obtained with Beverloo's formula with the experimental results of Miller (2013) in Table VII shows a good correspondence. As Ashour et al. (2017) recommends, the pellets are modelled by spheres of equivalent volume. The minimum mass flow rate of the silo must be 10 t/h. To achieve the minimum flow rate of the hopper of 10 t/h, an outlet diameter of about 0.105 m must be used. Adding a safety factor of 2, and thus designing for 20 t/h capacity, the outlet diameter must be 0.13 m.

Considering the unpredictable nature of biomass and

TABLE VII: Comparison of Experimentally Measured and Theoretic Mass Flow Rates for Wood Pellets with a Diameter of 8 mm and Mean Length of 10 mm

Outlet Diameter	Miller (2013) (Experimental)	Beverloo's Equation (Theoretical)
55 mm	1.4 t/h	0.9 t/h
63 mm	1.6 t/h	1.4 t/h
83 mm	5.7 t/h	4.6 t/h
154 mm	36.4 t/h	34.1 t/h
247 mm	95.1 t/h	132.6 t/h

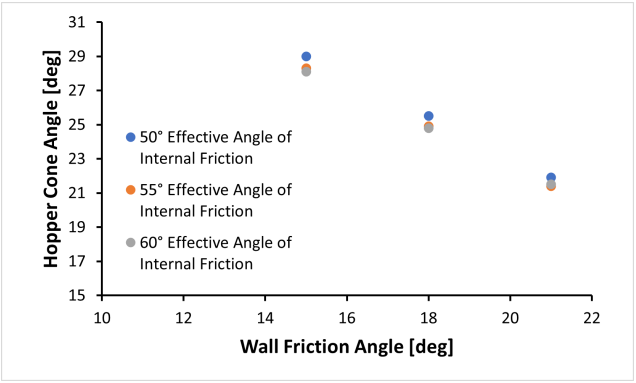

Fig. 17: The Effect of Fines on the Flowability of all Pellets for all Consolidation Stresses Combined

waste markets, it is plausible that different types of pellets with less favourable flow properties are used. Hence, it is essential to investigate the sensitivity of hopper design to variations in flow properties. Suppose the hopper design proves to be highly sensitive to specific properties. In that case, we recommend being safe and over-designing the hopper to ensure mass flow, even with poorer flowing pellets. To facilitate the analysis of hopper design sensitivity to measurements, Jenike's design procedure is automated based on the work of Oko et al. (2010).

In Figure 16, the combined effect of the wall friction angle and effective angle of internal friction on the hopper cone angle is studied. The effect of the effective angle of internal friction is negligible. The wall friction angle has a significant impact on the hopper cone angle. When a pellet with just a 3° higher wall friction angle is used, the cone angle must be increased to 21° from 25°. The effect of the wall friction angle and the effective angle of internal friction on the outlet diameter is negligible.

Another important material property in the design of a hopper is flowability. The flowability is used to draw the flow function, and the intersection with the hopper flow factor determines the size of the outlet. We study the sensitivity of the hopper design on the flowability by shifting the flow function by increasing the unconfined yield strength at every consolidation stress. This approach is shown graphically in Figure 16. In this Figure, 100% flowability represents the base scenario. 200% flowability means the unconfined yield strength is halved at every consolidation stress. 50% flowability represents a much worse flowing BSM, where the unconfined yield strength is doubled at every consolidation stress.

Figure 18 shows the sensitivity of the outlet diameter when changing the flowability. The 100% scenario is based on our measurements with 100% WW fines and thus already represents a worst-case scenario. Flowability has a significant effect on the minimum outlet diameter. When the flowability is halved, the outlet diameter must be three times larger. Therefore, it is essential to incorporate a sufficiently large safety factor in the design of the outlet diameter. The bulk density also has a linear influence on the minimum outlet diameter.

Figure 19 shows the effect of the particle size and hopper angle on the mass flow rate. The particle size is again the equivalent diameter of a sphere of equal volume. A steeper hopper cone results in a slightly increased mass flow rate.

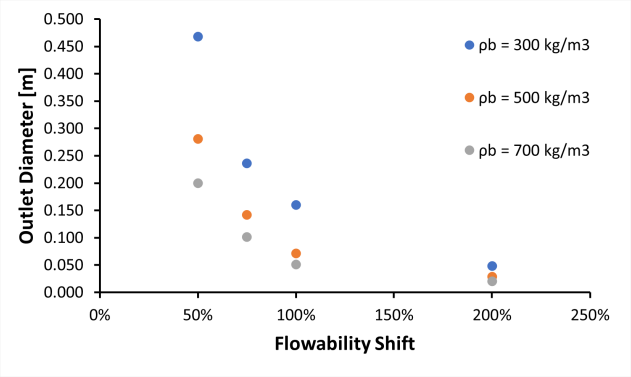

Fig. 18: Effect of Flowability and Bulk Density on the Minimum Outlet Diameter

The mass flow rate is more sensitive to the particle size. A particle with an equivalent sphere diameter of 0.015 m (e.g., a 20 mm long and 10 mm diameter pellet) loses about a quarter of the mass flow rate compared to a pellet of 11 mm long and 8 mm diameter. Furthermore, the mass flow rate depends on the outlet diameter, as shown in Table VII and linearly on the bulk density.

The hopper cone angle is mainly affected by the wall friction angle. A large range of wall friction angles can be found in literature, ranging from 14-28°. The wall friction angle also depends significantly on the wall material. Due to the wide differences in the tested pellets, in terms of roughness and mechanical durability, it is unexpected that a new pellet shows a much larger wall friction angle with the tested cold-rolled steel. The highest measured ϕ_x is 19°. Designing a hopper for a BSM with a ϕ_x of 23° results in a hopper angle of 19°. The hopper will still empty completely in the unlikely scenario of a pellet with even higher wall friction. The minimum hopper angle to ensure complete emptying is $\theta = 65 - \phi_x$, thus resulting in a minimum hopper angle of $\theta = 42°$ (Schulze, 2007).

The cohesive arching is mainly influenced by the flowability and bulk density of the BSM. A hypothetical bulk solid with unconfined yield strength 1.5 times higher than our worst measurement and a bulk density of 400 $\mathrm{kg\,m^{-3}}$ has a minimum outlet diameter of 0.18 m. Salehi et al. (2019) compared the minimum outlet diameter determined by Jenike's procedure with experimentally measured values. They found that the Jenike overestimates the required critical outlet size for pine forest residue chip of 4 to 8 mm by about

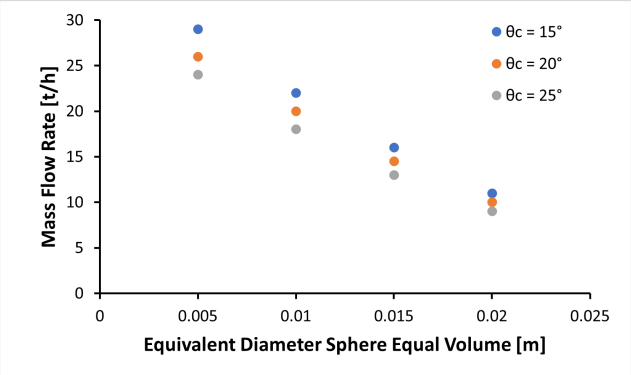

Fig. 19: The Effect of the Particle Size and Hopper Angle on the Mass Flow Rate

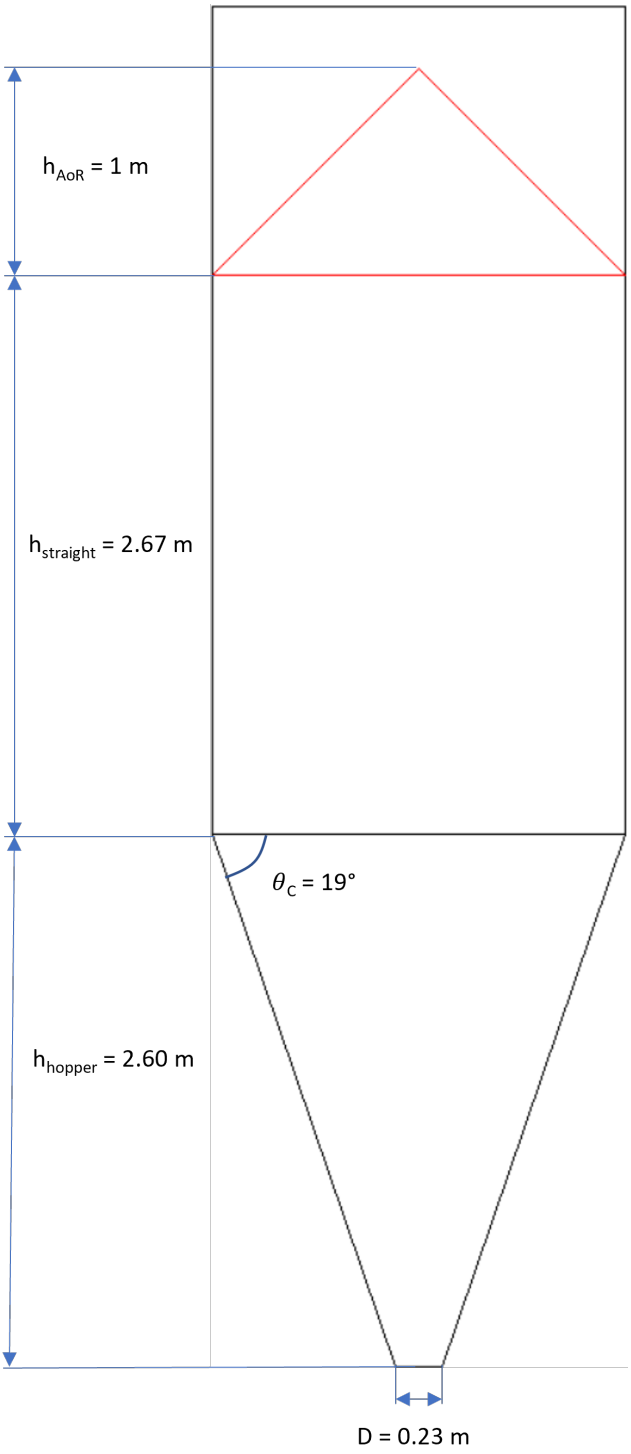

Fig. 20: Conservative Silo Design.

1.5 times.

The mechanical arching depends on the particle size and shape. We will consider the D90 pellet length and design the outlet 6 times larger. This results in a minimum outlet diameter of 0.15 m for FW pellets. Larger pellets often have a larger aspect ratio and, thus, a larger tendency to bridge. Therefore, a safety factor of 1.5 is used to obtain a minimum outlet diameter of 0.23 m. The BSM density and pellet size mainly influence the mass flow rate. A mass flow rate of 10 t/h is desired. If, once again, we consider a bulk density of 400 $\mathrm{kg\,m^{-3}}$ and a particle with a diameter of 10 mm and a mean length of 20 mm, the required outlet diameter to reach double the required mass flow rate is 0.17 m. Thus

mechanical arching is the critical mechanism to consider when designing the outlet diameter, and an outlet diameter of 0.23 m is recommended.

Finally, the hopper design procedure is automated in an Excel tool connected to a database with our experimental results for ease of use in industry. Additional pellets can also be added when the measurements are known. The results for the design in this paper are shown in Figure 20, assuming a diameter of 2 m and a capacity of 5 tonnes.

IV. Conclusions

In this study, the flow properties of RDF, FW, and WW with fines contents ranging from 0% to 30% were analyzed by Schulze Ring Shear Testing, angle of repose, angle of tilt, and Hausner ratio. The collected data enabled us study the effects of the fines on the flowability, to design a mass flow hopper and to establish relationships between flowability and the angle of repose, angle of tilt, and Hausner ratio.

The fines content substantially impacts the wall friction angle, with noticeable effects observed at just 10% fines content. The fines content hurts the flowability, with the sample's flowability with 30% fines content approaching the fines fraction's flowability. The pellet mixtures analysis revealed that the mixtures' flowability was consistent with the individual materials. The most prevalent material mainly influenced the wall friction of the mixtures. Adding a small percentage of a material with higher wall friction had a minimal impact on the overall wall friction. The bulk density is barely affected by the fines. Although the bulk density of 100% fines is much lower than the bulk density of the pellets, the fines occupy the voids between the pellets and thus do not lower the bulk density.

The flowability results were compared to the AoR, AoT and HR to see if more straightforward tests could be used to predict the flowability of pellets. All three descriptors show the expected trend of decreasing flowability with an increasing AoR, AoT and HR. However, their predictive accuracy was limited, and we do not recommend relying on them for hopper design purposes.

The wall friction angle primarily influences the hopper cone angle. Given the highest measured ϕ_x of 19°, designing a hopper for a BSM with a wall friction angle (ϕ_x) of 23° results in a hopper angle of 19°. Even in the unlikely scenario of encountering a pellet with an even higher wall friction angle, the proposed hopper design will still ensure complete emptying. Mechanical arching is the critical mechanism to consider when designing the outlet diameter, and we recommend a minimum outlet diameter of 0.23 m. Still, mechanical arching for pellets was much less likely than often thought and is only critical when the pellets are unusually long and thick. The minimum outlet diameter mechanical arching is sufficiently larger than the outlet diameter required for the mass flowrate.

References

Abou-Chakra, H., & Zuk, U. T. (1999). *Coefficient of friction of binary granular mixtures in contact with a smooth wall part i: Direct shear box measurements of the effects of particle size ratio and particle surface roughness*.

Al-Hashemi, H. M. B., & Al-Amoudi, O. S. B. (2018). A review on the angle of repose of granular materials. *Powder Technology*, *330*, 397–417. https://doi.org/10.1016/j.powtec.2018.02.003

Ashour, A., Wegner, S., Trittel, T., Börzsönyi, T., & Stannarius, R. (2017). Outflow and clogging of shape-anisotropic grains in hoppers with small apertures. *Soft Matter*, *13*, 402–414. https://doi.org/10.1039/c6sm02374f

Barletta, D., Berry, R. J., Larsson, S. H., Lestander, T. A., Poletto, M., & Ramírez-Gómez, Á. (2015). Assessment on bulk solids best practice techniques for flow characterization and storage/handling equipment design for biomass materials of different classes. *Fuel Processing Technology*, *138*, 540–554. https://doi.org/10.1016/j.fuproc.2015.06.034

Basu, P. (2013). *Biomass gasification, pyrolysis and torrefaction* (2nd). Elsevier Inc.

Bernhart, M., & Fasina, O. O. (2009). Moisture effect on the storage, handling and flow properties of poultry litter. *Waste Management*, *29*, 1392–1398. https://doi.org/10.1016/j.wasman.2008.09.005

Bradley, M. S. (2016). *Biomass fuel transport and handling*. https://doi.org/10.1016/B978-1-78242-378-2.00004-3

Cheng, Z., Leal, J. H., Hartford, C. E., Carson, J. W., Donohoe, B. S., Craig, D. A., Xia, Y., Daniel, R. C., Ajayi, O. O., & Semelsberger, T. A. (2021). Flow behavior characterization of biomass feedstocks. *Powder Technology*, *387*, 156–180. https://doi.org/10.1016/j.powtec.2021.04.004

Craven, J. M., Swithenbank, J., & Sharifi, V. N. (2015). Investigation into the flow properties of coarse solid fuels for use in industrial feed systems. *Journal of Powder Technology*, *2015*, 1–12. https://doi.org/10.1155/2015/786063

Dooley, J. H., Lanning, C. J., Yi, H., & Puri, V. (2020). Overview of doe flowability measurement and modeling project at forest concepts and penn state university. *ASABE 2020 Annual International Meeting*. https://doi.org/10.13031/aim.202000080

Fasina, O. O., & Sokhansanj, S. (1993). *Effect of moisture content on bulk handling properties of alfalfa pellets*.

Gilvari, H. (2021). Degradation of biomass pellets during transport, handling and storage an experimental and numerical study. https://doi.org/10.4233/uuid:aecd60c9-f7f9-416a-92ff-80261d7c954c

Hann, D., & Strazisar, J. (2007). Influence of particle size distribution, moisture content, and particle shape on

the flow properties of bulk solids. *Instrumentation Science and Technology*, *35*, 571–584. https://doi.org/10.1080/10739140701540453

Hinterreiter, S., Hartmann, H., & Turowski, P. (2012). Method for determining bridging properties of biomass fuels-experimental and model approach. *Biomass Conversion and Biorefinery*, *2*, 109–121. https://doi.org/10.1007/s13399-012-0033-7

Igathinathane, C., Tumuluru, J. S., Sokhansanj, S., Bi, X., Lim, C. J., Melin, S., & Mohammad, E. (2010). Simple and inexpensive method of wood pellets macro-porosity measurement. *Bioresource Technology*, *101*, 6528–6537. https://doi.org/10.1016/j.biortech.2010.03.034

Jenike, A. W. (1964). Storage and flow of solids. *Bulletin of the University of Utah*, *53*.

Kákonyi, M., Bárkányi, Á., Chován, T., & Németh, S. (2021). Modelling of refuse-derived fuel gasification reactor. *Chemical Engineering Transactions*, *88*, 211–216. https://doi.org/10.3303/CET2188035

Kalman, H. (2021). Quantification of mechanisms governing the angle of repose, angle of tilting, and hausner ratio to estimate the flowability of particulate materials. *Powder Technology*, *382*, 573–593. https://doi.org/10.1016/j.powtec.2021.01.012

Kaza, S., Yao, L., Perinaz, B.-T., & Frank, v. W. (2018). *What a waste 2.0*. World Bank.

Klinghoffer, N. B., Themelis, N. J., & Castaldi, M. J. (2013). *Waste to energy (wte): An introduction*. Elsevier Ltd. https://doi.org/10.1533/9780857096364.1.3

Liu, Y., Lu, H., Guo, X., Gong, X., Sun, X., & Zhao, W. (2015). An investigation of the effect of particle size on discharge behavior of pulverized coal. *Powder Technology*, *284*, 47–56. https://doi.org/10.1016/j.powtec.2015.06.041

Lu, H., Guo, X., Jin, Y., & Gong, X. (2018). Effect of moisture on flowability of pulverized coal. *Chemical Engineering Research and Design*, *133*, 326–334. https://doi.org/10.1016/j.cherd.2018.03.023

Luo, B., Wang, X., You, M., Liang, C., Liu, D., Ma, J., & Chen, X. (2023). Effect of gas permeation and consolidation stress evolution on powder flow properties in the gas pressurization process. *Granular Matter*, *25*. https://doi.org/10.1007/s10035-023-01315-0

Massaro-Sousa, L., & Ferreira, M. C. (2019). Spent coffee grounds as a renewable source of energy: An analysis of bulk powder flowability. *Particuology*, *43*, 92–100. https://doi.org/10.1016/j.partic.2018.06.002

Mattsson, J. E. (1990). Basic handling characteristics of wood fuels: Angle of repose, friction against surfaces and tendency to bridge for different assortments. *Scandinavian Journal of Forest Research*, *5*, 583–597. https://doi.org/10.1080/02827589009382641

Miller, M. (2013). *Bestimmung des auslaufmassen-stroms von holzpellets in abhän-gigkeit des auslaufdurchmessers*. ThyssenKrupp Uhde GmbH.

Minglani, D., Sharma, A., Pandey, H., Dayal, R., Joshi, J. B., & Subramaniam, S. (2020). A review of granular flow in screw feeders and conveyors. *Powder Technology*, *366*, 369–381. https://doi.org/10.1016/j.powtec.2020.02.066

Oko, C. O. C., Diemuodeke, E. O., & Akilande, I. S. (2010). *Design of hoppers using spreadsheet* (2).

Pachón-Morales, J., Colin, J., Casalinho, J., Perré, P., & Puel, F. (2020). Flowability characterization of torrefied biomass powders: Static and dynamic testing. *Biomass and Bioenergy*, *138*. https://doi.org/10.1016/j.biombioe.2020.105608

Rezaei, H., Lim, C. J., Lau, A., & Sokhansanj, S. (2016). Size, shape and flow characterization of ground wood chip and ground wood pellet particles. *Powder Technology*, *301*, 737–746. https://doi.org/10.1016/j.powtec.2016.07.016

Salehi, H., Berry, R., Farnish, R., & Bradley, M. (2019). A new uniaxial compression tester: Development and application. *Chemical Engineering Transactions*, *74*, 463–468. https://doi.org/10.3303/CET1974078

Schulze, D. (2007). *Powders and bulk solids*. Springer.

Schwedes and Schulze. (2013). *Ermittlung von fließeigenschaften von biomasse und siloauslegung für massenfluss*. Schwedes + Schulze Schuettguttechniek GmbH.

Schwedes and Schulze. (2022). *Measurement of flow properties of waste-pellets and silo design for mass*. Schwedes + Schulze Schuettguttechniek GmbH.

Shen, Z., Guo, X., Wang, S., Lu, H., & Liu, H. (2022). Compression behaviour of pulverized coal under gas pressurization for the gasification process [article size plays an important role in compression-behaviour. When the SMD of pulverized coal is greaterthan approximately 46m (HR ¡ 1.25), there is no signif-icant compression under gas pressurization in the experi-mental rangerate more important than final pressureFinal pressure not of significant influence on the compression]. *International Journal of Energy Research*, *46*, 19064–19071. https://doi.org/10.1002/er.8509

Sokhansanj, S. (1996). *Effect of fines on storage and handling properties of alfalfa pellets*.

Sorrell, S. (2015). Reducing energy demand: A review of issues, challenges and approaches. *Renewable and Sustainable Energy Reviews*, *47*, 74–82. https://doi.org/10.1016/j.rser.2015.03.002

Stasiak, M., Molenda, M., Bańda, M., & Gondek, E. (2015). Mechanical properties of sawdust and woodchips. *Fuel*, *159*, 900–908. https://doi.org/10.1016/j.fuel.2015.07.044

Stasiak, M., Molenda, M., Bańda, M., Wiacek, J., Parafiniuk, P., Lisowski, A., Gancarz, M., & Gondek, E. (2019). Mechanical characteristics of pine biomass of different sizes and shapes. *European Journal of Wood and Wood Products*, *77*, 593–608. https://doi.org/10.1007/s00107-019-01415-w

Wang, C., Song, S., Gunawardana, C. A., Sun, D. J., & Sun, C. C. (2022). Effects of shear cell size on flowability of powders measured using a ring shear tester. *Powder Technology*, *396*, 555–564. https://doi.org/10.1016/j.powtec.2021.11.015

Wiese, N., & Schwedes, J. (1993). *The variation in the behaviour of bulk solids as a result of sudden pressure changes in the surrounding gas phase*.

Wiese, N., & Schwedes, J. (1991). Effects of sudden pressure changes in the surrounding gas phase on flow properties of bulk solids [Its distribution along the height resembles that of compressive strength. Therefore, the forces resulting from the pressure gradients are responsible for the consolidation of limestone.]. *Chemical Engineering Technology*, *14*, 53–59. https://doi.org/10.1002/ceat.270140108

Wu, M. R., Schott, D. L., & Lodewijks, G. (2011). Physical properties of solid biomass. *Biomass and Bioenergy*, *35*, 2093–2105. https://doi.org/10.1016/j.biombioe.2011.02.020